12-2004

Evaluation of Seal Integrity of Flexible Food Polytrays by Destructive and Non-Destructive Techniques

William James Barlow Jr.
University of Tennessee, Knoxville

To the Graduate Council:

I am submitting herewith a thesis written by William James Barlow Jr. entitled "Evaluation of Seal Integrity of Flexible Food Polytrays by Destructive and Non-Destructive Techniques." I have examined the final electronic copy of this thesis for form and content and recommend that it be accepted in partial fulfillment of the requirements for the degree of Master of Science, with a major in Polymer Engineering.

Kevin M. Kit, Major Professor

We have read this thesis and recommend its acceptance:

Marion G. Hansen, Roberto S. Benson

Accepted for the Council:
Carolyn R. Hodges

Vice Provost and Dean of the Graduate School

(Original signatures are on file with official student records.)

To the Graduate Council:

I am submitting herewith a thesis written by William James Barlow, Jr. entitled "Evaluation of Seal Integrity of Flexible Food Polytrays by Destructive and Non-Destructive Techniques." I have examined the final electronic copy of this thesis for form and content and recommend that it be accepted in partial fulfillment of the requirements for the degree of Master of Science, with a major in Polymer Engineering.

Kevin M. Kit

Major Professor

We have read this thesis
and recommend its acceptance:

Marion G. Hansen

Roberto S. Benson

Accepted for the Council:

Anne Mayhew

Vice Chancellor and
Dean of Graduate Students

(Original signatures are on file with official student records.)

Evaluation of Seal Integrity of Flexible Food Polytrays by Destructive and Non-Destructive Techniques

A Thesis Presented for the Masters of Science Degree

The University of Tennessee, Knoxville

William James Barlow, Jr.

December 2004

This thesis is dedicated to the following:

My Parents

William J. Barlow, Sr. and Mariella D. Barlow

My Brother

Michael P. Barlow

My Professors

Dr. Kevin Kit, Dr. Marion Hansen, Dr. Roberto Benson, Dr. Joseph Spruiell, Dr. Ray Buchanan, Dr. William Becker, Dr. Charlie Brooks, Dr. George Pharr, Dr. Carl Lundin, Dr. Jochen Weiss, Dr. Phillip Davidson, Dr. Bin Hu, Dr. Tom Meek, Dr. Tony Pedraza, Dr. Jack Fellers

&

My Friends

Jerrid, Pate, Brian, Justin, Mike T., Steve L., Pat, Hutton, Drew, Brad, Charles, Jeannie, Kat, Daryl, Songqing, Greg, Tony, John P., House, Truck, Scott, Jallo, Rusty, Jen, Veronica, Dan, Libby, Steve W, Mike B., Bryan B., Neel, Atul, Jose, Trent, Landon, J-Rock, Jason F., Livia, Seth, Corey F., CPD, Ben S., Brad E., Aaron, Sean, Stephanie, Frank

Acknowledgements:

The author would like to sincerely thank and extend his gratitude to Dr. Kevin M. Kit for his continuous support and knowledge for this project over the past two years. He would also like to thank Dr. Marion G. Hansen and Dr. Roberto Benson, his committee advisors, for their encouragement and help throughout his tenure at the University of Tennessee, Knoxville in Materials Science and Engineering.

The author also extends his gratitude to Dr. Joseph Spruiell, Dr. Pat Taylor, and Dr. Ray Buchanan for being excellent department heads in the Materials Science & Engineering over the past seven years and allowing him to become a leader among the students within the department. The author appreciates your support and faith in him.

The author also thanks Doug Fielden and the machine shop for all of their hard work, Van Brantley in TANDEC for help with film testing, Kshitish Patankar for all of his help on this project, Sherry Liu for her help with the FTIR spectroscopy, Dr. Weiss, Dr. Davidson, Kelly Burris and Lilia Santiago for their help with the microbial challenge testing, and COMSOL support group for their help with FEMLAB® simulations.

Abstract:

The military has recently suffered a reduction in production capacity due to the rejection of their flexible food packaging. The rejection of these polytrays was due to sealing defects and the high standards set forth for the sealing quality. These standards set by the military were likely too conservative and until a test could be developed and optimized to quantitatively measure seal integrity, the standards will remain very high. The optimized test, whether destructive or non-destructive, must show that a particular defect, which might currently cause rejection, will not affect the quality of the items contained if passed as a good package. The unavailability of such a test was the basis for the project.

Common tests, both destructive and non-destructive, were performed on the polymeric packaging to develop a basis for an optimized test. Destructive tests such as peel testing and tensile testing were performed to gain a perspective on the strength and rigidity of the seal in the packaging. Tensile testing provided materials properties, such as the elastic modulus. An average elastic modulus value of 1.4 $x10^9$ Pa and 1.8 x 10^9 Pa was used for the lid-stock and tray respectively and were used for the material properties input of finite element analysis.

.

Peel testing was also performed to gain a perspective on the strength of the both good seals and defective seals. Polytrays with no defects from Wornick Food Company proved to have the highest peel strength of all samples with a maximum and minimum peak load of 43.83 lb_f and 18.27 lb_f respectively. A large variation in peak load among all of the samples tested, suggested some uneven thermal sealing of the polytray during production. The first set of defective polytrays used in peel testing was from the Center for Advanced Food Technology at Rutgers University, where a good representation of "short seal" defects on the polytrays was obtained. These seals proved to have one of the lowest maximum and minimum peak loads of 24.01 lb_f and 8.42 lb_f respectively. Peel tests involving polytrays with artificial defects such as entrapped matter made at Stegner

Food Company Trial 2 were tested as well. It was found that solid entrapped matter in the seals, such as noodles, performed poorly in peel compared to the control samples. The entrapped noodle samples proved to be the worst performing of all peel test sets with an average peak value of 15.31 lb_f and the lowest recorded peak force value at 7.17 lb_f.

Burst tests were performed to detect leaks in polytrays with both naturally occurring and artificial defects in the sealing area. These results were the basis for improving and implementing a PC integrated burst test system and for predicting whether or not a seal is good based on defect present. Defective seals were tested and compared to the values of good seals. Leaks were detected in channel defects as small as 50.8 mm. Leaks were also detected in seals with solid entrapped matter; the polytrays with noodles entrapped in the seal, just as in the peel test, proved to be the weakest seals. The defective seals were classified, and a basis for the rejection of certain defects in the sealing area was specified. Although these destructive tests were effective in the determination of seal quality, 100% of production packages can not be inspected by these methods. These tests only provide visual basis for which a polytray can be rejected. The results will hopefully be used increase production without affecting the design or materials selection of the polytrays currently in use.

Finite element analysis, using programs such as FEMLAB®, was used to simulate different loading conditions that the polytrays might endure while in service. These simulations provided vital information as to the way the polytrays behaved under different conditions, especially in the seal area. Pressurizations (2.9 psi through 29 psi) and corner load (10 N through 200 N) simulations on the polytrays were examined in this project. It was found that Mode I and Mode II of fracture dominate in the pressurization simulations and Mode I and Mode III of fracture dominate in the corner force loading simulations. The results, stresses produced in Mode I, II, and III of fracture at the seal, were examined within cross-sectional plots and were reported. A linear increase in maximum stresses was also observed, which was expected.

Non-destructive testing techniques, such as ultrasonic C-scan inspection, were examined as a way to provide an economic means of reducing the incidence of defective packages reaching the consumer. The ultrasonic techniques did not result in the permanent change in the medium; maintained the integrity of the food package and did not alter the mechanical properties of the polytray. The pulse-echo technique was used for this project. Polytrays were sealed specifically for ultrasonic inspection which included all four channel defects on one side of the polytray. Although the wires were detected in both ultrasonic B and C-scans, this technique was ultimately not useful. The clarity and resolution of the images captured were not of high quality even with the largest of channel defects present. Smaller defects, such as the 50.8 micron channel defect, could not be captured in the images.

Post failure characterization was carried out using FTIR/ATR spectroscopy techniques. Failed burst test specimens, lid-stock side, were utilized in an attempt to correlate the failed lid-stock layer to a particular defect. The FTIR/ATR spectroscopy provided information as to what material(s) was present on the surface of the failed burst test specimen. Through visual inspection, it was concluded that the failed burst test samples delaminated in two places; at the actual seal between the polypropylene of the lid stock and the polypropylene of the tray and between the aluminum and the polypropylene of the lid stock. ATR/FTIR spectroscopy was used to examine 119 failed sample surfaces surrounding various defects. 72 of the failed samples displayed the polypropylene spectrum; 60.5% of the total samples examined. The remaining failed samples, 47, displayed a polyester spectrum which is equivalent to 39.5%. It was determined that the defects present in the seal, whether artificial or naturally occurring, had no adverse effect on the particular failure surface of the samples from the burst test experiments.

Table of Contents:

List of Tables:

List of Figures:

Chapter 1: Introduction

1.1 History:

The military's reduction in production capacity of their flexible food ration packaging due to sealing defects will be investigated in this project. These polytrays are an essential life line to the United States military in the field of action. The military's current standards are set to the highest level to ensure quality food product is delivered to our military in the field. There is now a major push for the development and optimization of test for seal integrity of these polytrays. Destructive and non-destructive testing techniques on the seals of these polytrays, along with their feasibility, will be examined. The results of these tests will ultimately be used to quantitatively classify current production defects in the seal that might cause rejection in production. Once defects are quantitatively classified, the development and implementation of a test(s) that specifies which sealing defects affect the quality of food, or integrity of the contents, can take place. Ultimately this test(s) and specifications can be used to increase production without affecting the design or materials selection of the polytrays currently in use.

A military group ration package, or polytray, consists of a tray composed of five layers, polypropylene (PP)/recycled PP/EVOH copolymer/recycled PP/PP, and a four-layered film (lid-stock) made from polypropylene/aluminum/nylon/polyester (PET) which is thermally bonded together under pressure and vacuum. They are designed to keep food from spoiling for at least 18 months at 80°C. This demanding requirement dictates the use of materials with excellent gas barrier properties such as ethylene-vinyl alcohol copolymers and aluminum. A schematic of the polymer package can be seen in Figure 1.1.

Both the lid and tray are constructed of multiple laminated layers. Li et al. [1] state that peelable sealants are rarely composed of a single component or layer. A single layer cannot meet the high demands for packaging food which includes high barrier to oxygen and moisture and a balance of flexibility and rigidity. According to Kit, polymers

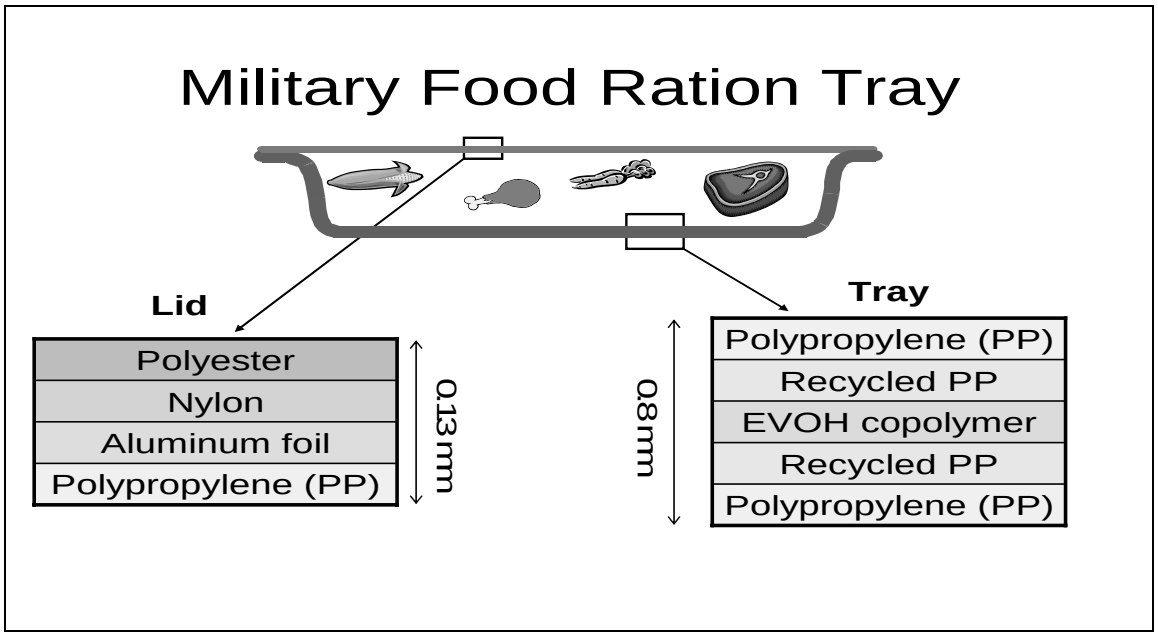

Figure 1.1: Schematic drawing of polytray showing the materials used in both the lid-stock (film) and the tray [2].

such as polypropylene provides good moisture barrier and impact properties, while nylon provides good puncture resistance for the lid [2]. The food is stored, heated, and served all in the same polytray.

The food ration packaging is a continuous process in which the plastic trays are filled with uncooked food one at a time then sealed with the quad-layered film, or lid-stock under a heated, vacuum press. One polytray is successfully produced every 3-4 seconds. The heated press creates a heated seal between the bottom layer of the lid stock (PP) and the top of the tray (PP). No adhesive is used in the process. The polytrays, especially the sealing area, are visually inspected as they come off the production line. The polytrays are then loaded into racks and are placed in retort, where a 255ºF steam bath cooks and sanitizes the food for 3-4 hours. The polytrays are once again visually inspected after the retort process because of the high possibility of defect development during the retort process. The polytrays are then wiped dry and packaged in sets of four in cardboard boxes ready for shipping.

1.2 Objective:

The objective of this project is to develop and optimize a test for the seal quality of the military polytray. Common tests, both destructive and non-destructive, will be performed on the flexible polymeric polytrays. Destructive tests such as peel testing, tensile testing and burst testing will first be performed on good polytrays (no sealing defects) to actually test the strength and rigidity of the seal area. These destructive tests will provide a quantitative figure which will be the basis for which a seal is deemed good. Polytrays with sealing defects, both artificial and naturally occurring, will then be tested and compared to the data obtained from polytrays with good seals. It is here that defects in the sealing area can be qualitatively and quantitatively classified and the basis for rejection of a certain polytray can be established. Although these destructive tests are effective in the determination of seal quality, 100% of packages can not be inspected by these methods. This is not feasible and these tests ultimately only provide a visual basis for which a package can be rejected. Non-destructive analysis such as finite element analysis, FEMLAB®, can and will be used to simulate actual stresses generated by these destructive tests.

An effective non-destructive method, such as ultrasonic inspection could provide an economic means of reducing the incidence of defective packages reaching the consumer. Ultrasonic techniques do not result in permanent change in medium. Used either in pulse-echo technique or in transmission technique, it maintains the integrity of the food package and does not alter the mechanical properties of the package. This method is a means by which 100% of the packaging can be examined. The feasibility of this type of testing will also be discussed.

Chapter 2: Literature Review

2.1 Mechanical Properties:

2.1.1 Material Properties:

Mechanical properties are the essential issue in the initial selection of materials for the specific application. Properties such as ultimate tensile strength, yield strength, elastic modulus, and barrier properties are extremely important in the design of flexible food packaging and ultimately play an important role in the seal strength. Li [1] et al. states that peel strength is a direct relation to the mechanical properties of the lid film. A peel test emulates a tensile test because the sealant experiences a tensile deformation up the sealant fails. The peel strength used in this project is given by the following;

$$P = \frac{F\left(load\ ,lb_f\right)}{in.} \tag{1}$$

Li [1] states that small deformation is important because the mechanics of the deformation are directly related to that of the layers in a tensile test. This deformation or plastic flow does take a large amount of energy and is equal to tensile energy [2]. This energy will contribute to the peel strength because the peel strength is the total energy consumed by the elastic and plastic deformation [2]. These properties along with peel and burst strength will be evaluated in this project and utilized especially in finite element analysis for loading simulations of the packaging.

The engineering stress, given in Pascal (N/m^2) or psi, is found by dividing the force or load by the initial area of the specimen tested. Strain (in/in or m/m) is found by taking the total change in length after testing by the initial gage length of the specimen. Values are plotted and a stress versus strain plot is generated. The ultimate tensile strength, σ_{uts}, is found by taking the maximum stress, σ, of the stress versus strain plot seen in Figure 2.1. The 0.2% offset yield strength, σ_y, can be found, as well as the modulus of elasticity, E, (slope of the linear portion of the curve).

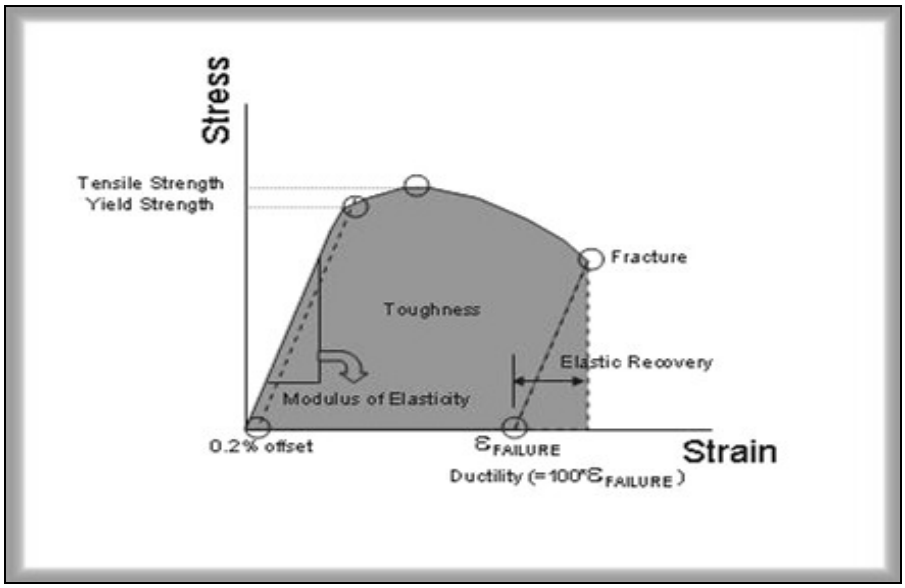

Figure 2.1: Stress versus strain diagram showing tensile strength, yield strength, and modulus of elasticity [3].

Good gas barrier properties are essential to keeping the food inside the flexible polytrays fresh and free of outside contamination. The flexible packaging must also have properties such as impact toughness and a high moisture barrier. Toughness of a material or total energy absorbed can be found by taking the area under the stress versus strain plot. Toughness or the ability to absorb impact is given either as ft*lb or N*m.

2.1.2 Adhesion:

Not only are the preceding properties important, but the ability for these materials selected to bond and adhere to one another is also important in keeping the integrity of the seal. The adhesion of the seal area, PP to PP, of the polytray is ultimately the most important property that will be tested in this project. The film layers of the lid-stock are also adhered together and are necessary to keep the polytray together as well. There are three basic types of adhesion: chemical, diffusive, and mechanical. The following paragraphs describe these types of adhesion. Adhesion cannot be described as a single theory, but rather as a combination of theories.

Bonding an adhesive to some object substrate can be considered to be a sum of the mechanical, physical, and chemical forces that can coincide with one another [4]. The forces can not be separated from one another and thus are split and referred to as mechanical interlocking, electrostatic forces, and the other adhesion mechanisms dealing with intermolecular and chemical bonding [4]. The chemical adhesion can be further explained in terms of the intermolecular forces by the adsorption theory, and also in terms of chemical interactions [4]. The seal area in the polytrays can be described by the diffusion theory in which the bonding consists of similar types of thermoplastic high-polymer materials, such as PP/PP bonding.

The adsorption theory explains that the final adhesion results from intermolecular contact between two materials or substrates, and the surface forces that develop between the atoms in the two surfaces keeps the bond together [4]. According to Lee [5], the absorption theory is the most important mechanism in achieving adhesion. The most common forces that result from the adhesion interface are van der Waals forces (see Figure 2.2) [4]. Glendhill, Kinloch, and Shaw [6-7] have shown through research that the mechanism of adhesion in many adhesive joints only involves interfacial secondary forces. The forces between two surfaces are quite a bit higher than the experimentally measured strength of the adhesion which has been accredited to defects or irregularities that cause stress concentrations during loading [4, 8].

According to the mechanical interlocking theory of adhesion, good adhesion occurs when the adhesive penetrates into the pores, holes or crevices of the adhered substrate; the adhesive can then lock mechanically to the substrate [4]. The adhesive must be able to wet the substrate properly and have proper rheological properties to quickly penetrate the substrate in order to ensure adhesion. The mechanical interlocking does help promote the adhesion, but because adhesion can occur between smooth surfaces as well, the interlocking mechanism is not a generally applicable adhesion mechanism [4]. Figure 2.3 shows mechanical interlocking between adhesive and substrate.

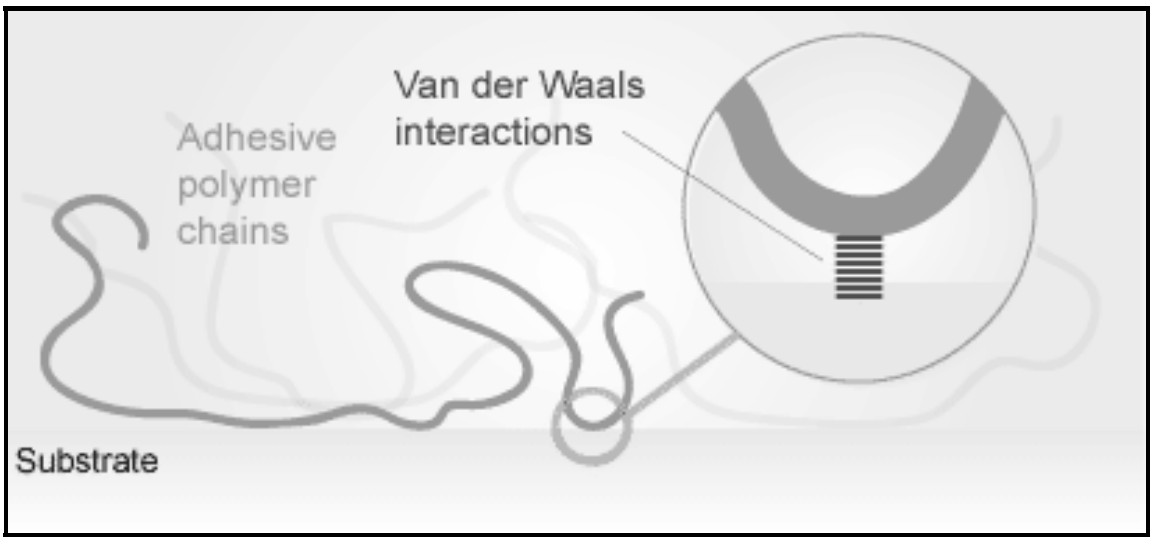

Figure 2.2: Adhesive polymer chains showing van der Waals interactions with the substrate [4].

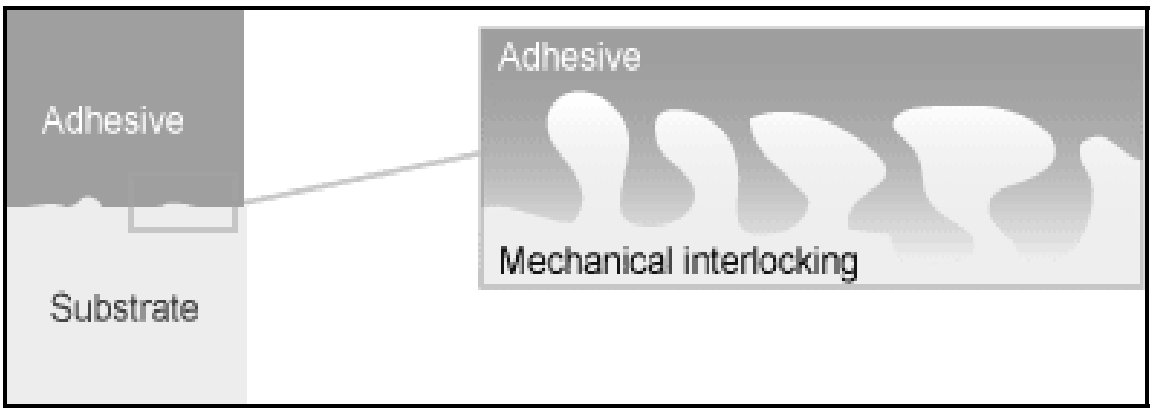

Figure 2.3: Mechanical interlocking between the adhesive and substrate [4].

Clearfield, McNamara, and Davis [9] state that pretreatment methods applied to surfaces can enhance adhesion. Surface pretreatments produce a micro-roughness on the adherent surface that could really improve the bond strength by providing a mechanical interlocking mechanism [4]. According to the chemical bonding theory, this mechanism suggests that primary chemical bonds form at the interface of the adhesive and the substrate [4]. These chemical bonds are strong, and in some instances, can make a big contribution to the overall adhesion [4]. Figure 2.4 shows chemical bonding of an adhesive and substrate. Kinloch [10] states that primary chemical forces have energies ranging between 60-1100 kJ/mol, which are considerably higher than the bond energies secondary forces have (0.08-5 kJ/mol).

According to the diffusion theory, the adhesion of polymeric materials, different or like is due to the inter-penetration of the polymer chains at the interface [4]. According to Voyutskii [11], the driving force for polymer auto-hesion and hetero-hesion is due to a mutual diffusion of polymer molecules at the interface of adhesion. The diffusion theory does require that both the adhesive and adherent are polymers that are miscible with each other and are mutually compatible [4]. Figure 2.5 shows diffusive adhesion between two polymeric materials. Some parameters that affect the diffusion process between polymeric materials are: contact time, temperature, molecular weight of polymers and physical form (liquid, solid) [4]. The process for producing polytrays involves physically solid materials and conditions such as pressure, temperature and time for the sealing of the lid-stock to the tray; closely resembles the diffusive adhesion theory.

The electrostatic theory of adhesion is given as the difference in electonegativities of the adhering materials [4]. Adhesive forces are due to the transfer of electrons across the interface of the adhesive and substrate, thus creating positive and negative charges that attract [4]. As an organic polymer makes contact with a metal, the electrons are transferred from the metal into the polymer which creates an attracting electrical double layer (EDL) [4]. According to Deryagin [12], the electrostatic theory tells us that these electrostatic forces at the interface (i.e. in the EDL), are responsible for resistance to separation. Figure 2.6 shows the electrostatic theory of adhesion.

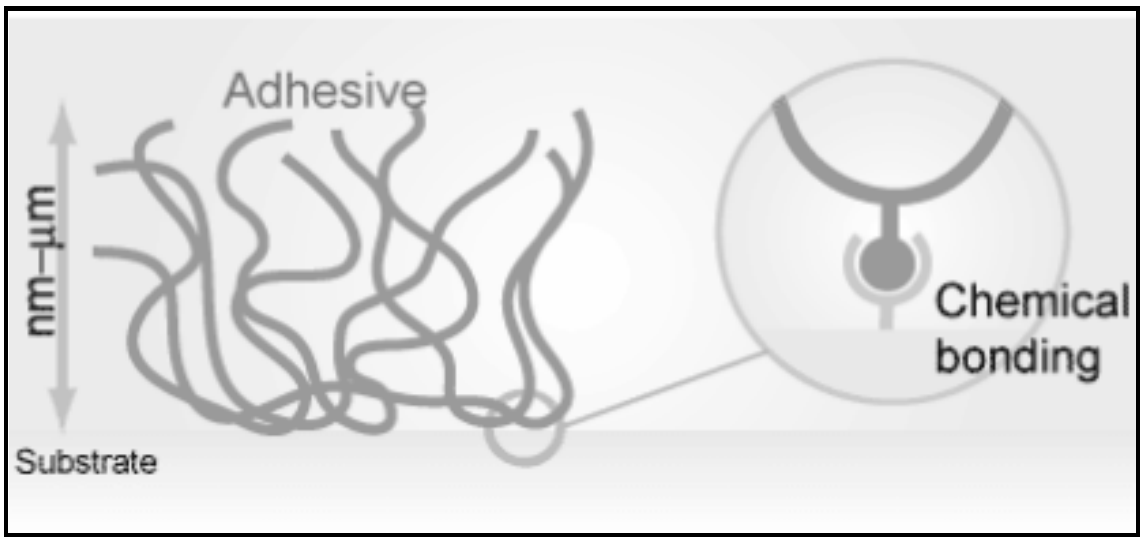

Figure 2.4: Chemical bonding of adhesive and substrate [4].

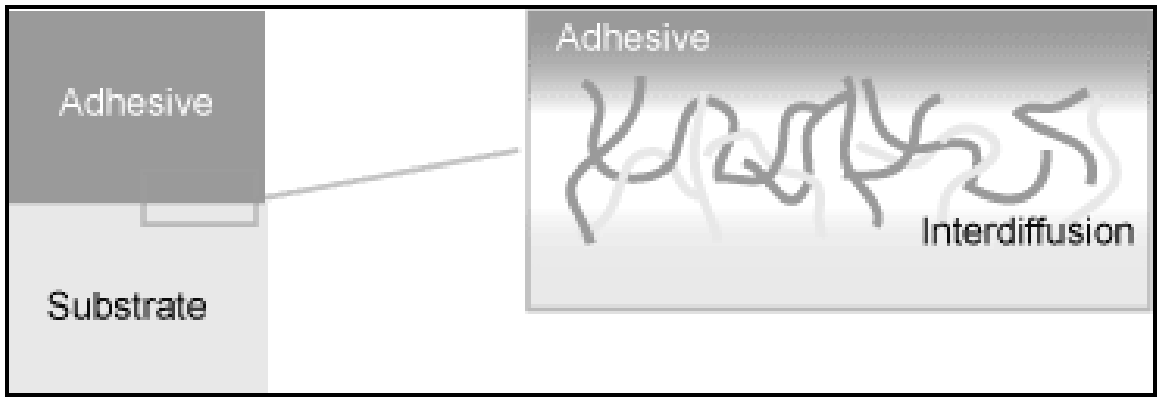

Figure 2.5: Diffusive adhesion between two polymeric materials showing interdiffusion of their polymer chains [4].

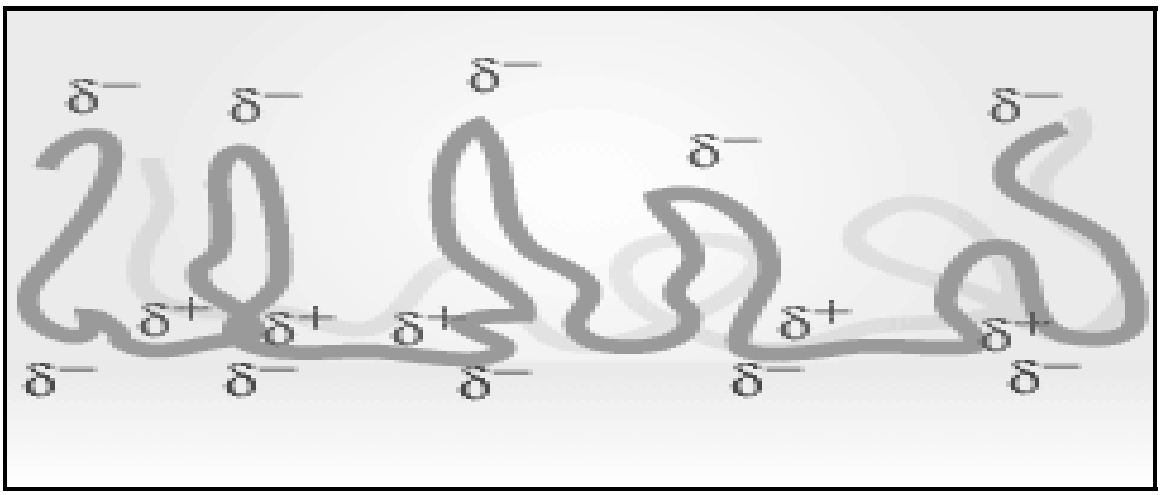

Figure 2.6: Electrostatic theory of adhesion showing positive and negative charges across the interface [4].

2.1.3 Cohesive vs. Adhesive Properties:

According to Li [1] et al., the basic sealing process involves bonding of two polymer surfaces by forcing them into intimate contact while they are in at least a partially molten state. They also state that the failure of a heat seal bond will always start at the weakest point in the seal; which can be adhesive failure, cohesive failure, or interlaminar failure [1].

Li [1] et al. states that cohesive and interlaminar failures are preferable in some consumer product applications that require hot filling and pasteurization. The military polytrays require this type of failure because of the retorting process involved in the production of the polytray. In an adhesive failure, the interface of the peel and the seal is the same and the seal strength has to be compromised to allow for a peel that is reasonable [1]. A reasonable peel is not desired in the polytray packaging because of the packing and shipping conditions the polytrays will endure. Seal strength does not need to be compromised in this project. Li et al. also state that the peeling of adhesive failure is usually a bursting peel that does require higher strength to initiate failure and the peel strength of adhesive failure is sensitive to the processing variables [1].

A cohesive failure may require only a single layer film. A cohesive failure occurs when the sealant materials are immiscible and have low interfacial tension and when the overall seal between the lid and the bottom web is stronger than the cohesive strength of the sealant [1]. Li [1] states that if the bottom web is polypropylene, the sealant should contain polypropylene to seal to the polytray or container. The sealant used should be a blend of polymers that can vary the peel strength and materials in the blends can be polymers that provide limited miscibility to the major component [1].

2.2 Packaging Materials

According to Li [1], the selection of materials is critical to a peelable seal because it ultimately determines the seal and peel properties and processing conditions. The sealant must closely match the container or packaging materials in a structure to ensure a reasonable bond at the joint of the seal [1]. Multilayer co-extruded flexible packaging materials have been a significant influence into the development of modern packaging. These multi-layered packages are be used in such as applications as food, pharmaceutical, medicinal, cosmetics and electronics industries [13]. The packages usually combine several desired properties such as barriers to gases and water vapor, mechanical strength, machinability and low cost which no single material can provide [13].

Packaging materials must be carefully selected to ensure quality of the food contained. In this project, materials for the multilayered flexible packaging were pre-selected by the military and used in production before any testing was initiated. Some common co-extruded materials produced that are used in the food packaging industry include: LLDPE/tie/EVOH/tie/LDPE which can be used for wine and fruit juices, polyamide/ethylene-vinyl acetate (PA/EVA) which is used for frozen foods, PA/Ionomer and PA/LDPE for processed meat and dairy, and PP/EVOH/PP and HDPE/EVOH/HDPE used for ketchup, sauces, salad dressing and juices [13]. In this project, polytrays consisted of the PP/EVOH/PP combination type as discussed in Section1.1.

The lid-stock of the flexible food packaging is also constructed of multiple laminated layers to increase the barrier properties. A large number of combinations of single materials can be used in a coextrudate, but most multilayered structures have a polyolefin base [polyethylene (PE) and polypropylene (PP)] [13]. These polyolefins are cheap and are essentially easy to process and polyolefins such as low-density polyethylene (LDPE) and linear low-density polyethylene (LLDPE) are used widely for their toughness and sealability [13]. Barrier materials such as ethylene-vinyl alcohol (EVOH), polyvinylidene chloride (PVDC), and aluminum are used when outside elements such as gas, vapor, and aroma are unwanted [13]. Ethylene-vinyl alcohol (EVOH) copolymers and aluminum were used for good gas barrier protection this project. The selection of a polymer such as polypropylene in both the lid and tray provided good moisture barrier and impact (toughness) properties, while nylon in the lid-stock provides good puncture resistance for the lid-stock.

2.3 Destructive Testing:

2.3.1 Seal Strength:

Peel testing will be performed using the T-Peel ASTM Standard D1876. This standard is used to understand seal strength and cohesive and adhesive properties of the seal. Burst testing on the polytray will be performed using design modified equipment based on current industry implementation. This test, not based on ASTM standards, will be used in characterizing the strength of the heat seal in flexible food packaging. Peel and burst tests will be performed and a correlation will be examined to determine if the tests are related in the relative strength of the seal.

Researchers [14] have tried to correlate these tests using flexible food pouches. Feliu et al. [14] have developed theoretical equations based on force diagrams to try to describe the food pouch behavior while undergoing a restrained burst test. Feliu et al.'s [14] resulting equation is given as, $P = 2\ S/D$, where the burst pressure (P) increases directly with seal strength (S) and inversely with the restraining plate (D) distance and

after restrained burst tests and a peel tests were run on Tyvek/plastic pouches, they found that the theoretical equation did not explain burst test results in terms of peel test values. Feliu [14] has found that their formula (P = 2 S/D) overestimates the burst pressure based on the seal strength and the overestimation increases at smaller gaps (distance between restraining plates). The results indicate that their formula cannot be used to correlate burst and peel strength and it suggests an oversimplification; it might work for particular materials at a particular set of testing conditions [14].

Li et al. state that there are many factors influencing the seal and peel properties [1]: processing variables including temperature, dwell time, and pressure, materials including the lidding and bottom web, miscibility and morphology, peel rate and angle, thickness and location of layers in a multi-layer film, and mechanical properties of the sealant materials. Effects on peel properties in regards to molecular weight were not discussed, although higher molecular weight polymers used for sealing might require longer sealing times and higher sealing temperatures because of the higher viscosity upon melting.

Properties of materials selected, of course influence the sealing temperature; higher sealing temperatures usually create higher peel strengths [1]. Processing values such as pressure and dwell time are typically less material-dependent, but the dwell time must be long enough to bring the interfacial temperature to a desired level [1]. Longer times will not improve the seal properties and can ultimately distort a sealing surface [1]. The pressure applied typically has to be high enough to place the seal components into contact with one another to achieve good wetting, while higher pressure do not improve the seal properties or appearance of the seal [1].

Peel tests are typically performed on consumer products to test for seal quality and ease of delamination; a common ground is not always easily met for these consumer products. It is ultimately extremely difficult to compromise seal strength with the ease at which the sealed packaged can be opened. In this project, the polytrays do not require ease of delamination for the lid-stock from the tray. The seal strength and integrity must

be kept at a high standard while producing a uniform quality seal with no defects. Peel tests in this project were performed to quantitatively categorize visually good seals containing no defects and seals with artificial and naturally occurring defects.

Sanchez et al. [15] state that coextrusion is a widely used process in food packaging industry because it allows for the design of multilayered films that have different functional properties associated to each layer. When layers of a coextruded film show incompatibility, a `tie' layer can be incorporated to promote and improve the adhesion, but it makes for a more expensive and complex manufacturing process [15]. Sanchez [15] has also reported that polymer blend compatibility can be improved if the adhesion between different phases is increased. Sanchez's group has studied blends of LLDPE and LLDPE-gMA that is used to help the adhesion to nylon in a three layer coextruded film without using an adhesive tie layers. Sanchez [15] studied the T-peel strength and oxygen and water vapor transmission rate of the coextruded films. The failed or peeled films surfaces were then characterized using a scanning electron microscope. Sanchez [15] found that the films with 10% and higher levels of maleated LLDPE in the blend increased in T-peel strength, which ultimately suggests good adhesion between the layers.

2.3.2 Microbial Challenge:

Microbial challenge experiments will be performed on media filled polytrays with various artificial channel defects in the sealing area. This testing is vital to the seal integrity of the polytray and will provide a basis for minimum passable defects during the process. According to Wilson et al. [16], the ability of foods to support the growth of microorganisms and food-borne pathogens has been assessed by inoculating with an organism of interest, and monitoring the growth of that organism over a set time. Wilson states [16], "Information gained from such challenge tests, together with knowledge of the organoleptic stability of the product, can then be used to determine an appropriate shelf-life for the food. Whilst this approach may be seen as the "gold-standard" of microbiological assessment of food it is both time-consuming and costly."

Researchers [17] have studied microbial challenge testing of ready-to-eat (RTE) foods containing *Listeria monocytogenes*, which is recommended to assess the potential for growth. The study was to evaluate a protocol for microbial challenge testing applied to RTE cooked meat products [17]. Uyttendaele et al. [17] state, "In order to choose *L. monocytogenes* strains with a representative behavior, initially, the variability of the response of multiple *L. monocytogenes* strains of human and food origin to different stress and growth conditions was established." Researchers [17] performed microbial challenge testing of *L. monocytogenes* in modified atmosphere packaged sliced cooked ham and pâté.

Uyttendaele et al. [17] describe, "A mixed inoculum of four *L. monocytogenes* strains and an inoculum level of ca. 1–10 CFU/g was used. On vacuum packed sliced cooked ham, the concentration of 100 CFU/g, the safety limit considered as low risk for causing listeriosis, was exceeded after 5 days whereas ca. 10^5 CFU/g were obtained after 14 days when also LAB spoilers reached unacceptable numbers (ca. 10^7 CFU/g) whether standard or cold-adapted inoculum was used. The concentration of sodium lactate determined the opportunities for growth of *L. monocytogenes* in pâté. If growth of *L. monocytogenes* in pâté was noticed, the threshold of 100 CFU/ml was crossed earlier for the cold-adapted inoculum compared to the standard inoculum."

2.4 Post-Failure Characterization:

2.4.1 Attenuated Total Reflection ATR/FTIR

Attenuated total reflection (ATR) is utilized to examine failed seal surfaces from the burst tested polytrays. Internal reflection spectrometry or attenuated total reflectance infrared spectrometry provides vital information regarding the chemical composition of the selected material. Mid-infrared spectra can be captured obtained by pressing small pieces of a material against an internal reflection element (IRE) such as zinc selenide (ZnSe) or germanium (Ge), Ge is this project, where the infrared radiation is focused onto one end of the IRE [18-22]. As the light enters the IRE, it is reflected down the length of

the crystal and at each reflection, the radiation will penetrate a short distance into the polymeric material [18-22]. Figure 2.7 shows an example of an internal reflection element. For FTIR/ATR spectrometry, the depth of penetration, d_p, varies with the crystal angle and the incident angle, θ.

In the mid-infrared, absorption of radiation can be related to vibrations produced by the chemical bonds [18-22]. The internal reflection spectrometry can provide information regarding the presence or absence of functional groups, as well as the chemical make up of the material tested; absorption bands are assigned to functional groups such as the C=O stretch and the C-H bend [18-22]. When the frequencies of absorption bands shift, the relative band intensities change and ultimately the chemical structure changes [18-22].

Although this project does not involve any surface modifications, ATR/IR spectrometry can also be used to examine surface modifications by chemical or physical treatments such as exposure to surfactants or chlorine and temperature annealing and can also be used to identify unique features on the surface after these modifications [18-22]. Researchers [18-22] have studied the chemistry of viable biological fouling and hoe it affects the materials performance and fouling potential, which is ultimately critical in optimizing function, performance and design.

The following equations describe the math and physics behind the infrared total reflection spectroscopy. An appropriate optical setup can focus infrared light onto a face of the ATR crystal [23]. By selecting, θ (seen in Figure 2.7), which is the angle at which the infrared light enters the interface between the ATR crystal and the air, $\boldsymbol{W}$ which is the thickness of the crystal, and $\boldsymbol{L}$ which is the length of the crystal, the total number of reflections, $\boldsymbol{N}$, of the light can be controlled [23]. The equation for the number of reflections is given by the following equation:

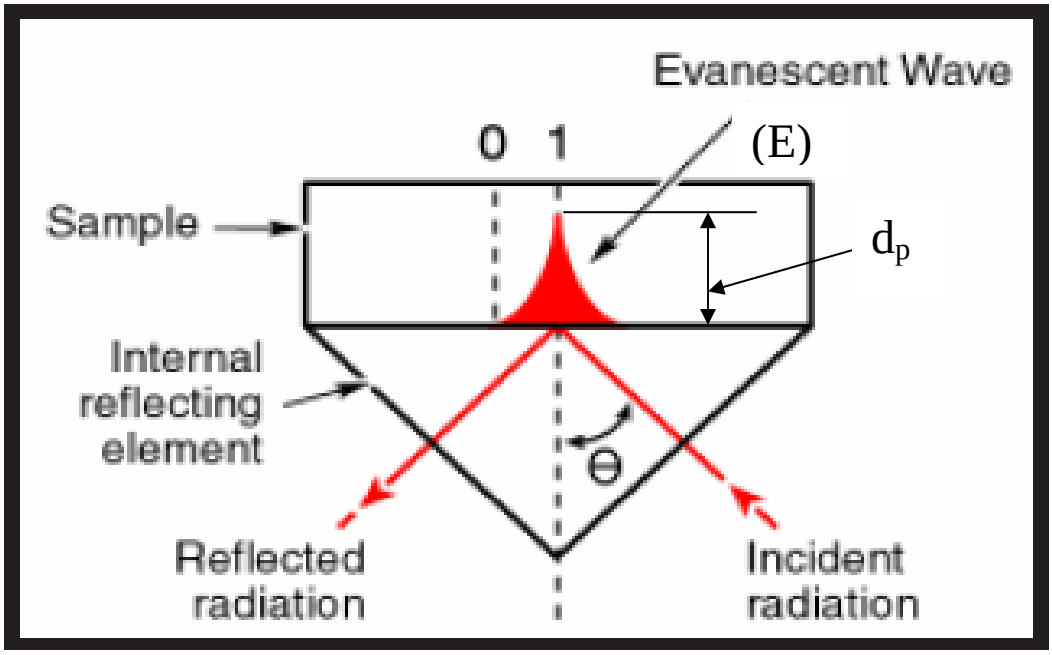

Figure 2.7: Total internal reflection at the interface of an internal reflection element showing a single reflection of the ATR [24].

$$N = \frac{L}{W}\cot(\theta) \tag{2}$$

An evanescent electric field (E) in the medium is produced at each reflection; the intensity of the evanescence will decay exponentially with a given distance (z) into the medium. The evanescence can be seen by the following equation below.

$$E = E_o e^{-\frac{z}{d_p}} \tag{3}$$

where E_o is the incident radiation intensity and d_p is the depth of penetration into the medium orthogonal to the surface of the medium [23]. The magnitude of the depth of penetration tells how deep one can see into the medium and is true for both the electric and the magnetic components of the light [23].

A polarizer can selectively absorb one of these components of the light [23]. Perpendicularly polarized light, perpendicular to the plane of incidence and when traveling through the ATR crystal, results in an electric field on the surface of the ATR crystal [23]. Only one component is at the surface and is given by the equation below:

$$E_o = E_y \tag{4}$$

As the entering light is polarized parallel to the incident plane, the equation then becomes [23]:

$$E_o^2 = E_x^2 + E_z^2 \tag{5}$$

The two components of the light beam are important to interpreting calculations of molecular orientations which are on the surface of the ATR and the presence of infrared absorbing material in the medium reduces the overall intensity of the reflected light at each reflection point [23]. The addition of small absorbances from each reflection will result in sensitivity of ATR surface [23]. The depth of penetration is given by and is shown in Figure 2.7:

$$d_p = \frac{\lambda}{2\pi n_1 \sqrt{\left(\sin^2\theta - n_{21}^2\right)}} \tag{6}$$

where λ, the wavelength of the light, n_1 is is the refractive index of the ATR crystal, n_2 is the refractive index of the rare medium, θ, is the angle of incidence and n_{21} is n_1/n_2 [23].

2.4.2 Ultrasonic Inspection:

Ultrasonic inspection will be utilized to in this project to examine polytrays with defective seals containing various channel defects. The objective will be to examine the seals and specify the minimum channel defect size that could detected with the system. The research will be conducted to specify the feasibility of this particular type of inspection. The C-scan with the pulse-echo technique will be utilized in which the polytrays are submerged into a water medium and scanned with varying frequency transducers.

Pascall et al. [25] investigated the feasibility of ultrasonic inspection for a non-destructive assessment of the seal strength of 335 ml polymeric trays. Pascall [25] filled sample trays with beef enchilada and then sealed the trays at temperatures of 170-260 degree C for 5 s at 3 bar [25]. Ultrasonic measurements were done by an immersion technique using pulse/echo signal in which signal amplitudes of the reflections were captured, digitized, and analyzed to ultimately develop C-scan images of the seals [25]. The data for each tray sample was analyzed and then used to compare with the seal strength of the trays.

Pascall et al. [25] also investigated the minimum channel leak size that could be detected using this ultrasonic equipment. Pascall [25] reported a direct correlation between the seal strength of the trays and sealing temperature, and the ultrasonic inspection did show that the scatter in the pulse-echo signal decreased as the sealing temperature of the trays increased. Pascall [25] correlated this reduction in the scatter to a trend of increasing uniformity in the fusion seal; between 170°C and 193°C, sharp changes in the scatter were observed and little change was seen for sealing temperatures greater than 193°C. The ultrasonic C-scan technique seemed to be a promising way to non-destructively test and predict the seal quality in the polymeric trays and will be examined in this project.

2.5 Finite Element Method/FEMLAB®:

Research has shown that finite element analysis (FEM) has not been used to a great extent in the field of food packaging. It was found that burst testing and side compression testing has not been modeled or simulated in the area of flexible food packaging. Modeling of rigid containers and film blisters has been done and the concepts gained from those experiments will be examined in this project to actually simulate pressurizations and side compression loading on the flexible polytrays.

Kaliakin [26] states that in continua analysis, dependent variables such as temperature, pressure, and displacement are functions of every point in the body being analyzed; these dependent variables have infinitely many values or an infinite number of degrees of freedom. The approximate solutions generated by finite element method are based upon: (1) governing equations which are recast into a weak or integral (variational) form and (2) a continuous problem is replaced by an approximated problem [26]. According to Kaliakin [26], the weak or integral form has its advantages because it is closer to the physical aspects of the problem involving an analysis of a solid; the weak or integral form of the equations of motion involve strain and potential energy due to outside loads applied to the body.

As the continuous problem is replaced by the approximated problem, a finite dimensional sub-space of values of the primary dependent variables is constructed [26]. The construction is based on the generation of a mesh which can approximate the domain $\boldsymbol{\Omega}$, where $\boldsymbol{\Omega}$ is divided into a finite number of elements or overlapping sub-domains given by $\boldsymbol{\Omega}^e$ [25]. The domain is given by the following equation:

$$\Omega = \sum_{e=1}^{NE} \Omega^e \qquad (7)$$

where NE is the total number of elements used [26]. Each element has a specific number of nodes or node points associated with it and these elements are connected at a specific number of nodes which are set along the boundary of the element [26]. Each nodal value represents the finite number of unknowns to be solved for and is given by $\hat{\phi}_m$ [26]. Kaliakin [26] states that every element Ω_e can characterized by the following: the geometry of Ω_e, the set of degrees of freedom defined on Ω_e, and the basis polynomial for the interpolation functions N_m. The sub-space construction also involves defining the finite space as a set of piecewise functions N_m that are restricted to the element domain and the approximation of the primary dependent variables can then be given by the following equation:

$$\hat{\phi} = \sum_{m=1}^{NDOF} \hat{\phi}_m N_m \tag{8}$$

where NDOF is the number of degrees of freedom for $\hat{\phi}$ within the element [26]. These approximations are thus continuous over each sub-domain and the finite number of degrees of freedom involved within the body of interest is approximated by a finite number or by the nodal unknowns $\hat{\phi}_m$ [26].

Margaritis et al. [26] have explored a finite element modeling (FEM) of an island blister test (IBT) which considers the plasticity of a film which can separate normal and shear components of fracture energy. The blister specimens are a polymer film, Amoco Ultradel 4212 HFDA-APBP Polyimide, on a chromium-coated silicon substrate and were tested to show that crack propagation occurs when mode I component of the fracture energy reaches a specific value [26]. The sample was mounted on an island and pressurized with dry N_2 at a controlled rate while the crack front at the island was examined through a microscope [26].

Margaritis [27] used axial symmetry and meshed the IBT by one row of 1000 axisymmetric eight-noded quadrilaterals which was determined from the average ratio of film thickness to blister radius, given as 1 to 1000. They [27] assumed the substrate to be completely rigid and all of the nodes over the island were pinned in rigidly. It was found that the system under the pressure had stresses greater than the yield stress which developed near the island as the film began to delaminate from the substrate [27]. Stresses, deflections, and fracture energies were all plotted versus the radial position of the film over the island. Margaritis [27] used a large deflection elastic-plastic FEM for the blister test which allowed for the mode I and mode II components of fracture energy and the specific plastic work to be quantified and separated.

Chapter 3: Experimental Procedure

3.1 Tray Production:

In order to successfully categorize sealing defects, polytrays with both artificial and naturally occurring defects had to be acquired from the manufacturing facilities. Many of these packages, especially with artificial defects, had to be manually produced at the manufacturing facilities. Polytrays, both empty and media filled with naturally occurring sealing defects ranging from excellent to very poor were also acquired from three of the manufacturers; Stegner Food Products in Cincinnati, OH, Sopakco in Mullins, SC, and Warnick located also in Cincinnati, OH. The sealing conditions of the as received packages will be categorized and described later.

3.1.1 Tray Production – Trial 1:

Trial 1 for polytray production took place at Stegner Food Products in Cincinnati, OH on June 3, 2003. Sample trays were made for both mechanical and microbial challenge testing. Artificial channel defects across the seals were created using fine nickel-chromium (Ni-Cr) wires with diameters of 50.8, 127, 254 and 381 microns. The wires were gently taped across the edge of the trays in various positions before sealing. Some experimenting with the wire placement was required before tray production could begin. A potential 12.7 micron wire was used and proved to be too fine for production. The 12.7 micron wire would break as the tray was sealed and the wire could not be pulled out of the seal to create the channel defect. A PTFE (Polytetrafluoroethylene Telomer) spray was used as dry release agent to aid in the removal of the more delicate 50.8 and 127 micron wires from the seals of the trays.

A total of 60 empty trays were produced for mechanical testing; 10 trays for control (no defects), 10 trays for each wire size (four wire sizes), and 10 trays with all the wire sizes in the seal (see Appendix A). Each wire was removed after the sealing and retort process to create a channel leak in the seal. The empty trays were used for non-

destructive and destructive testing. An additional 9 empty trays were made with the placement of a starch solution on the seal before sealing; 3 different viscosity solutions (3, 4, and 5% starch in water) in 3 different positions on the seal. These trays were used for mechanical testing as well and the production of polytrays with entrapped matter defects will be examined further in Trial 2.

A total of 80 media filled trays were produced for the microbial challenge testing (see Appendix A). Media was produced at Stegner Food Products and used to fill trays containing various artificial defects. Defects were created using the same nickel-chromium wires as discussed previously. Five trays for each wire size (four wire sizes) five defect free samples were made to be dipped into three different microbial environments. An additional five positive control samples were made to be post cool inoculated. The lab at Stegner was used to make the media for tray production. Two 10L pots were used to make a 20L batch of media. Each pot contained 10L of water, 300g tryptic soy broth and 500g (5%) starch (*Ultraspearse*). The solution was heated until boiling and was continuously stirred with a whisk until solids were completely dissolved. A total of 6.5 batches were made or a total of 130L of media.

Media was slowly poured into the trays with the various wires in place and the trays were then sealed under the following conditions: line speed of 16 trays/min, sealing temperature of 232° C, and a sealing pressure of 5.5 bars or 80 psi. Ten to fifteen trays at a time were put into production at random times during the production day (see Appendix A). Once all trays were produced, they were put through the retorting process using the ICON 2000. The retorting process required about 3.5 hours for each cycle. The sealed retort vessel was pumped with steam with a slow ramping temperature to around 124.5°C and then a cool down spray was used to return packages to room temperature. Tables in Appendix A shows the exact retort conditions used for our trays.

As stated previously, nine additional empty trays were made with artificial defects by placing different viscosity solutions on the seal area before sealing. For each viscosity solution, one drop was placed on three trays; the short side of one tray, long side of one

tray, and the corner of one tray. After sealing, it was clearly seen that there were defects in the seal where the drops had been placed. Future experiments will include a variety of different media to understand real processing/sealing problems encountered at the plant.

3.1.2 Tray Production – Trial 2:

Polytrays were again manufactured at Stegner Food Company in February 2004. The same process was used here for Trial 2 to fill and seal the packages. The 254 and 381 micron wires were not used in this trial because prior testing, which can be seen in the Results and Discussion section, proved the channel defects to be too severe. The 50.8 micron wire and ~12 micron carbon fibers were used in this trial to create channel defects. The carbon fibers proved to be entirely too small to create a channel defect. The fibers would break very similarly to the 12.7 micron wire in production. As the lid stock was sealed to the tray, the fibers would break and could not be pulled from the seal to create a channel defect. Sound samples were made along with samples with entrapped matter, see Appendix A.

To understand some of the problems occurring in process, soy bean oil, starch solution (6.5%) and blanched noodles were placed across the tray before sealing. This in turn creates an artificial defect in the sealing area. The defects were clearly visible and samples could then be cut from the area surrounding the defect for mechanical testing. The polytrays were not placed in retort at the Stegner plant for Trial 2; instead the media filled polytrays were placed in retort at the University of Tennessee, Knoxville in the Food Science and Technology Building. The retort conditions can be found in Appendix A for Trial 2.

3.1.3 Received Polytrays:

Several sets of polytrays were received at the University of Tennessee for testing. As the polytrays were received, they were documented and labeled accordingly. The condition of the as-received polytrays was recorded and defects were classified before

testing was conducted. The first polytrays received were from Sopakco in Mullins, SC and the second set of polytrays was received from Wornick in Cincinnati, OH. These packages were empty, meaning they were sealed with no media inside. The polytrays had no as-received visual defects in the seal area. These packages were used for initial peel, tensile, and burst testing to gain a better perspective on the seal strength of these polytrays. The preceding polytray sets were labeled as Wornick 1 and Sopakco 1, respectively.

A third set of polytrays received was from the Center for Advanced Food Technology at Rutgers University. These polytrays were also sealed empty. These polytrays had some major sealing defects mainly due to deformed (high variance) flanges on the polymer tray itself. As lid stock (quad-layered film) was heat-sealed to the tray, the resulting seal contained many areas that were not bonded and thus "short seals" were created. Some areas of the lid-stock did not bond at all with the tray; voids, or large channel defects, were created within the seal. Each polytray was labeled and each defect was taken into consideration and documented. A good seal is roughly 5 mm in width from the inside of the flange to the outside. A "short seal" defect was defined as any area of the seal that was less than 5 mm in width. The defect was then given as a percentage of a good seal remaining after the sealing process. Figure 3.1 shows a schematic drawing of a "short seal" defect. Shaded regions represent areas of the seal that remain unbonded after sealing process. These "short seal" polytrays were used for both peel testing and burst testing.

The last set of polytrays was sent from Sopakco. These packages were mainly used for the last version of the burst tester and were labeled as Sopakco 2. These polytrays were sealed with media inside such as baked beans, spaghetti, and meatballs. A large variety of defects was represented in this set of polytrays. Short seals, air bubbles, and wrinkles of varying sizes were all visible within the seals of these polytrays.

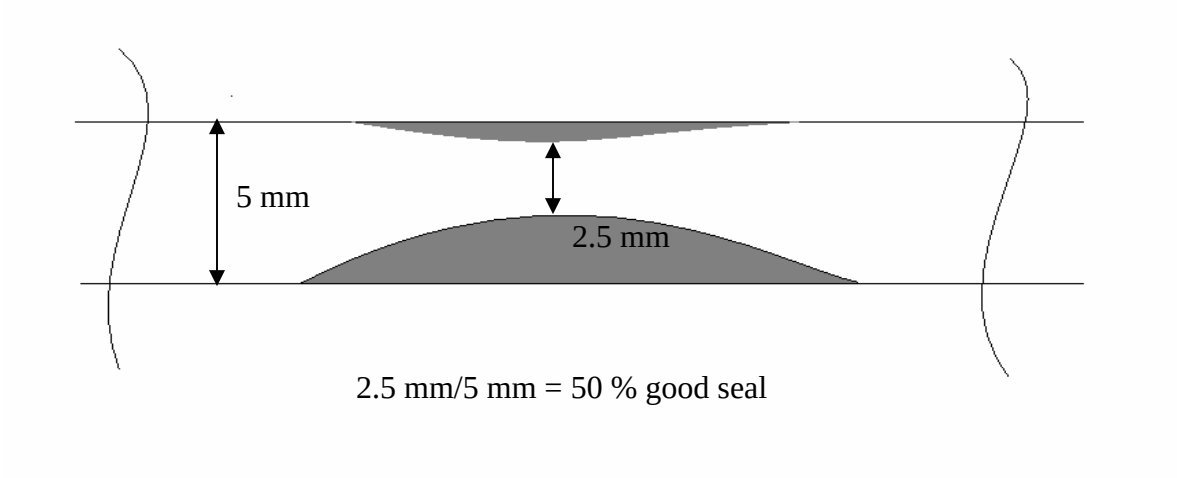

Figure 3.1: Schematic drawing of a “short seal” defect and calculation of remaining good seal after sealing process.

3.2 Mechanical (Destructive Testing):

Destructive testing is necessary to understand the strength or seal integrity of both sound polytrays and defective polytrays. As the polytrays are tested, the defects can be categorized and classified. Those defects which should be allowed to pass visual inspection without compromising the integrity of the seal can be specified. Reasonable changes to this specification based on the destructive test results could decrease the rejection rate and increase revenue. However, seal integrity must be held at the highest of standards to provide food that is safe to eat, especially food with a shelf life of 18 months.

3.2.1 Peel Testing:

Peel testing was performed using the T-Peel test according to ASTM D1876-01 [28] standard in conjunction with the ASTM F88 – 00 [29] standard test method for seal strength of flexible barrier materials. Specimens deviated from the standard because the bonded area or seal width is only about 5 mm. Samples were cut from the polytrays in 1 inch wide sections. Sound polytrays were tested first to understand the seal integrity of

polytrays deemed as in good condition. From these results we compared results from the samples cut from the polytrays surrounding the natural and artificial defects. The Instron® tensile testing machine was used for this experiment. A 100 lb load cell was used with a cross-head speed of 0.2 inches/minute. The sample was placed in between the grips, having a gage length of 0.5 inches, with 100 psi gripping pressure. Peel tests were conducted on the polymer trays in batches as they were sent to the University of Tennessee, Knoxville and as they were made at the manufacturing facilities. No spectroscopy such as SEM or optical was used to examine the possible variance in the seal region of the as received trays. As stated earlier, through visual examination one can see a variance in the seals from manufacturer to manufacturer. This variation was examined carefully in hopes to fully understand the strength of these polytrays and how they vary from polytray to polytray. Figure 3.2 shows an example of a T-peel test specimen from ASTM D1876-01.

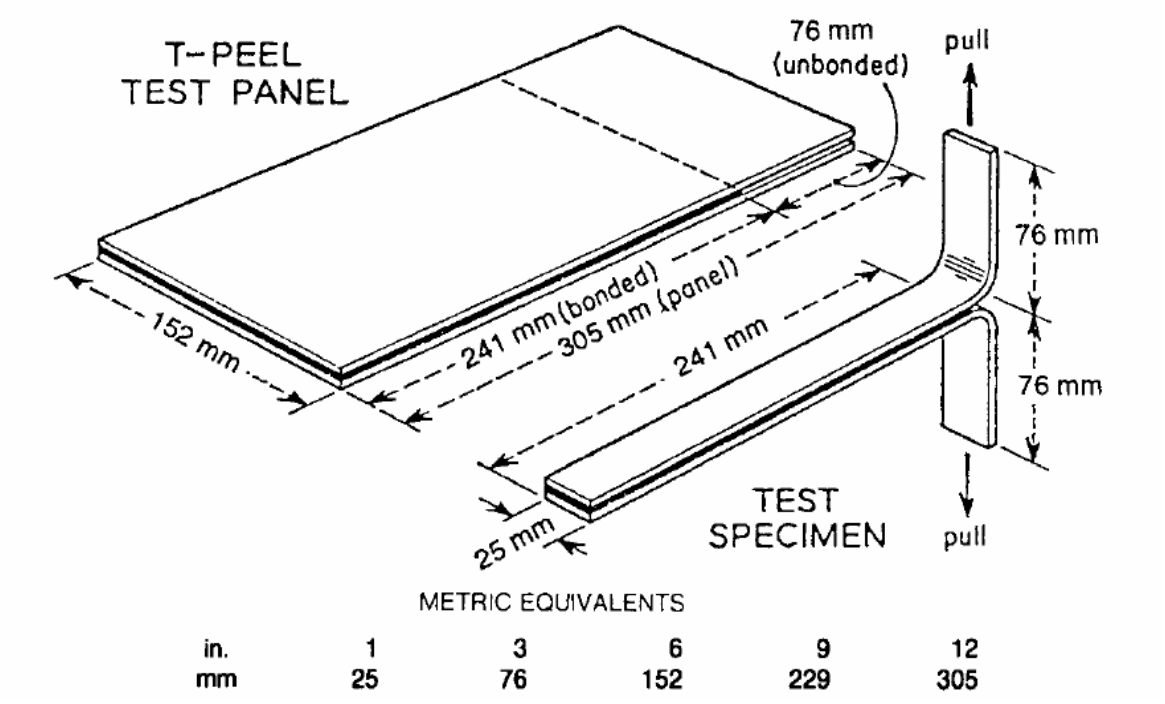

Figure 3.2: Example of T-peel specimen from ASTM Standard D1876 [28].

3.2.2 Tensile Testing (Lid Stock/Tray):

Tensile tests were performed on both the lid stock and the tray in order to get accurate input values for use in finite element analysis (FEMLAB®). Modulus values calculated from this data were used in conjunction with finite element analysis of these packages as a material property. The lid stock (film) tensile specimens were run with the same equipment used for the peel testing. ASTM D882-02 [30] standard was used for the testing of the film. Film specimens were pulled at 0.5 inches/minute while a 2 inch gauge length was used. Stress versus strain plots were generated and the modulus values were calculated from this data. The lid stock samples were taken from the same polytrays that were sent to us from the manufacturer Sopakco.

The tray tensile specimens were also taken from the same polytrays. Dog bone specimens with a standard gage length of 4 inches were cut from the tray itself. The samples were run using the Phoenix® tensile tester with a 2000 lb load cell while being pulled at a crosshead speed of 20 inches per minute. Stress versus strain plots were also generated for these samples and modulus values were then calculated for finite element analysis input.

3.2.3 Microbial Challenge:

The first microbial challenge was done using a total of seventy-five polytrays with sound trays and artificial channel defects ranging from 50.8 to 381 μm. These polytrays were produced along with five control (no defects) samples for the first experiment. After the polytrays were retorted and transported to the Food Science & Technology department at the University of Tennessee, Knoxville, the wires were pulled from the seals and then the packages were dipped in the microorganism *Enterobacter aerogene*. The concentrations of the microorganism can be seen in Appendix B. The polytrays were exposed for 2 min at 21-25°C in the varying concentrations and then were placed in incubation, at an elevated temperature of 35°C. The concentrations were as follows:

Chlorinated Water (negative control of 7-9 ppm FAC), 3 log colony formation units (CFU)/mL, and 6 log CFU/mL. Five positive control samples were post cool inoculated with the microorganism as well. Daily examination of the packages was conducted to check for gas formation or bacteria growth. Activity (swelling) was recorded as bacteria grow in the polytrays. Bacteria produce carbon dioxide (CO_2) gas as they grow and the polytray in turn swells.

The second microbial challenge trial was completed using similar procedures in the first trial. Retorting capabilities became available and was conducted at the University of Tennessee, Knoxville for this trial. The retort conditions can be seen in Appendix A. The conditions for the retorting process were programmed to match the conditions of the retort machine at Stegner Food Products. The concentrations of the microorganism were kept constant from Trial 1. The time that the polytrays were exposed to the microorganism was increased to 15 minutes instead of 2 minutes at room temperature. Polytrays were stacked on their side in crates and placed in an incubator at elevated temperatures. Polytrays were examined daily for 12 days and bacteria growth was indicated as carbon dioxide (CO_2) gas formation was present.

3.2.4 Burst Testing (Pressurized Package):

ASTM standard F 2054 – 00 [31] was used as a basis for the design of a burst test system in this project. This standard test method describes burst testing of flexible package seals using internal air pressurization within restraining plates. A burst test (pressurized polytray) was developed to simulate the testing performed at the manufacturing facilities. The burst test was used to compare results and correlate data with peel tests for the seal strength of the polytrays. A burst test system had to be built that would constantly monitor the air flow through the polytray versus increasing air pressure within the polytray. The first system was built as a calibration check for future PC integrated systems. The initial system set up was developed to check for the minimal

air flow or leak that could be detected. Once this initial leak detection was completed, the development of a more accurate system was pursued. A PC integrated system that could monitor and record air flow and pressure digitally every second was the ultimate goal and challenge.

The first system assembled consisted of a regulator, flow meter, a pressure gauge close to the package, a release valve, and the polytray chamber. Figure 3.3 shows the regulator and air flow meters run in series to the package chamber. Figure 3.4 is a picture of the burst chamber designed to hold the package in place while pressurization is taking place. Designs for the burst chamber were completed using the Solidworks® software and can be seen in Appendix C. Air was transferred into the polytray using 0.25 inch Tygon® rubber tubing. A 0.75 inch hole was drilled into the side of each polytray before testing. The polytray was then placed into the burst chamber. Once the polytray was in the burst chamber, the rubber tubing was inserted into the hole in the side of the polytray and was sealed air tight with a rubber stopper. Once the hole was sealed, the burst test was initiated.

The polytrays produced at Stegner Food Company on June 3, 2003 were used for the first round of the burst test experiment. Sound packages were run for calibration of the air flow system to the package and to check for leaks. Five packages of each artificial channel defect – 50.8, 127, 254, and 381 micron were tested. Five packages that had "short seals" were also tested (50 – 80% good seal in a certain area). Pressure versus flow was monitored and plotted as applicable. Only two polytrays with the 50.8 micron channel defects were tested. It was extremely difficult to remove the 50.8 micron wires from the seal without breaking even with the dry lubricant PTFE spray. Several polytrays were lost in the attempt to remove the wire (wires are still in the seal). Burst tests were continued using polytrays from production Trial 2 at Stegner Food Company. Three of each of the following was pressurized until failure: sound samples, samples with 6.5% starch solution entrapped, samples with soybean oil entrapped and samples with blanched noodles entrapped. Pressure versus flow was monitored, plotted, and analyzed.

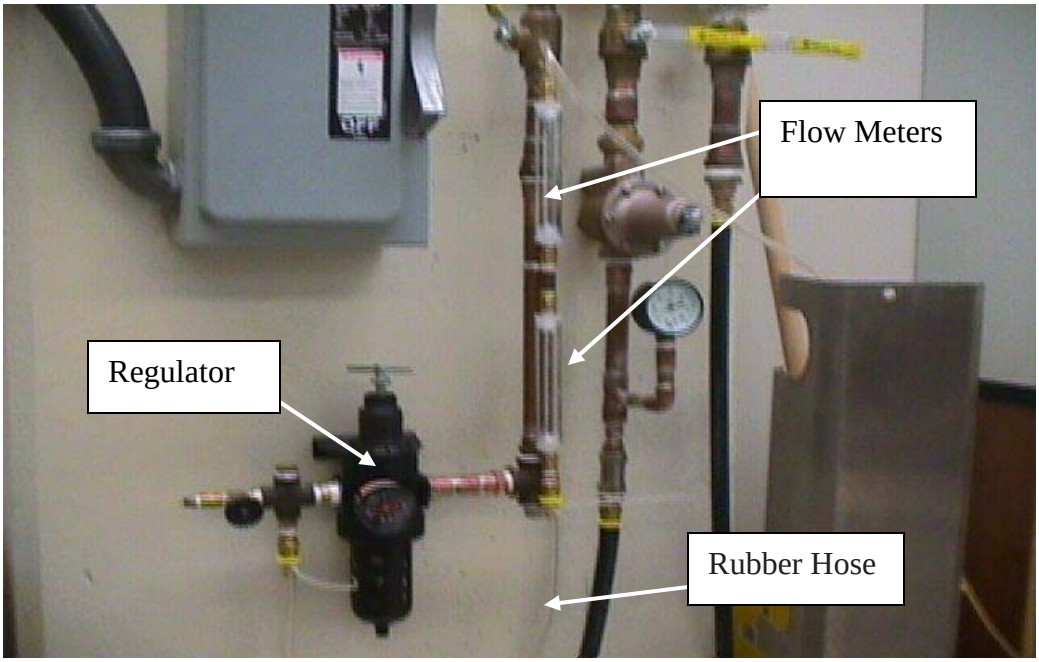

Figure 3.3: Picture of the air flow system for the burst tester consisting of a regulator and two flow meters in series.

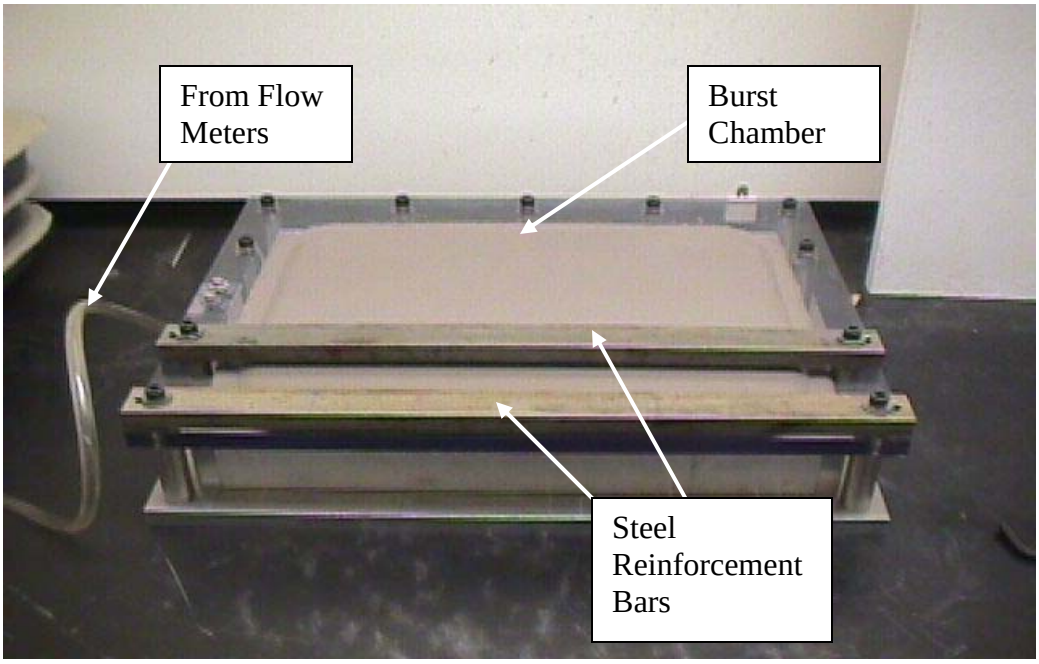

Figure 3.4: Picture of the burst chamber designed in Solidworks® used for the burst testing.

The first burst tester was replaced by the PC integrated system after the polytrays from Trial 2 were tested. The PC integrated system uses the Labview® 7.0 software in conjunction with the National Instruments® hardware. Sample polytrays were run with this system in which air flow and pressure was monitored and recorded every second. The drafted system schematic can be seen below in Figure 3.5. The maximum measurable air flow was 20 mL/min with an accuracy of 0.2 mL/min. As the polytray was pressurized and reached the set value, the air flow fell to 0.0 mL/min when there is no leak in the polytray.

The media filled samples from Sopakco, with various defects were tested and used for process checkout with the PC integrated system. Polytrays were tested until failure and data was recorded and saved through the Labview® 7.0 software. The initial pressure was set to 5 psi and a step program increased the internal pressure 5 psi every five minutes. This allowed ample time for the polytray to pressurize while allowing the flow rate to return to 0 mL/min if a leak did not develop. The pressure continued to rise until the polytray failed.

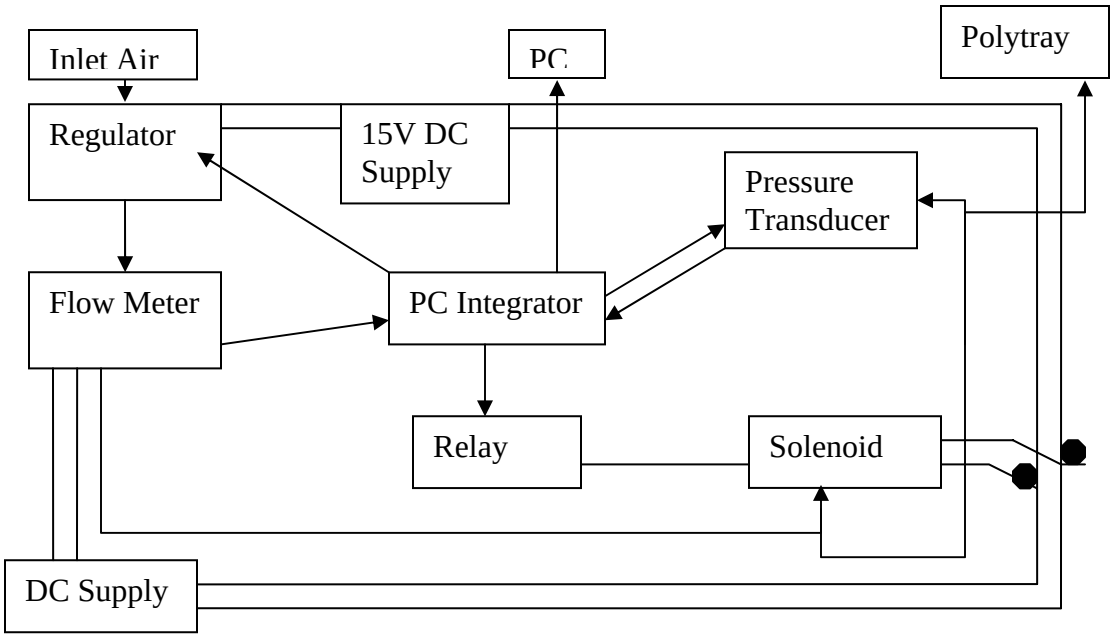

Figure 3.5: Schematic of PC integrated system for burst data analysis.

3.3 FEMLAB® (Finite Element Method):

Finite element method can model a computer generated 3D solid object such as the military polytray and subject that object to real life stresses and pressures through elemental linear integrations using an iterative solver. Simulation of pressurization on a polymer polytray, such as the polytray, or simulation of applied forces can be done in FEMLAB®. Simulations show the actual stresses and strains that are placed on any point within the object. Figure 3.6 shows a quartered polytray and the loading geometry for the corner forces applied to the quartered package. 3D modeling was done with the SolidWorks® program (see Appendix C) and was imported into the FEMLAB® software. Pressurized simulations were run at $2.0x10^4$, $5.0x10^4$, $1.0x10^5$, $1.5x10^5$, and $2.0x10^5$ Pa or 2.9, 7.25, 14.5, 21.8, and 29 psi. Corner forces were also simulated on the polytray at 50, 100, 150, and 200 N loads. Modulus values calculated from the tensile testing of the lid stock and tray were used as the input values for the simulations; $2.02x10^5$ psi and 2.66 $x10^5$ psi respectively. In order to reduce the simulation times, symmetry conditions were used; only one quarter of the polytray was used for the simulation.

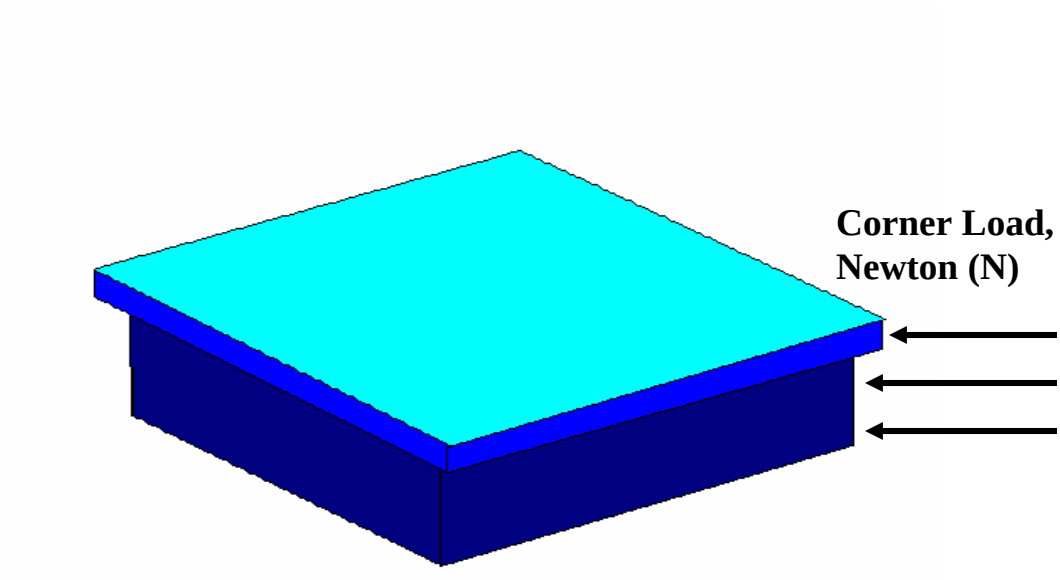

Figure 3.6: Quartered package showing the loading geometry for the corner loading.

The following settings were used to successfully model the pressurization and corner force loadings on the polytray in FEMLAB® software:

Meshing:

- Number of degrees of freedom: 86526
- Number of nodes: 4801
- Number of edge elements: 509
- Number of boundary elements: 14805
- Mesh edge size: 4.5
- Mesh growth rate: 2
- Mesh curvature factor:1
- Mesh curvature cut-off: 0.05

Elements:

- Lagrange – Quadratic

Solver:

- Stationary linear
- Solver options: Iterative solver
- Direct linear solver: Matlab®
- Linear Solver: Good Broyden
- Preconditioner: Geometric multigrid with Gauss-Siedel smoother

3.4 Ultrasonic C-scan:

Ultrasonic techniques provide an economic means of reducing the incidence of defective packages reaching consumers. There is absolutely no change in the object under test, thereby waste is not an issue. Ultrasonic inspection has two techniques that can be utilized, pulse-echo and through-transmission technique. In the pulse – echo technique, the pulse is sent from the transducer and, when it hits an object, a signal is bounced (echoed) back to the transducer in a certain time. The time is transformed into a signal that is recorded by the transducer and variations in the intensity of the signal are shown on the screen in waveform (see Figure 3.7).

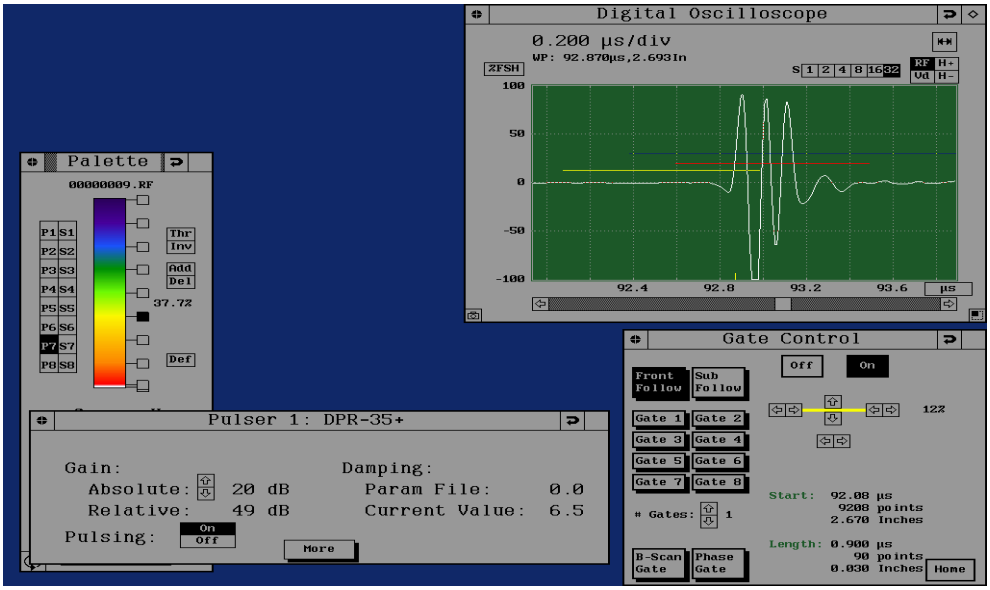

Figure 3.7: SONIX® software showing the waveform generated by the pulse-echo.

The SONIX® FlexSCAN-C 4.3 System was used for the C-scans of the defective polytrays. A 0.5 inch transducer having a frequency of 10 MHz and a focal length of 3 inches was used for the pulse-echo C-scans in this experiment. Important parameters in adjusting the c-scan include: gate locations, time of flight, and peak amplitude. Packages with artificial defects made from the Stegner Food Products polytray production Trial 1 were used for scanning as well as the “short seal” defective packages described earlier in the Sections 3.2.1 and 3.2.4. Polytrays were sealed specifically for ultrasonic scanning which contained all four channel defects on one side of the package. Before the polytrays were placed in the water medium, the wires were drawn out of seal creating the channel defects to be examined.

Polytrays were then completely submerged into the water medium and centered in the middle of the tank. The 10 MHz transducer was then used with varying gain and damping settings. Settings were adjusted accordingly to optimize resolution of the package as the transducer scanned and produced the reflective image. Gate locations were set for the area of good seal before the scans were initiated.

3.5 Fourier Transform Infrared (FTIR)/Attenuated Total Reflection (ATR):

Infrared spectrometry was utilized to examine the seals of burst polytrays. This technology can be used to examine surfaces and show what material is present on failure surfaces. An absorption spectrum is obtained by placing the material in between the spectrometer and an energy source which provides an electromagnetic radiation in the frequency range being studied [32]. Each chemical compound has a specific absorption spectra and respective intensity of absorption within the spectrum. The material exposed can be identified to a specific surface the lid stock.

Samples of the lid stock were cut from all burst polytrays surrounding specific defects. One to two inch sections surrounding the burst seal (defect area) were examined. The objective of using the ATR is to take the scans and correlate specific defects with a specific delamination of the lid stock. Because the samples are not transparent, attenuated total reflection (ATR) was used on the samples. The internal reflection element used is a Germanium crystal. The equipment utilized was the Bio-Rad FTS 6000e spectrometer in conjunction with the WinIR Pro 3.0 software. One hundred scans to co-ad were used for each sample tested with an angle of incidence of the infrared radiation being 45°. No change in incident angle was used in this experiment.

Chapter 4: Results and Discussion

4.1 Overview:

To ultimately develop an optimized test for the seal quality of the polytrays, some common tests were examined, both destructive and non-destructive. Destructive tests such as peel testing, tensile testing and burst testing were performed to gain a perspective as to the true strength of the seal area. The strength of a good sealing area was found and was used to compare strength values of seals with defects. Finite element analysis, using programs such as FEMLAB®, was used to simulate the actual stresses generated by these destructive tests.

Defective seals were then tested and compared to the values of the seals deemed good. Defects were then qualitatively and quantitatively classified and used as a basis for the rejection of polytrays with naturally occurring defects. Although these destructive tests are effective in the determination of seal quality, 100% of packages can not be inspected by these methods. These tests only give us a visual basis for which a package can be rejected. Two microbial challenge experiments were conducted on the polytrays produced at Stegner Food Products. The trays were produced with artificial channel defects of varying diameters. This destructive experiment provided a basis for what size channel defect would allow bacteria to infect the food in the polytray. It is these channel defects that must be discarded if present on the production line.

An effective non-destructive method, such as ultrasonic scanning could provide an economic means of reducing the incidence of defective packages reaching the consumer. Ultrasonic techniques do not result in permanent change in medium. Used either in pulse-echo technique or in transmission technique, it maintains the integrity of the food package and does not alter the mechanical properties of the package. This method is a means by which 100% of the packaging can be examined. The feasibility of this type of testing will also be discussed. Infrared spectroscopy was used to examine failed seal areas. This non-destructive post-burst test displays what material is present on

the failed surface. This technique was used to correlate various defects with their failure surfaces. The lid-stock is a quad-layered film, and the object was to determine whether or not a specific defect caused failure on any particular layer of the quad-layered film.

4.2 Destructive Testing:
4.2.1 Peel Testing:
4.2.1a Wornick Polytrays:

Peel testing was performed using the procedure explained in Section 3.2.1. Figures 4.1 and 4.2 show example plots of a peel test of polytrays sent from Wornick Food Company in Cincinnati, OH. Forty samples cut from five polytrays with no visual defects were used as the testing population. Two tests were conducted containing twenty samples each. The plots display the maximum and minimum peak loads for each test set. There is a wide variation in peak load within the sample set and the resulting standard deviation is high. The maximum peak and minimum peak peel for the forty sample population was 43.83 lb_f/in and 18.27 lb_f/in respectively. As stated before, no visual defects were present, but the wide variation in peak peel, 7.67 lb_f/in standard deviation, suggested some uneven thermal sealing of the polytray.

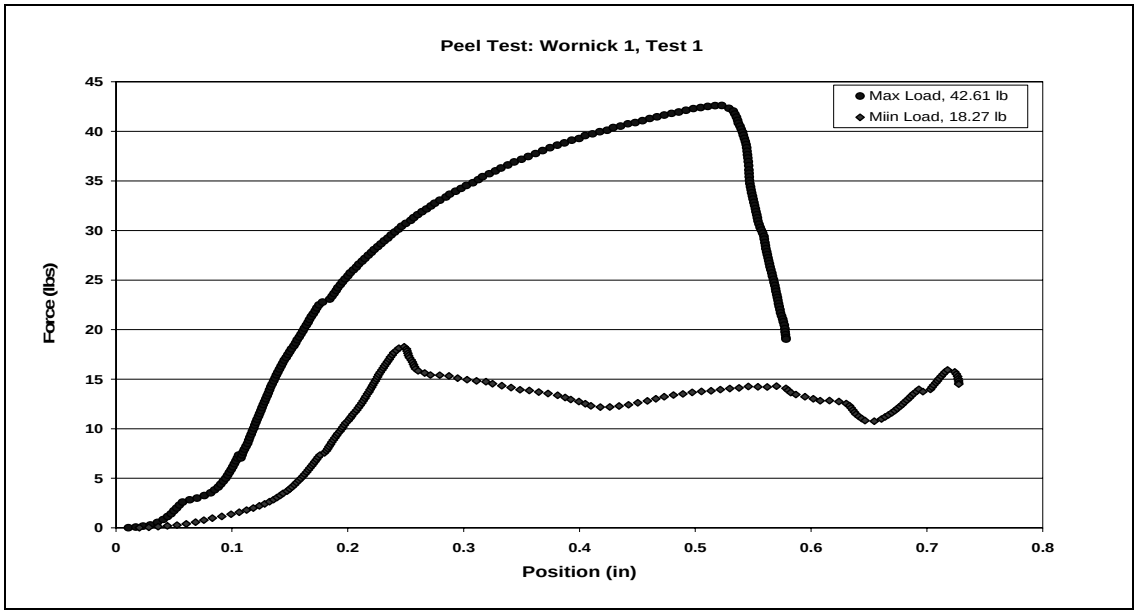

Figure 4.1: Plot of peel test data for Wornick 1 polytrays, Test 1; seals in good condition.

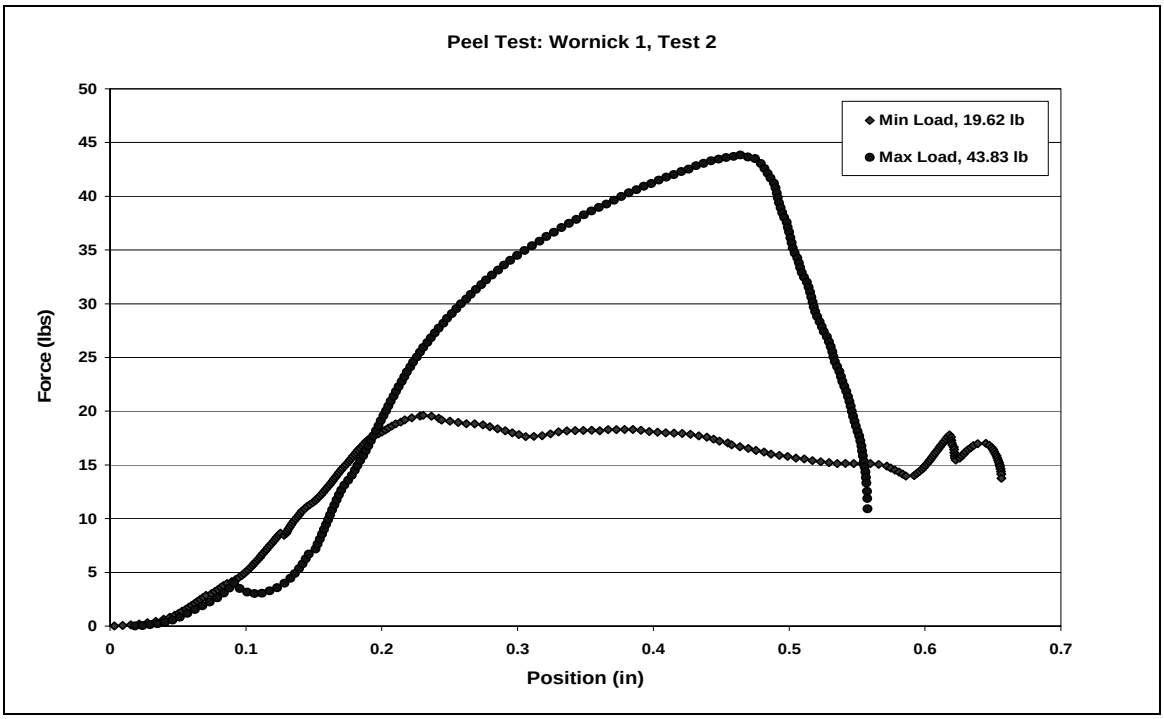

Figure 4.2: Plot of peel test data for Wornick 1 polytrays, Test 2; seals in good condition.

4.2.1b Sopakco Polytrays:

Peel tests were conducted on polytrays sent from Sopakco Food Products in Cincinnati, OH as well. A forty polytray population was repeated for these tests. These polytrays also had no visual defects in the sealing area. Two tests were conducted containing twenty samples each. Although the variation in peak load within these sample sets is smaller than that of the Wornick polytrays, the overall maximum peak peel is 12 – 15 lb_f/in lower than that of the Wornick polytrays. The maximum peak and minimum peak peel for the forty sample population was 30.35 lb_f/in and 17.42 lb_f/in respectively. Again, no visual defects were present in the Sopakco polytrays, but the variation in peak peel, 3.34 lb_f/in standard deviation, suggests some uneven thermal sealing of the polytray. The burst test was used to clarify this variation in peak peel. The burst test data discussed later was used to correlate these peel tests.

4.2.1c Rutgers Polytrays:

A set of defective polytrays tested was sent from the Center for Advanced Food Technology at Rutgers University in New Jersey. These polytrays had many visual defects; mainly short seal defects due to deformed (high variance) flanges on the polymer tray itself. These defects were described earlier in the as received polytrays in Section 3.1.3. As lid stock (quad-layered film) was heat-sealed to the tray, the resulting seal contained many areas that were not bonded and thus "short seals" were created. Again, some areas of the lid-stock did not bond at all with the tray. Voids, or large channel defects, were created within the seal and the peel tests verify that fact with low peak load.

The samples were cut from several of the polytrays at random. No specific defect was cut to be tested, but rather a good representation of the defects on the polytrays was obtained. Samples were tested with areas of the seal within the sample ranging from 0% to ~90% good seal. A total of ten "short seal" samples were used for the sample sets. The maximum and minimum peak peels were 24.01 lb_f/in and 8.42 lb_f/in respectively. The average peak load was obviously lower than that of Wornick and Sopakco polytrays. Again, a large standard deviation of peak peels was obtained, 4.48 lb_f/in, but it can be justified here by the presence of the visual defects. The peak peels measured can not be correlated with the percent good seal because the percent good seal value was not recorded specifically for each sample tested.

Rutgers polytray samples that appeared visually intact (100% good seal) were also tested in two subsets. A total of seventeen samples were tested, eight in the first test and nine in the second test. The maximum and minimum peak peels were plotted for each test and are 31.21 lb_f/in and 20.54 lb_f/in respectively for that population. There is still variation of peak peel, but this particular set of polytrays has one of the lowest standard deviations of all the populations, 3.38 lb_f/in. This is most likely due to the fact that these samples were not picked at random. The seals that were most visually sound were selected and cut from the polytrays.

4.2.1d Stegner Polytrays:

The last set of peel tests involved polytrays with artificial defects such as entrapped matter made at Stegner Food Company Trial 2. Surprisingly, the entrapped oil and starch samples performed just as well or better than the control (defect free) samples produced. The entrapped noodle samples, on the other hand, performed poorly compared to the control samples. There is a wide variation in all of the sample groups especially in the control samples. Again, this variation in the control samples may be due to uneven sealing or processing conditions on the particular production day, even though visual inspection showed no difference in seal appearance before the samples were tested. SEM or optical microscopy was not used in this project. These particular polytrays with entrapped matter were burst tested as well and the data was correlated to the peel test data obtained.

An analysis of the peel data for the Stegner Trial 2 polytrays can be seen in Table 4.1. The analysis for the entire peel testing group can be seen in Table 4.2. Figure 4.3 displays a bar chart for the data with corresponding error bars, showing (+/-) deviation from the average, comparing the different polytrays. Table 4.2 shows the maximum and minimum peak loads for each sample within its respective sample group as well as the standard deviation and mean value. It is here that the sample sets can be compared and analyzed.

Wornick polytrays obviously have the strongest seals with an average peak peel of 32.35 lb_f/in but at the same time have the highest standard deviation of all the polytray sets with a corresponding value of 7.67 lb_f/in. The Sopakco polytrays and good samples (100% good seal) from the Rutgers polytrays seem to have the best standard deviation of all coming very close in value at 3.34 lb_f/in and 3.38 lb_f/in respectively. The entrapped noodle samples proved to be the worst performing of all peel test sets with an average peak value of 15.31 lb_f/in and the lowest recorded peak force value at 7.17 lb_f/in.

Table 4.1: Analysis of Stegner Trial 2 polytray peel test data.

	Max Peel (lb_f/in)			
Sample	**Entrapped Oil**	**Entrapped Starch**	**Entrapped Noodle**	**Sound Samples**
1	27.83	30.81	23.54	13.02
2	27.54	17.35	18.65	19.76
3	22.44	28.69	12.69	24.11
4	27.87	19.6	21.17	11.98
5	29.44	32.49	11.38	16.74
6	23.91	17.2	7.17	20.78
7	28.64	22.49	11.48	16.76
8	22.33	21.25	11.37	14.71
9	18.01	30.28	23.39	27.82
10	23.95	18.3	12.24	15.68
11				13.45
12				23.77
13				27.12
14				16.13
15				13.36
16				25.68
17				23.1
18				22.36
19				21.36
20				22.81
STDEV	**3.653**	**6.072**	**5.838**	**5.021**
Mean	**25.196**	**23.846**	**15.308**	**19.525**

Entrapped Oil Samples

Max (lb_f/in)	**Min (lb_f/in)**
29.44	18.01

Entrapped Noodle Samples

Max (lb_f/in)	**Min (lb_f/in)**
23.54	7.17

Entrapped Starch Samples

Max (lb_f/in)	**Min (lb_f/in)**
32.49	17.2

Sound Samples

Max (lb_f/in)	**Min (lb_f/in)**
27.83	11.98

Table 4.2: Analysis of all peel test data showing maximum, minimum, and average peak peels and standard deviation.

			Population	
Peel Samples	**Maximum Peak Peel (lbf/in)**	**Minimum Peak Peel (lbf/in)**	**Average Peak Peel (lbf/in)**	**Std Dev (lbf/in)**
Sopakco 1 - Good Samples	30.25	17.41	23.77	3.35
Wornick 1 - Good Samples	43.83	18.27	32.36	7.68
Rutgers Polytrays - Good Samples	31.21	20.53	25.49	3.38
Rutgers Polytrays - Short Seals	24.01	8.42	18.86	4.49
Stegner Trial 2 – Sound Samples	27.83	11.72	19.53	5.02
Stegner Trial 2 - Entrapped Oil	29.44	18.01	25.20	3.65
Stegner Trial 2 - Entrapped Starch	32.49	17.35	23.856	6.07
Stegner Trial 2 - Entrapped Noodle	23.54	7.17	15.31	5.84

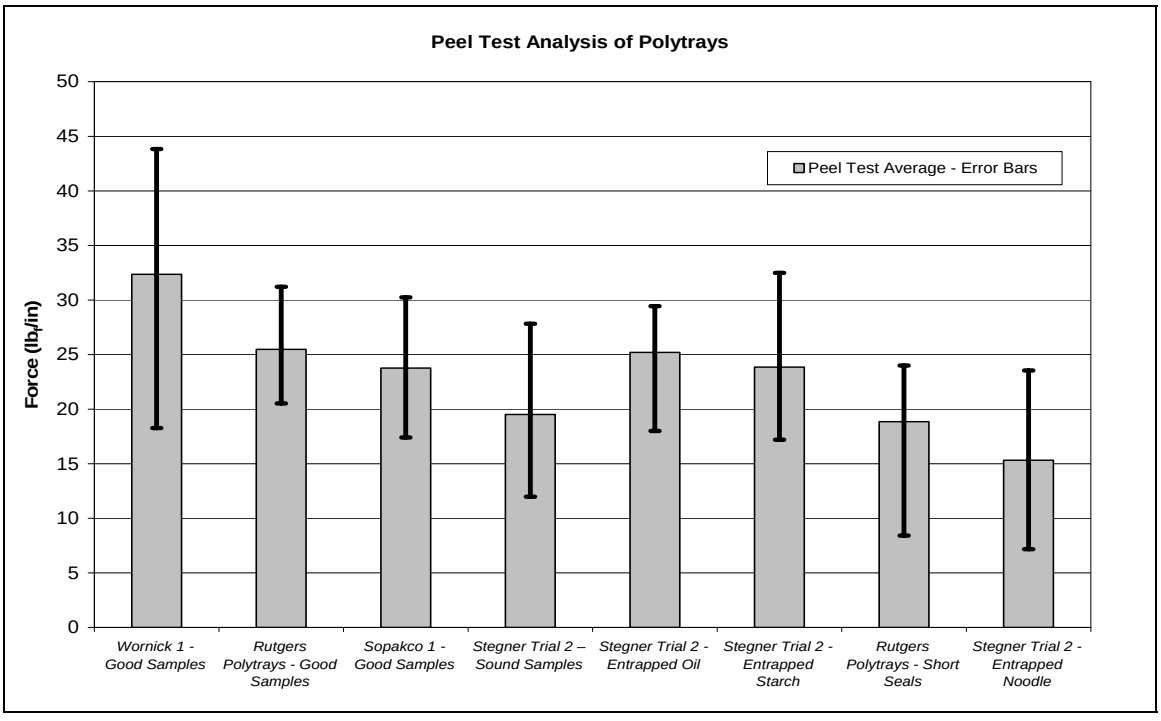

Figure 4.3: Bar graph of peel test data for all polytrays showing average peak load and corresponding error bars.

4.2.2 Tensile Testing:

To better understand the mechanical properties of the polytrays, tensile tests were performed on both the lid stock and the tray. Stress versus strain plots were generated and modulus values were calculated from this data. The material properties such as the elastic modulus, E, were gathered from the tensile plots and were eventually used in conjunction with finite element analysis of these polytrays. The film tensile specimens were run with the same equipment (Instron® Tensile tester) used for the peel testing and the tray specimens were run on the Phoenix® Tensile tester.

Figure 4.4 shows stress versus strain plots for the film (lid-stock) tensile test. These film samples were taken from the same Sopakco 1 polytrays used for the peel tests. A total of twenty film samples were tested; two sample sets with ten samples each. The average elastic modulus value of 1.4 $x10^9$ Pa will be used for the material properties input of finite element analysis. Figure 4.5 is a plot of the stress versus strain for five polytray specimens. An average modulus value of 1.8 x 10^9 Pa will be used in conjunction with the finite element analysis for the tray. Table 4.3 displays the statistics for the polytray tensile specimens and the lid-stock specimens. The elastic modulus, E, was calculated using the following equation:

$$E = \sigma/\varepsilon \tag{9}$$

where stress, σ, in divided by the strain, ε.

Strain values of 0.04 and 0.01 in/in were used for the calculation of the elastic modulus for the lid-stock and tray specimens respectively. These values were chosen as the maximum strain within the elastic region of the plot. Corresponding values of stress were then used to ultimately calculate the elastic modulus, E. The values were examined and reported as an average to be used in the finite element analysis.

Figure 4.4: Plot of stress versus strain for lid-stock specimens from Sopakco 1 polytrays, Test 1.

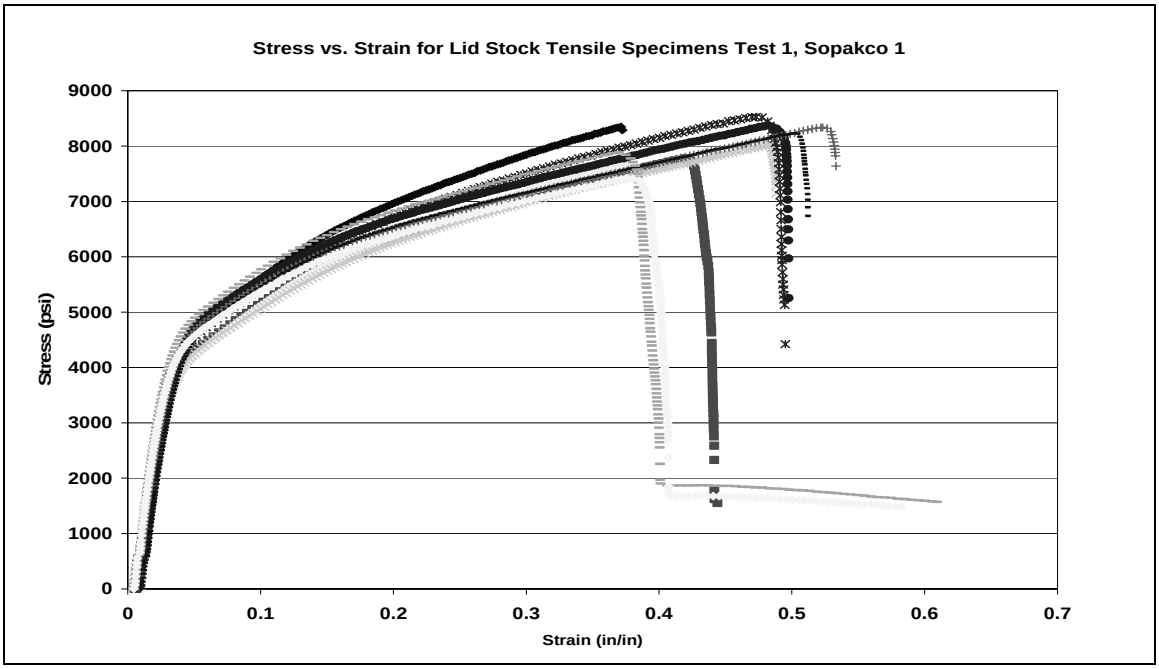

Figure 4.5: Plot of stress versus strain for tray specimens from Sopakco 1 polytrays.

Table 4.3: Tensile analysis of lid-stock and tray samples from Sopakco 1 polytrays.

Lid-stock	Tray	Lid-stock	Tray
Average Modulus (Pa) 1.39E9	Average Modulus (Pa) 1.84E9	Average Modulus (psi) 2.02E5	Average Modulus (psi) 2.67E5
Max Modulus,E (Pa) 1.51E9	Max Modulus,E (Pa) 1.95E9	Max Modulus,E (psi) 2.19E5	Max Modulus,E (psi) 2.83E5
Min Modulus, E (Pa) 1.29E9	Min Modulus, E (Pa) 1.70E9	Min Modulus, E (psi) 1.87E5	Min Modulus, E (psi) 2.47E5
STDEV (Pa) 6.39E8	STDEV (Pa) 1.05E8	STDEV (psi) 9.27E4	STDEV (psi) 1.53E4

4.2.3 Microbial Challenge:

4.2.3a Challenge #1:

Two microbial challenge experiments were carried out to see if artificial defects such as channel defects would affect the seal integrity of the polytray when exposed to bacteria. Polytrays, described in Sections 3.1.1 from Stegner Trial 1 production were used for this experiment. The detailed results of the first microbial challenge that was carried out at the Food Science & Technology department at the University of Tennessee, Knoxville can be seen in Appendix B. A (+) sign indicates gas formation from the growth of bacteria within the polytray. As gas forms within the polytray, the package gets pressurized. Pressurized packages from gas formation can be seen in Figure 4.6.

As mentioned previously, a total of seventy-five polytrays with artificial channel defects having diameters ranging from 50.8 to 381 μm were produced along with five control (no defect) samples for Stegner Trial 1. The wires were pulled from the seals and then the polytrays were dipped in the microorganism Figure 4.7 is a bar chart that displays the total number of polytrays that failed, or showed CO_2 gas production (bacteria

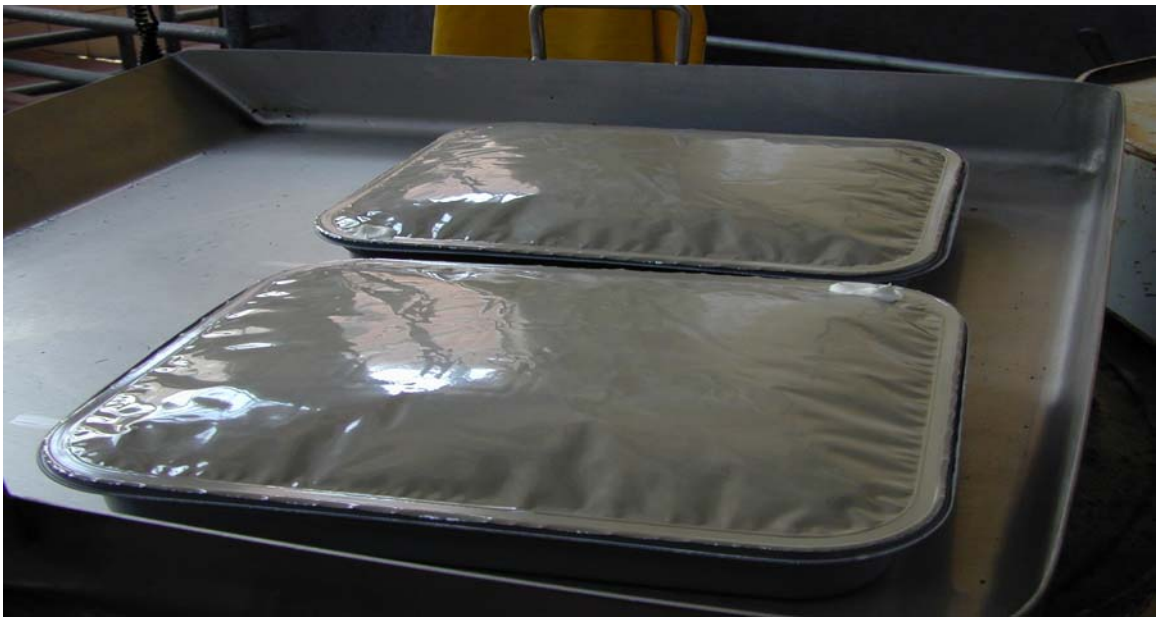

Figure 4.6: Photograph of pressurized polytray due to gas formation from bacteria growth.

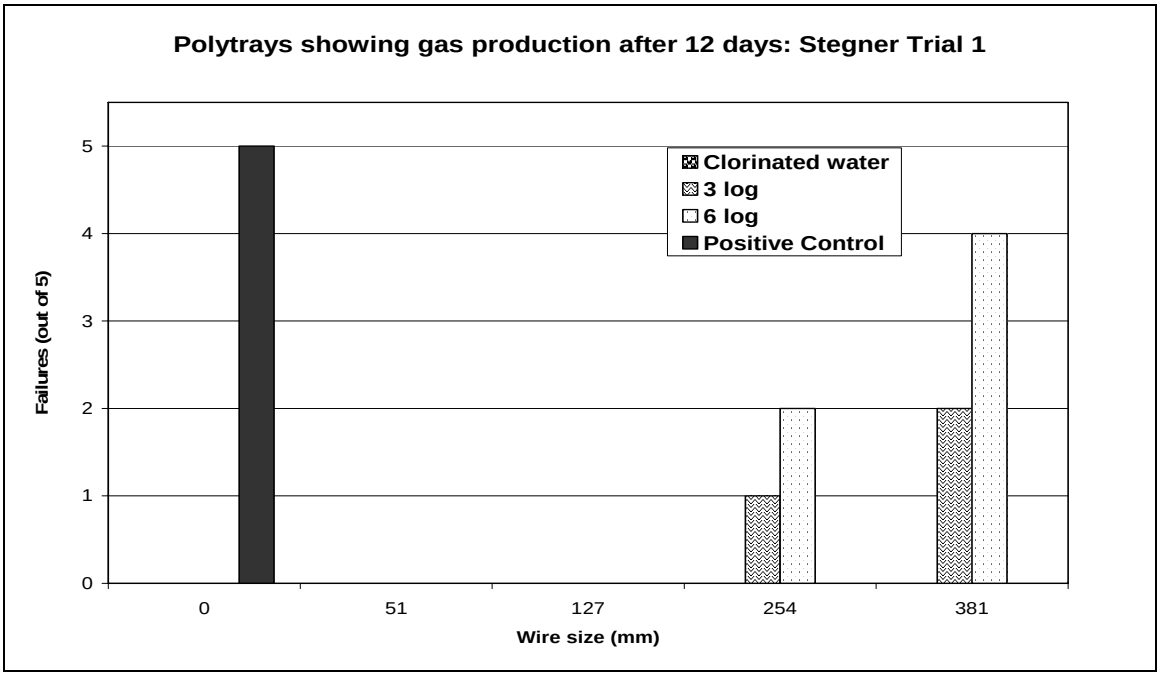

Figure 4.7: Microbial challenge results for polytrays produced in Stegner Trial 1.

growth), after 12 days of incubation. *Enterobacter aero gene*. Concentrations of the contaminated water (see Appendix B) are given as 3 log CFU/mL and 6 log CFU/mL; 10^3 and 10^6 microorganisms per 1 mL of water. Polytrays were exposed for 2 min at 21-25°C. Six out of fifteen polytrays with the 381 micron channel defect were positive (+) for CO_2 gas production. Three out of fifteen polytrays with the 254 micron defect were positive (+) for gas production. All five inoculated polytrays (positive control) were positive (+) for gas production, where as none of the sound samples failed. Fifteen polytrays were also dipped into negative control, chlorinated water (10 ppm FAC), after which none of the polytrays produced gas while in incubation. The most valuable result from this challenge was that none of the trays with the 50.8 and 127 μm channel defects failed.

The challenge #1 results clearly give a basis for smallest channel defect that could be allowed to pass during inspection. The trays with channel defect less than or equal to 127 μm were obviously not as serious as the other channel defects. These same trays will be used in the burst test; the leak detection results of the channel defects will be correlated with the results from this microbial challenge

4.2.3b Challenge #2:

Polytrays, described in Sections 3.1.2 from Stegner Trial 2 production were used for this experiment. Again, the detailed results of this second microbial challenge carried out at the Food Science & Technology department at the University of Tennessee, Knoxville can be seen in Appendix B. The positive (+) sign again, indicates gas formation from the growth of bacteria within the polytray. The concentrations of the microorganism were kept constant from Trial 1. As stated previously, the time that the polytrays were exposed to the microorganism was increased to 15 minutes instead of 2 minutes at room temperature. Polytrays were stacked on their side in crates and placed in an incubator at an elevated temperature. Polytrays were examined daily for 12 days and bacteria growth was indicated as carbon dioxide (CO_2) gas formation was present.

An experimental mistake made results difficult to interpret. The polytrays were stacked on their sides in crates rather than on a flat surface. Liquid media leaked out of some of the polytrays and quite possibly contaminated other polytrays. Media and bacteria covered the trays and the incubator which made examination of the polytrays very difficult. Due to this mistake in experimental procedure, the results seen in Figure 4.8, shown as a bar graph, are considered invalid but do need to be considered with regards to experimental error. For this reason, a negative control is used in the experiment. Failure, or gas production, within the negative control polytrays (chlorinated water), makes these results invalid. Seven polytrays dipped in the 3 log CFU/mL water failed along with six polytrays that were dipped in the 6 log CFU/mL contaminated water. All five positive control samples produced CO_2 gas.

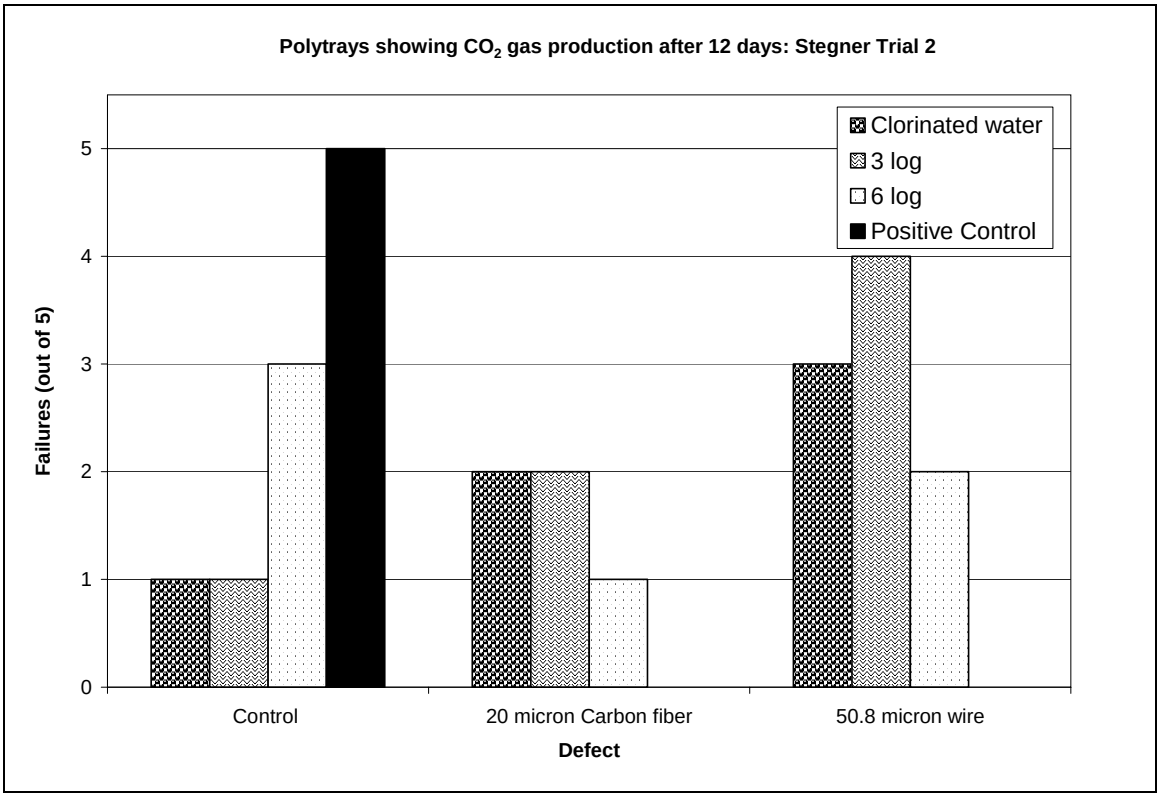

Figure 4.8: Microbial challenge results for polytrays produced in Stegner Trial 2.

4.2.4 Burst Test Development:

An initial system was constructed to monitor air flow through the polytray versus increasing pressure. As discussed in Section 3.2.4, this system consisted of a manual regulator, an analog flow meter, an analog pressure gauge close to the package, a release valve, and a polytray chamber. The flow meter ranged from 0.0 mL/min to 110 mL/min with glass ball inserted into the tube and 0.0 mL/min to 250 mL/min with the steel ball inserted into the tube. Interpolation of the inserted ball within the flow meter was easily done on the smaller leaks; less than 10 mL/min. As leaks were detected on the higher end of the scale, estimates of the ball placement within the flow meter were increasingly difficult.

Experiments were carried out and a basis for further experiments and development was established. Once the system was complete, three packages, without defects, were run with increasing pressure from 0 to 40 psi for the calibration. One package burst up to 40 psi, one package did not burst at 40 psi, and one package burst at 30 psi. Flow meter readouts for all three calibration experiments were from 0 to 0.5 mL/min which indicates that the system connections are sealed nicely. The small air flow present, 0.5 mL/min was probably due to the creep, or peel, of the seal under increasing pressure. Table 4.4 shows an example of a calibration polytray under increasing pressure.

The packages produced at Stegner Food Company Trial 1 were used extensively for the first round of burst testing. Several control polytrays were used for calibration of the new air flow system to the polytray. Five packages of each artificial channel defect created having diameters of 50.8, 127, 254, and 381 micron were tested. An additional five packages from the Rutgers polytrays, having short seal defects, were also tested. The Rutgers polytrays had short seal defects ranging from 50 to 80% good seal in a certain areas. The pressure versus flow was monitored and plotted as applicable. Only two polytrays containing the 50.8 micron channel defects were tested due to the extreme difficulty of removing the 50.8 micron wire from the seal without breaking.

Table 4.4: Air flow readout of the calibration polytray as pressure increases in the polytray from 0-40 psi.

Pressure (psi)	Flow (mL/min)
0	0.0
5	0.2
10	0.5
15	0.5
20	0.5
25	0.0
30	0.0
35	0.0
40	Burst

A total of four polytrays were lost in attempt to remove the wires. These polytrays were then used for non-destructive testing such as ultrasonic-inspection. Air flow versus pressure was monitored and plotted which can be seen in Figure 4.9. Air flow was detected going into the polytray with as little pressure as 5 psi. The sharp increase in air flow on the plot, around 20 psi, was most likely due to human error in estimation on the analog flow meter.

Figure 4.10 shows an example of a polytray with a 50.8 diameter micron channel defect that had burst at a pressure of 30 psi. The X's mark the area of failed seal after failure. It cannot be determined if the seal initially failed at or around the defect site based on data and observation, but this is a possibility.

Five polytrays with 127 micron diameter channel defects were tested from 0 to 30 psi. The flow versus pressure was monitored and then plotted as above. Every polytray burst at or around 30 psi. Because there is no digital readout for the pressure gage, the actual value at which the polytrays burst can not be determined with great accuracy. Only one of these polytrays did not fail in the seal area surrounding the channel defect.

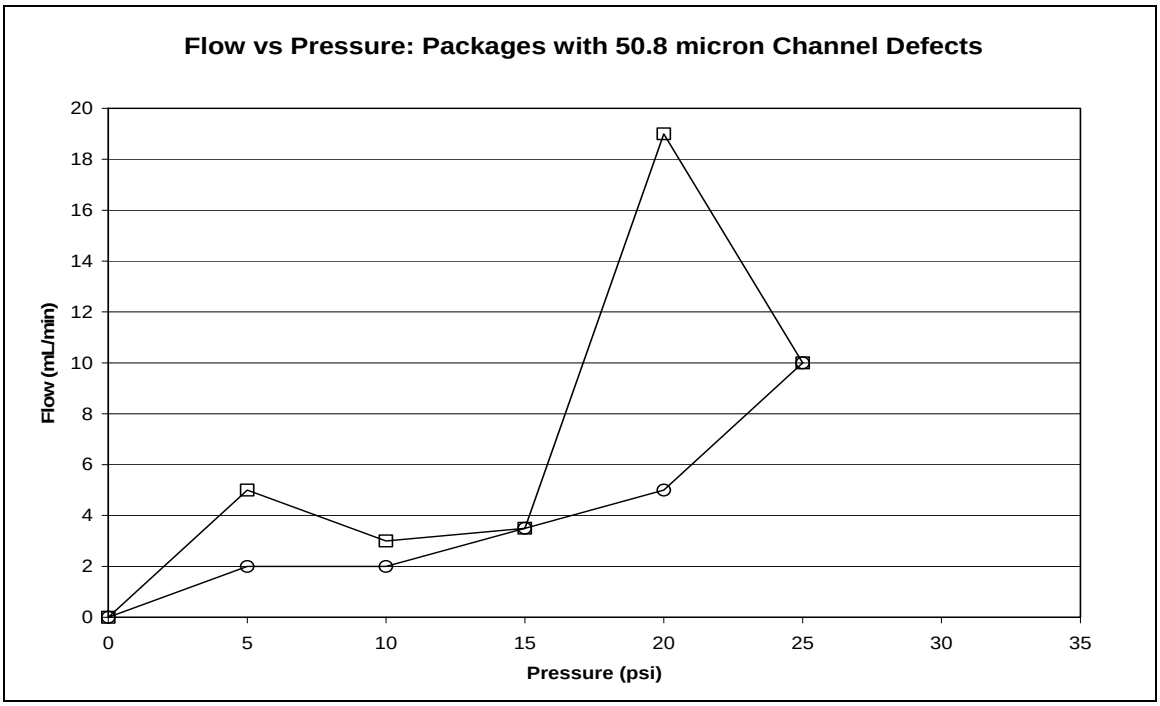

Figure 4.9: Plot of the air flow versus the increase in pressure for polytrays with 50.8 micron diameter channel defects.

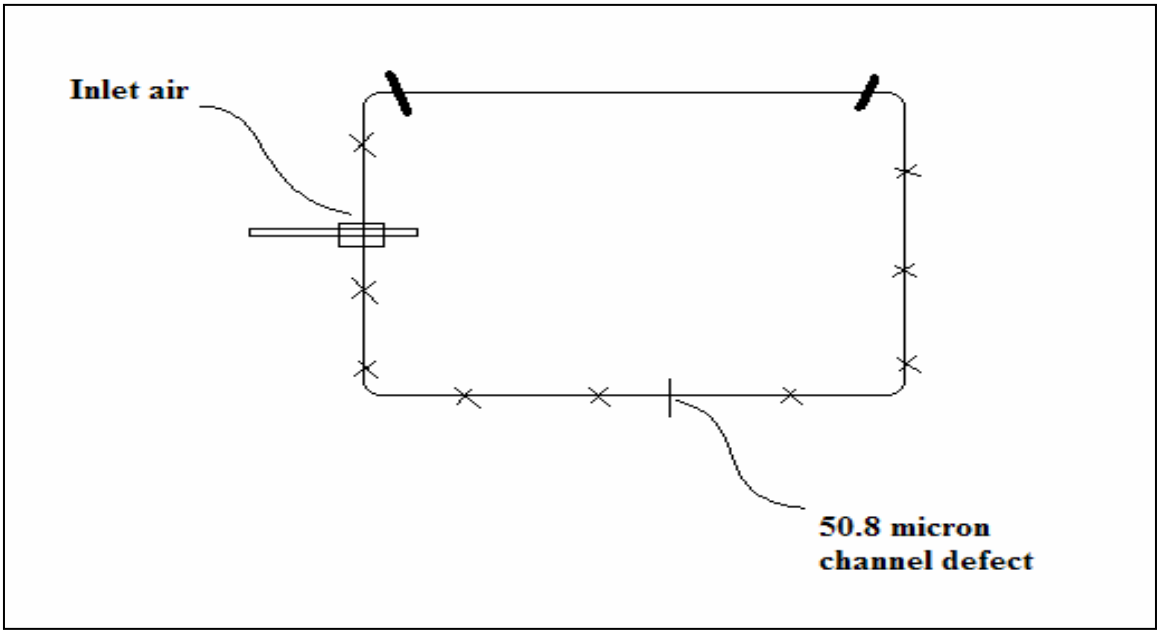

Figure 4.10: Example of the 50.8 micron channel defect package after failure.

Figure 4.11 is a plot of the air flow versus increasing air pressure for the 127 micron diameter channel defects. All 127 micron diameter channel defect polytrays tested had detectable leaks. A more linear pattern was seen in this experiment as compared to the polytrays with the 50.8 micron diameter channel defects. All five polytrays burst between 25 and 30 psi. Figure 4.12 is an example of a package with a 127 micron channel defect that failed due to the high pressure, but the seal area surrounding the defect did not fail. The X's mark the area of burst seal. The other four polytrays all burst around the defect site, but determining exactly where the failure initiated is unclear based on the data and observation.

Five polytrays were tested with the 254 micron diameter channel defects. Three of the polytrays burst at 35 psi. Two polytrays did not burst, but rather formed severe leaks in the area surrounding the sealing defect. Along with the severe leak, delamination, or peel of the seal, occurred at and around the area surrounding the channel defect. The minimum seal width required to protect the contents of the polytrays was not specified. Once these polytrays leaked so severely, the polytray could no longer maintain regulator pressure. Air flow with an internal pressure of 5 psi and greater was off the scale of the flow meter; the leak was too great. A plot of the pressure versus air flow could not be generated because data could not be collected from the flow meter. Figure 4.13 is an example of how the seal delaminated around the 254 micron diameter channel defect.

The same results were seen for the polytrays with 381 micron diameter channel defects. None of the polytrays burst due to the increasing pressure. The leaks became larger with increasing regulator pressure; 0 to 30 psi. The polytrays could not maintain regulator pressure because the flow was again too great through channel defect. Plots for air flow versus pressure could not be generated for these polytrays because the flow meter data was off the scale. Although air flow data could not be obtained, Table 4.5 shows data for the pressure of polytray with increasing regulator pressure. Notice the difference in the actual pressure of the polytray compared to the regulator pressure.

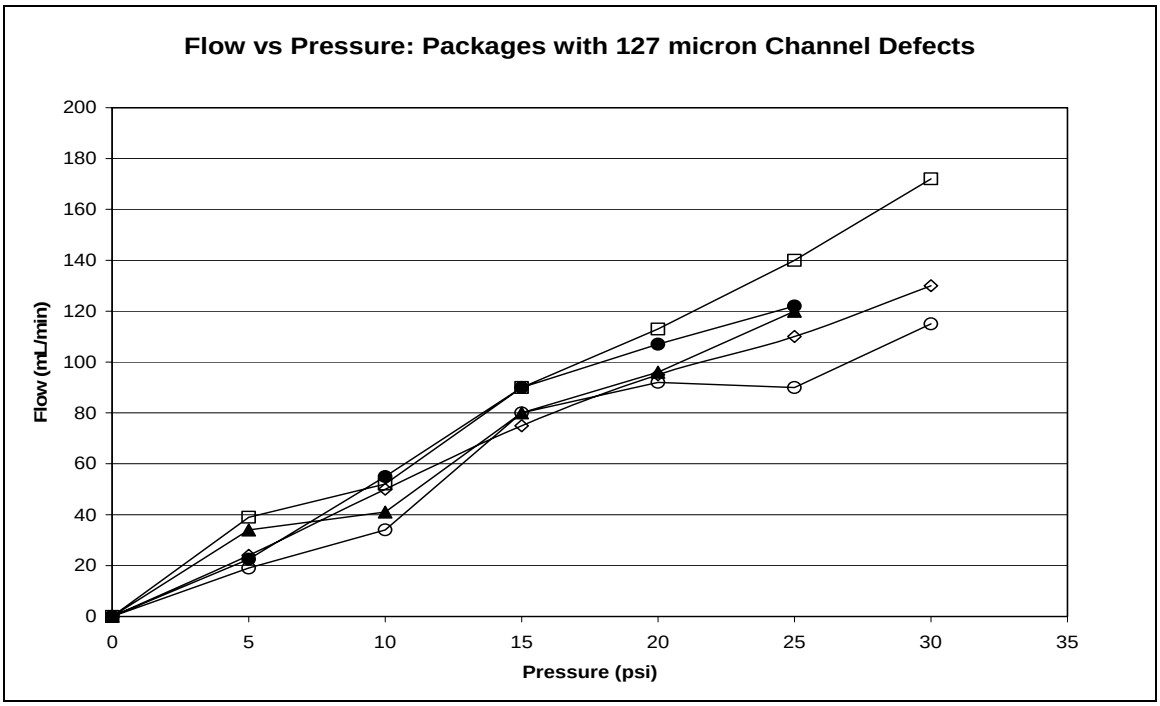

Figure 4.11: Plot of the air flow versus increasing air pressure within the 127 micron diameter channel defect polytrays.

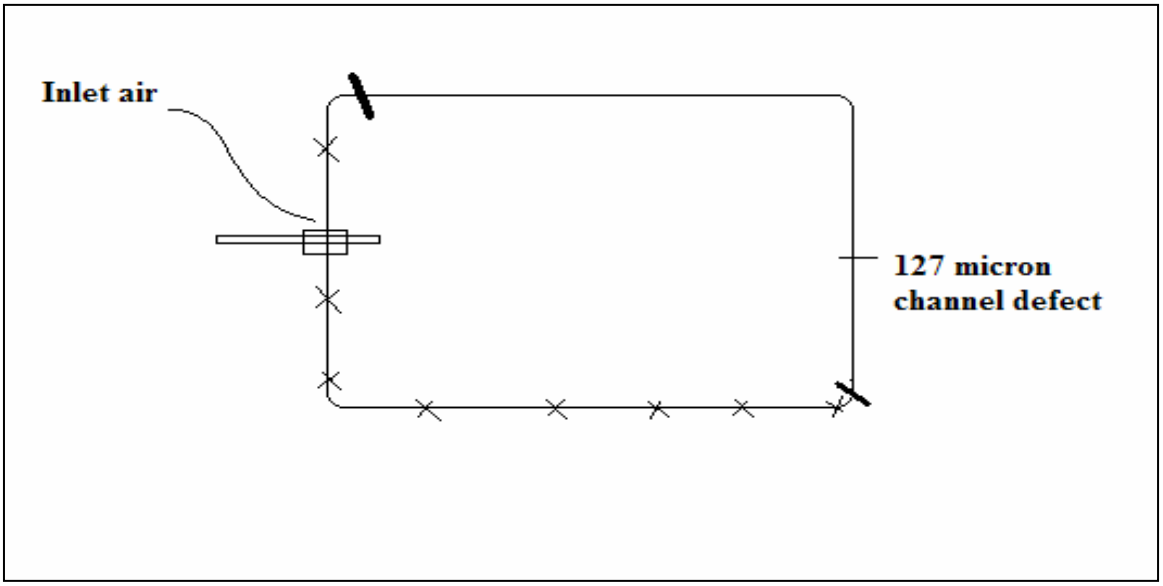

Figure 4.12: An example of a package with a 127 micron channel defect that failed but the seal area surrounding the defect did not fail.

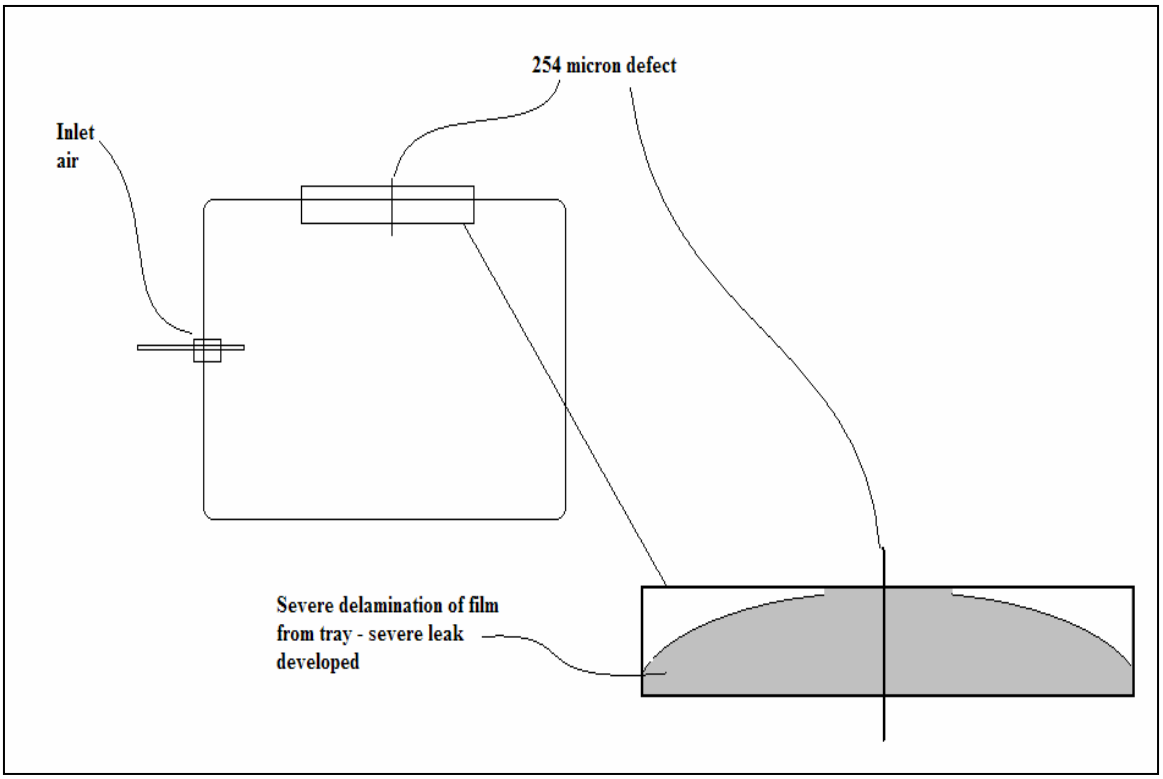

Figure 4.13: Example of polytray with a 254 micron diameter channel defect that did not burst, but formed severe delamination around the defect site.

Table 4.5: Data from the pressure gage on the package with increasing regulator pressure.

Regulator Pressure (psi)	Actual Pressure on Package (psi)
0	0
5	4
10	7
15	11
20	15
25	19
30	22

Air flow versus pressure for the polytrays with various short seal defects can be seen in Figure 4.14. The development of leaks could be seen in these samples. Five polytrays from the Rutgers group with short seal defects were also tested. Three of these polytrays burst at 30 psi; one polytray with an seal area having 60% good seal and two packages with seal areas having 50% good seal. One polytray having an area of the seal with 70% good seal did not burst but rather leaked severely around 30 psi at the defect site. The last polytray, containing another area with a 70% good seal defect maintained pressure to 40 psi and did not burst. These results demonstrate that visual inspection and interpretation of a defect is not always correct and this issue needs to be evaluated carefully. Burst tests were also conducted for polytrays made in Trial 2 at Stegner Food Company. Three of each of the following polytrays were pressurized until failure: sound samples, samples with entrapped 6.5% starch solution, samples with entrapped soybean oil and samples with entrapped blanched noodles. All polytrays failed at pressures less than 35 psi. The sound sample, entrapped oil, and entrapped starch (6.5%) all performed similarly. The entrapped noodle polytrays did perform as expected producing leaks and failing at lower pressure values than the other polytrays.

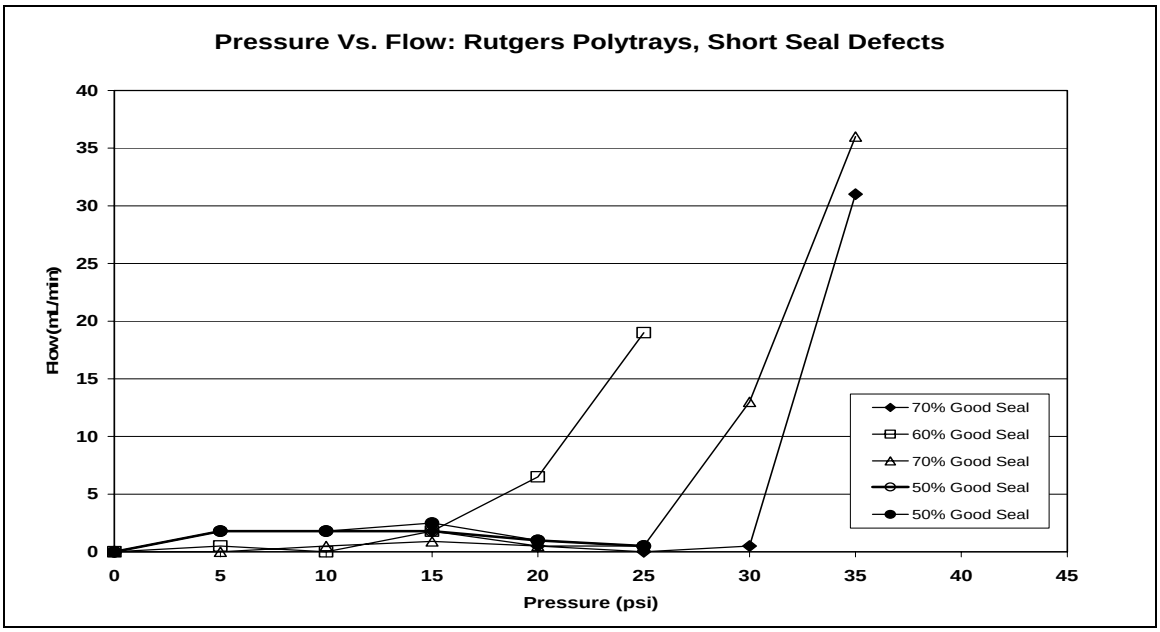

Figure 4.14: Plot of the pressure versus air flow for the packages with short seal defects.

The results from these burst tests, three polytrays for each defect, correlated very nicely with the peel results for the same polytrays seen previously. FTIR/ATR post failure examination was completed, but there no indication regarding the changes in composition of the seals. Figure 4.15 shows a bar graph of the data for the Stegner Trial 2 polytray burst tests. A comparison of the burst and peel tests data for these polytrays along with the Rutgers polytrays can be seen in Figure 4.16. Another plot was made to emphasize the fact that these peel and burst tests do correlate fairly well. A correlation plot given in Figure 4.17 displays peel (lb_f/in) versus burst strength (psi) for the various polytrays tested. The PC integrated system described in Section 3.2.4 was a result of the preliminary testing using an analog system. Based on these results, it was determined that a volumetric flow rate sensitivity of 0.2 mL/min was appropriate to detect leaks in these polytrays. The internal workings of this PC integrated system can be seen in the picture in Figure 4.18. This system will be used in future burst test experiments. The ultimate goal of designing a test and implementing it was achieved and is extremely useful in the examination of the seal integrity of the polytrays.

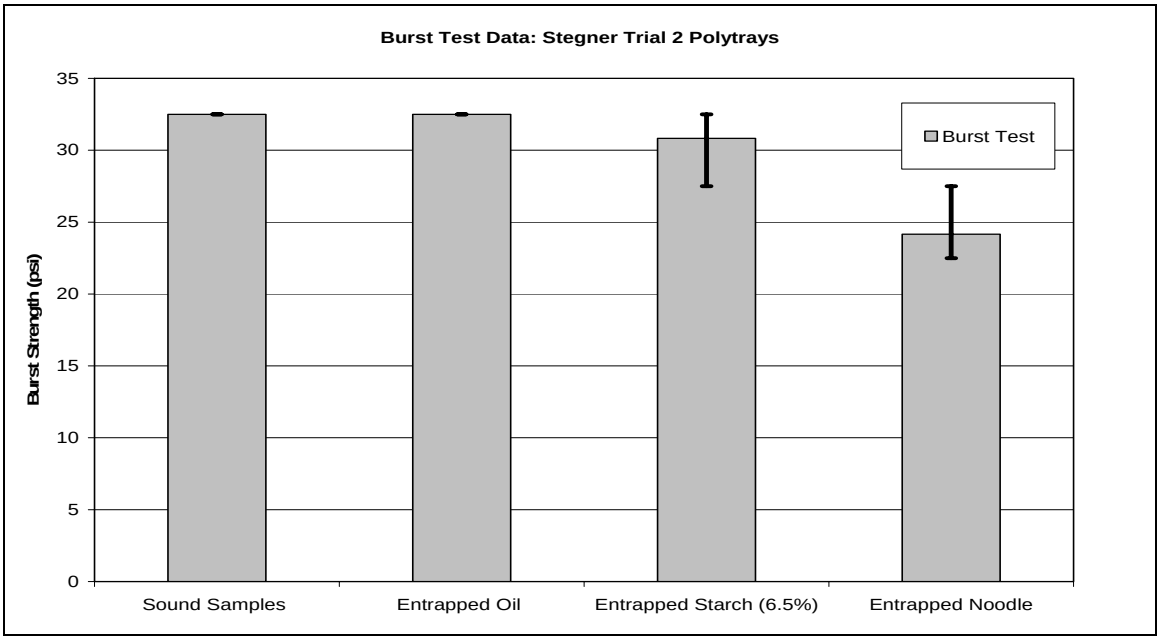

Figure 4.15: Burst test data for polytrays produced in Trial 2 at Stegner.

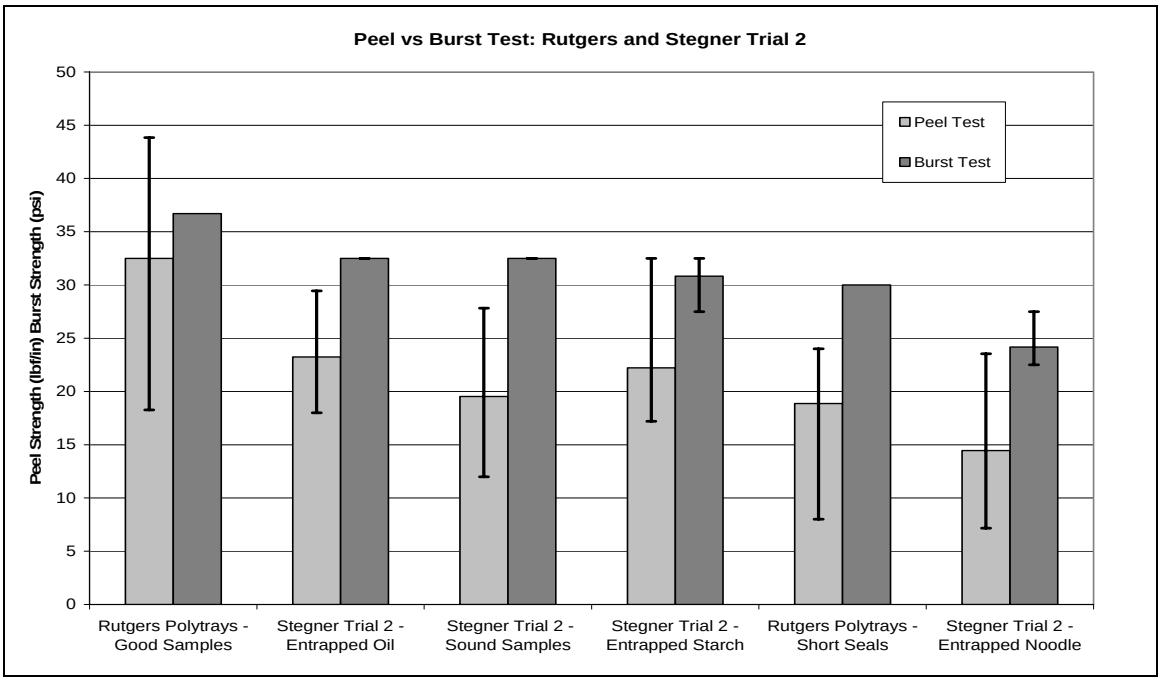

Figure 4.16: Comparison bar chart of burst test and peel test for Rutgers and Stegner Trial 2 polytrays.

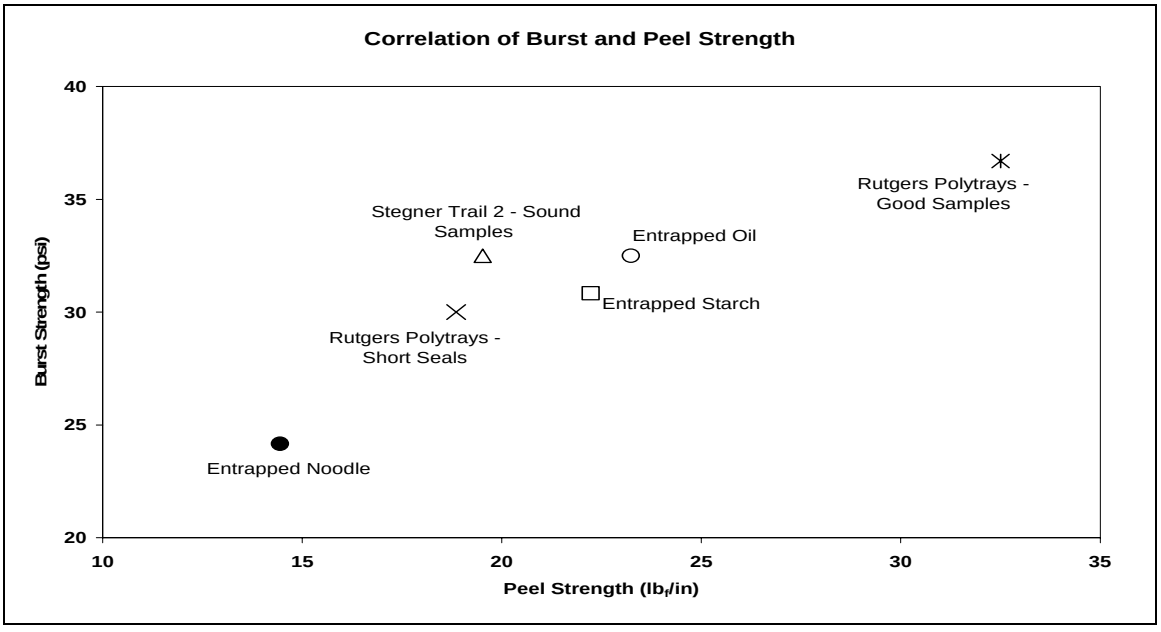

Figure 4.17: Correlation of burst versus peel strength of Rutgers and Stegner Trial 2 polytrays.

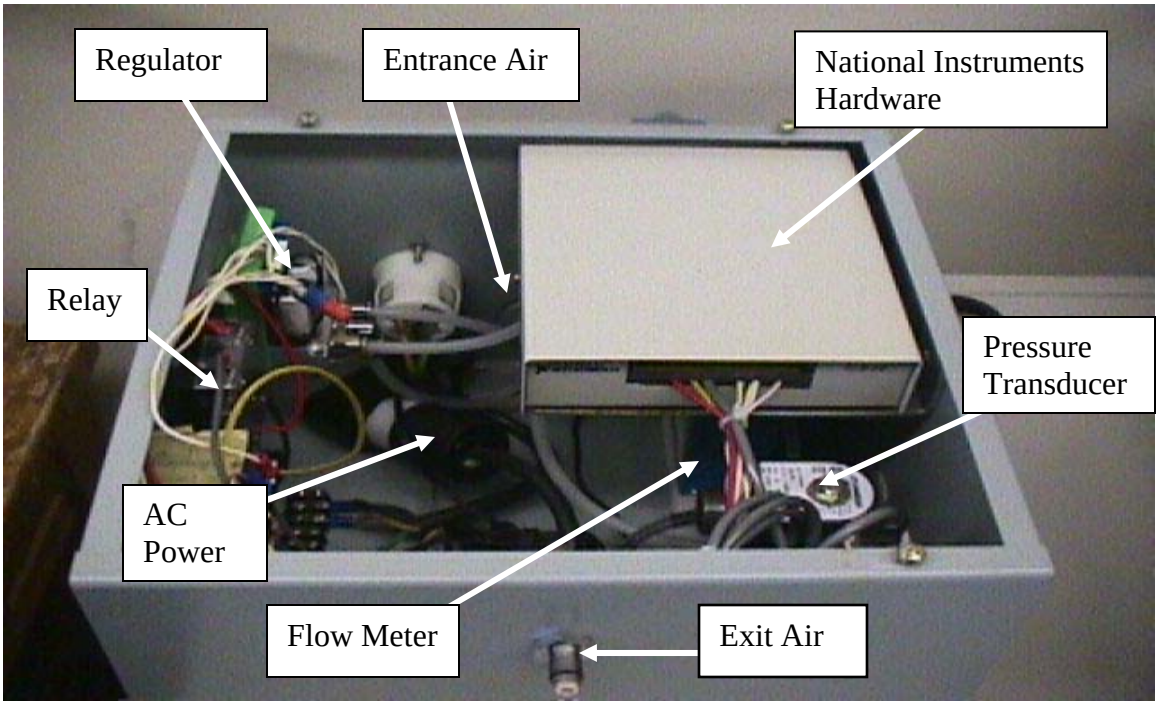

Figure 4.18: Picture of PC integrated burst test system.

4.3 FEMLAB® (Finite Element Analysis):

As stated previously, finite element analysis can take a 3D solid model such as the military polytray and subject that object to stresses and pressures through elemental linear integrations using iterative solvers. Using a program such as FEMLAB®, simulations of these actual stresses and strains can be generated within any point of the model. The 3D modeling was done with the SolidWorks® program and was imported into the FEMLAB® software. The 3D model generated in the SolidWorks® software can be seen in Appendix C.

Symmetry conditions within the FEMLAB® software can be utilized for simulation. Quartering the actual 3D model takes place in the SolidWorks® program before importing into the finite element analysis program. Since the polytray is symmetrical, it can be cut into sections and simulated as an entire polytray instead of simulating the entire polytray. This saves simulation time because the software requires so much virtual memory. Boundaries for maximum displacement were set to zero for the x and z directions within FEMLAB®. This would allow the polytray to be simulated without any movement in the x and z direction. Because our polytray does not move in actual testing, the simulation must have these restrictions to accurately depict the stresses produced during testing.

There are three modes of loading that a crack can experience with respect to testing of materials or objects; Mode I, II, and III. The polytray seal can ultimately be viewed as an initial crack surface. Mode I loading is seen as normal to the crack plane. The crack surfaces of the seal area will tend to separate symmetrically with respect to the initial crack plane [33-38]. Mode II, or shear mode, is related to the in-plane shear load which slides one crack face over another [33-38]. This stress is parallel to the crack growth direction [33-38]. Finally, Mode III corresponds to out-of-plane shear, or tearing of the material [33-38].

Figure 4.19 shows the modes of fractures as a schematic. A cracked body can be loaded in any of these modes, or in any combination of these modes. "Each mode of loading produces the $1/\sqrt{r}$ singularity at the crack tip. In a mixed mode problem (more than one mode is present), due to the principle of linear superposition, the individual contributions to the stress component are additive [33]". In the case of the pressurization and corner or side load simulations we see all modes in combination; Mode III is negligible for pressurization simulations and Mode II is negligible for side load simulations on the polytrays. These modes of fracture can be separated using the FEMLAB® software. The cross section plots shown are a result of these simulations and display Mode I, II, and III stresses.

The internal pressure simulations, which model the burst test, were run at $2.0x10^4$, $5.0x10^4$, $7.5x10^4$, $1.0x10^5$, $1.5x10^5$, and $2.0x10^5$ Pa or 2.9, 7.25, 10.875, 14.5, 21.8, and 29 psi respectively. Corner forces, described in Section 3.3.1, were also simulated on the model polytray. Modulus values calculated from the tensile data of the lid stock and tray were used as material property input values. Figures 4.20 and 4.21 are results from the simulations for a pressurization of a polytray at 2.9 psi. They represent von Mises stresses and show the deformed shape of the package as it is pressurized. The Figures 4.22 through 4.33 are cross section plots from the pressurization and corner load simulation results for the minimum and maximum loading conditions described above. The cross section plots were observed at the interface of the lid-stock and the tray (seal), or the PP/PP diffusion seal.

From the cross-section plots in the xz plane, maximum stresses (σ_{yy}, σ_{xy}, σ_{yz}), were obtained and can be seen in Table 4.6; Mode I and Mode II dominate in the pressurization simulations and Mode I and Mode III dominate in the corner load simulations. Notice the linear increase in maximum stress as the pressure and load is increased for the burst and corner force simulations respectively. Figures 4.34 and 4.35 are plots of these linear curves for the burst and corner simulations respectively.

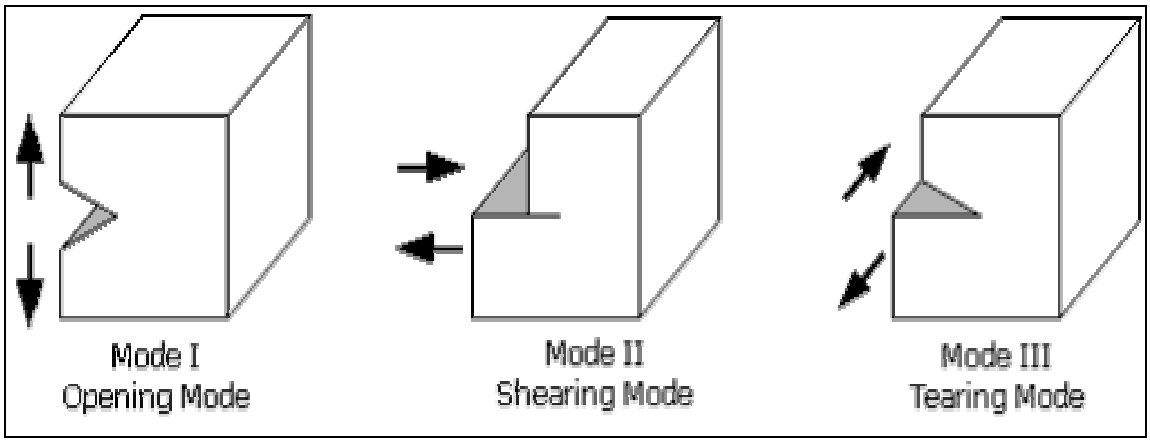

Figure 4.19: Schematic of the three modes of fracture [33].

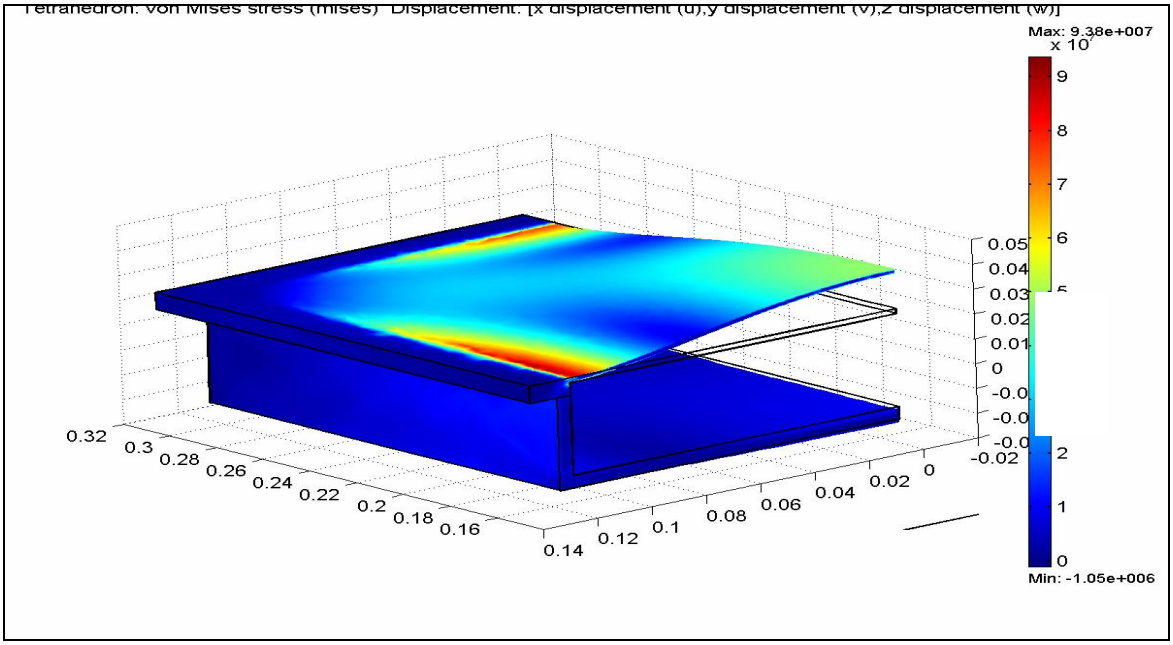

Figure 4.20: Von Mises stress pressure simulation of a quartered package run at 2.9 psi showing deformed shape**.**

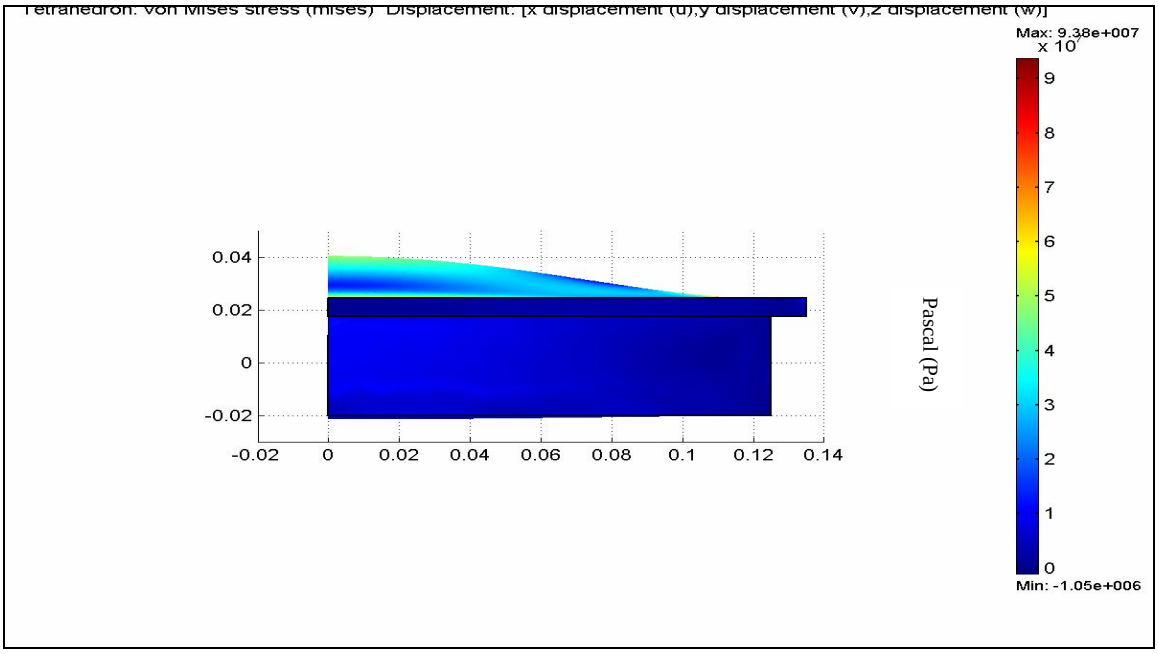

Figure 4.21: Side view of quartered package pressure simulation run at 2.9 psi.

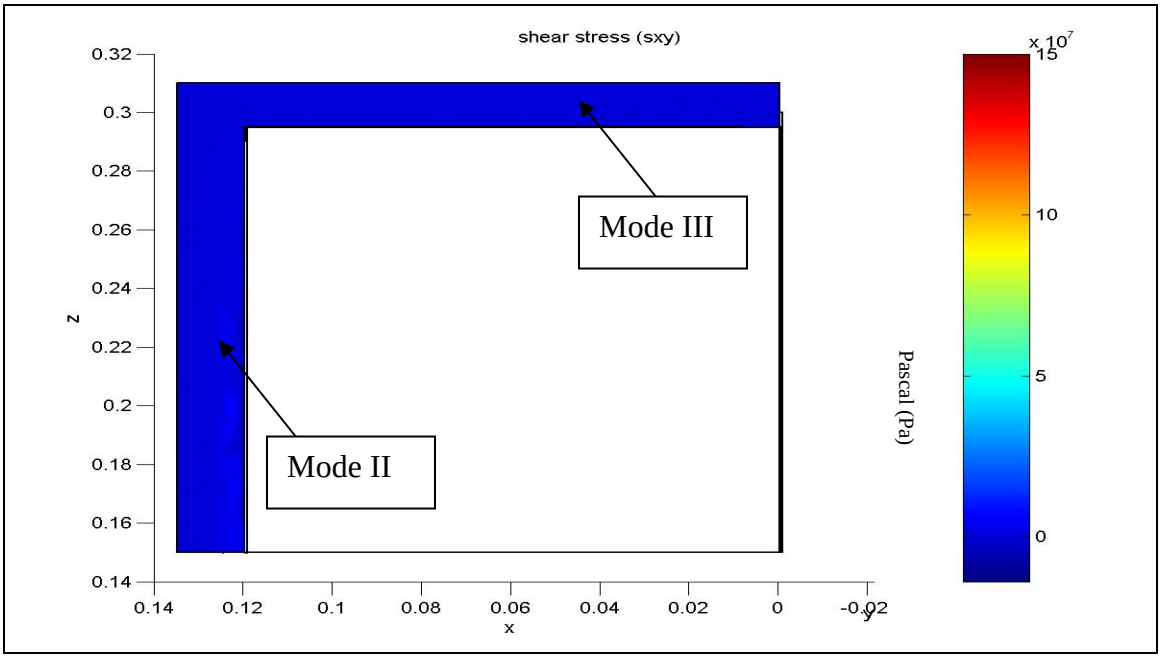

Figure 4.22: Cross-section plot of pressure simulation at 2.9 psi showing shear stress, σxy, in xz plane.

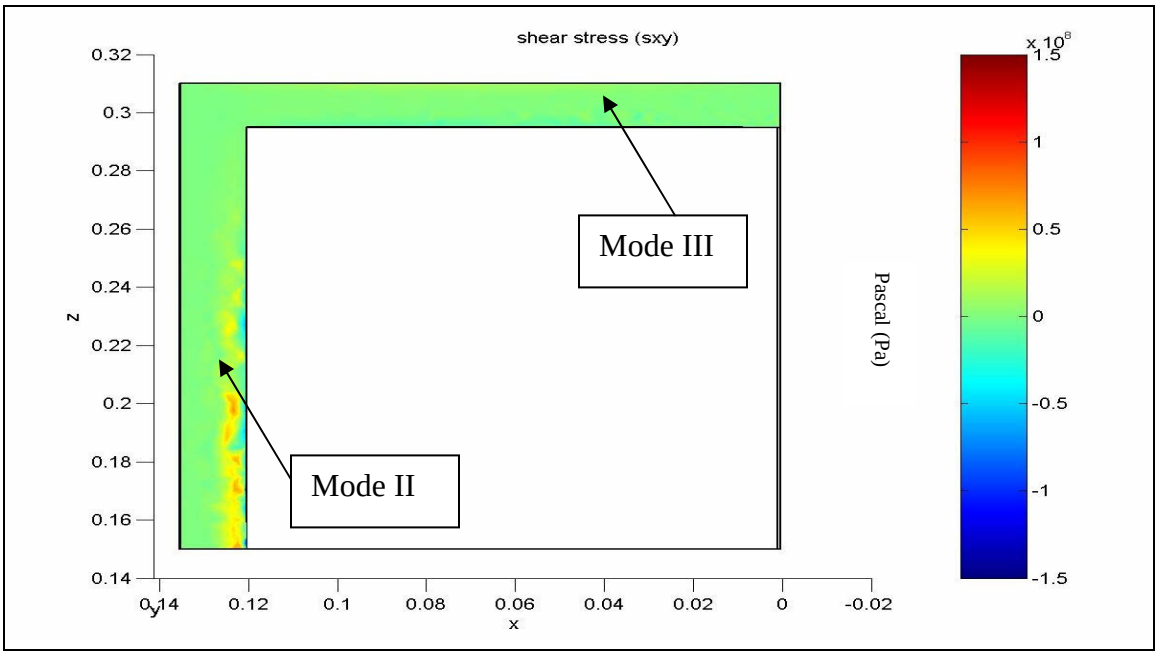

Figure 4.23: Cross-section plot of pressure simulation at 29 psi showing shear stress, σxy, in xz plane.

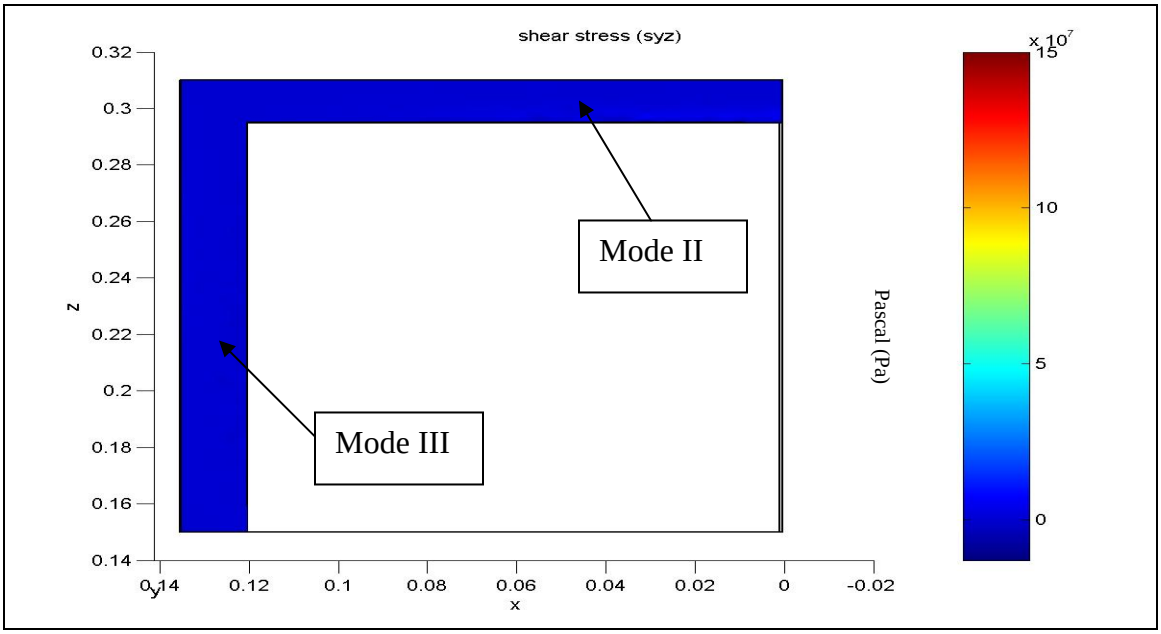

Figure 4.24: Cross-section plot of pressure simulation at 2.9 psi showing shear stress, σyz, in xz plane.

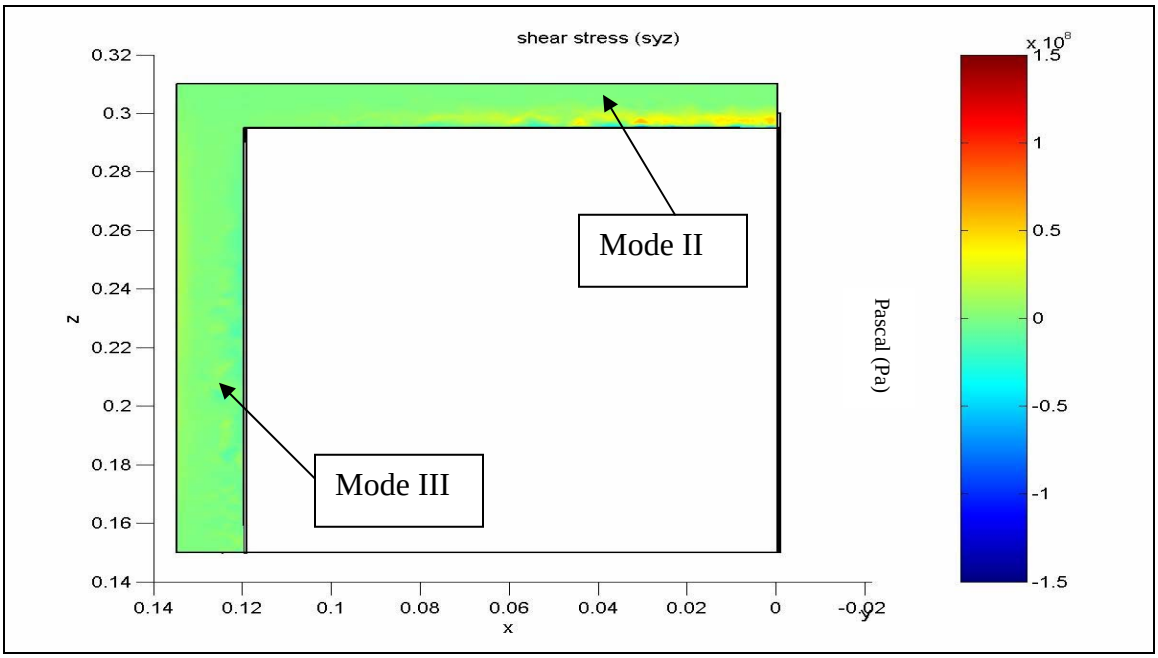

Figure 4.25: Cross-section plot of pressure simulation at 29 psi showing shear stress, σyz, in xz plane.

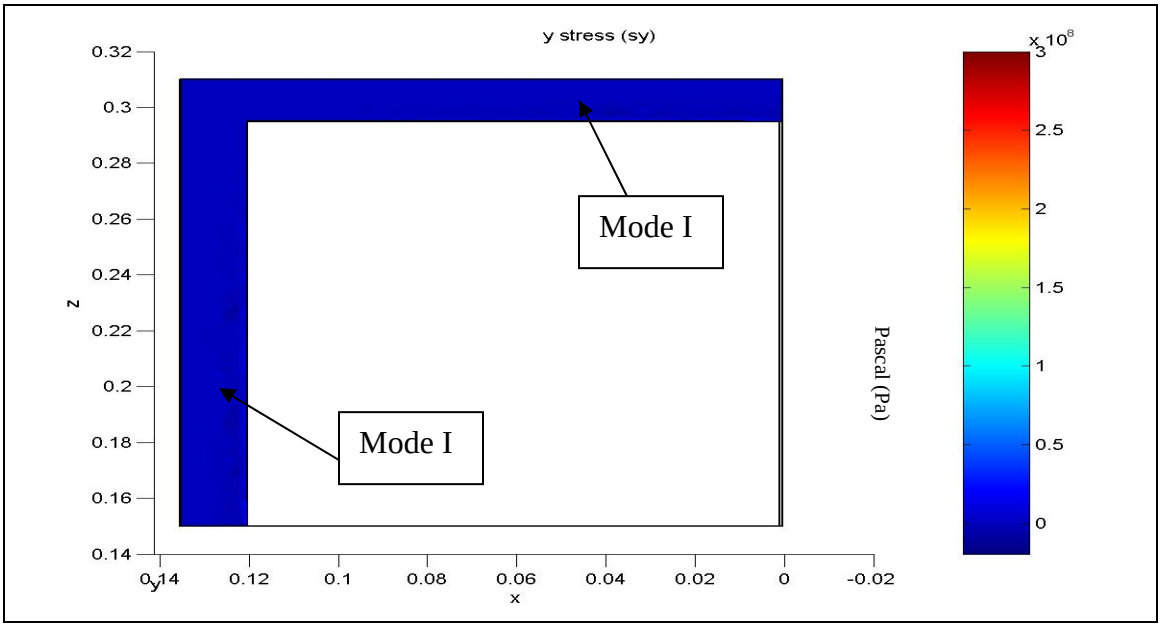

Figure 4.26: Cross-section plot of pressure simulation at 2.9 psi showing normal stress, σyy, in xz plane.

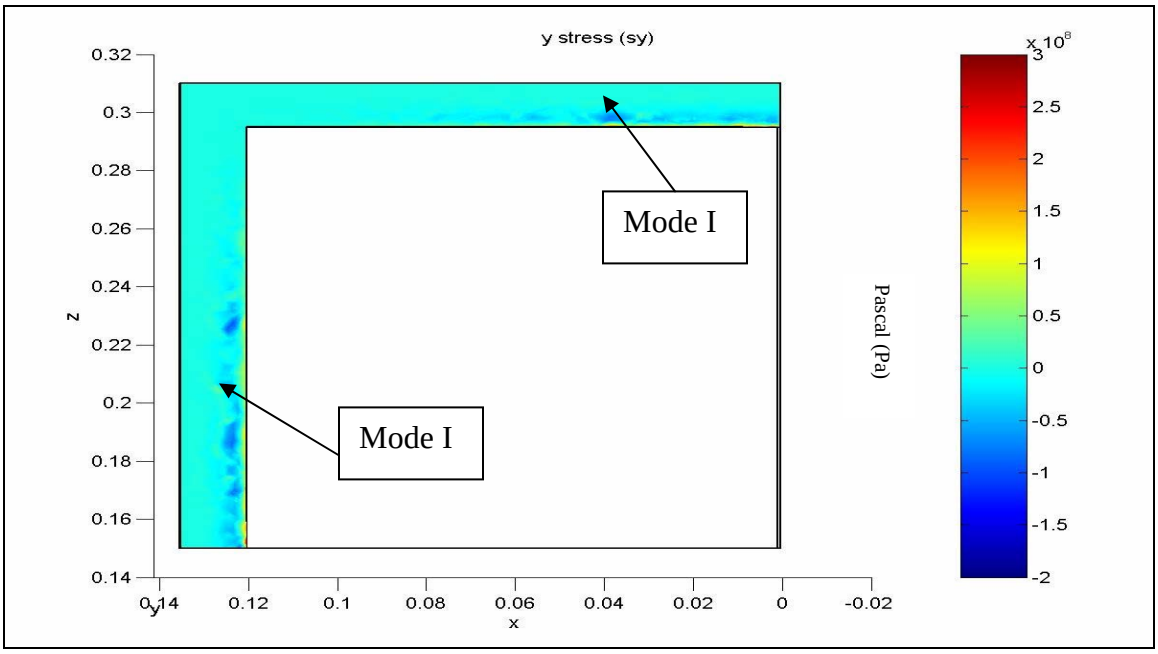

Figure 4.27: Cross-section plot of pressure simulation at 29 psi showing normal stress, σyy, in xz plane.

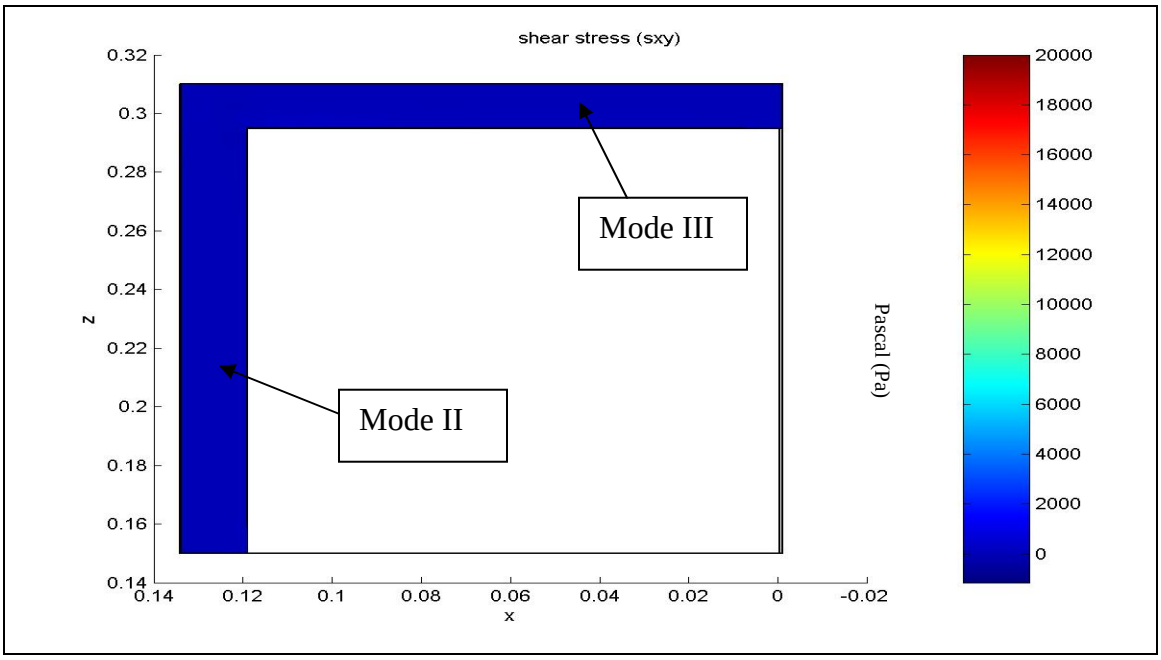

Figure 4.28: Cross-section plot of corner force simulation at 10 N load showing stress, σxy, in xz plane.

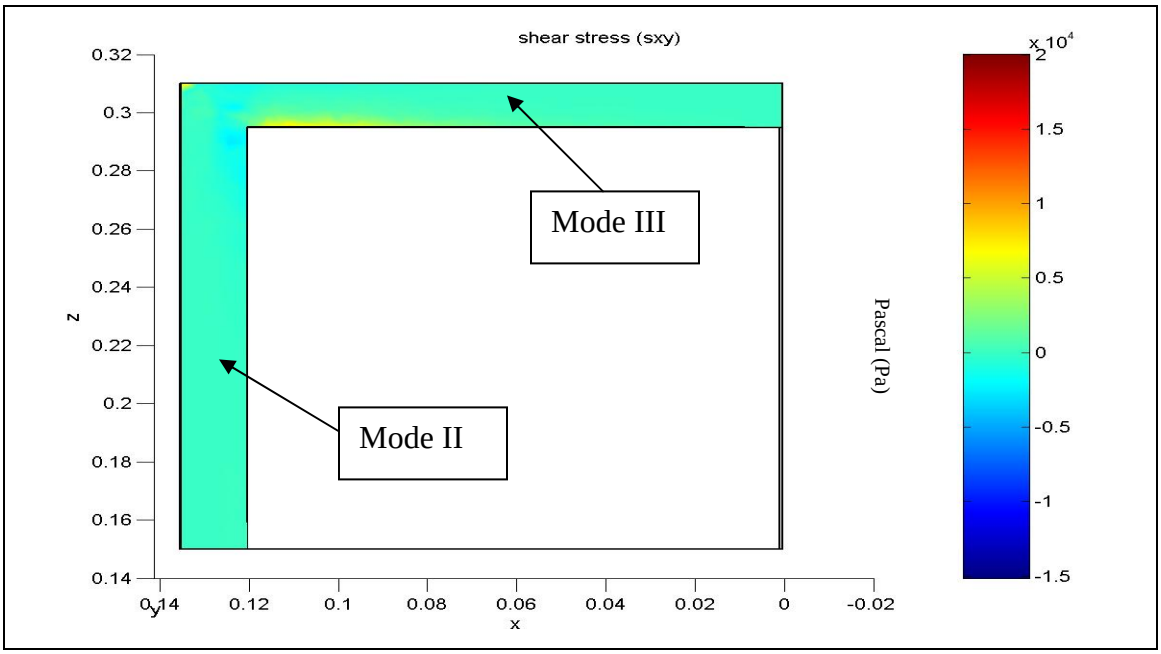

Figure 4.29: Cross-section plot of corner force simulation at 200 N load showing stress, σxy, in xz plane.

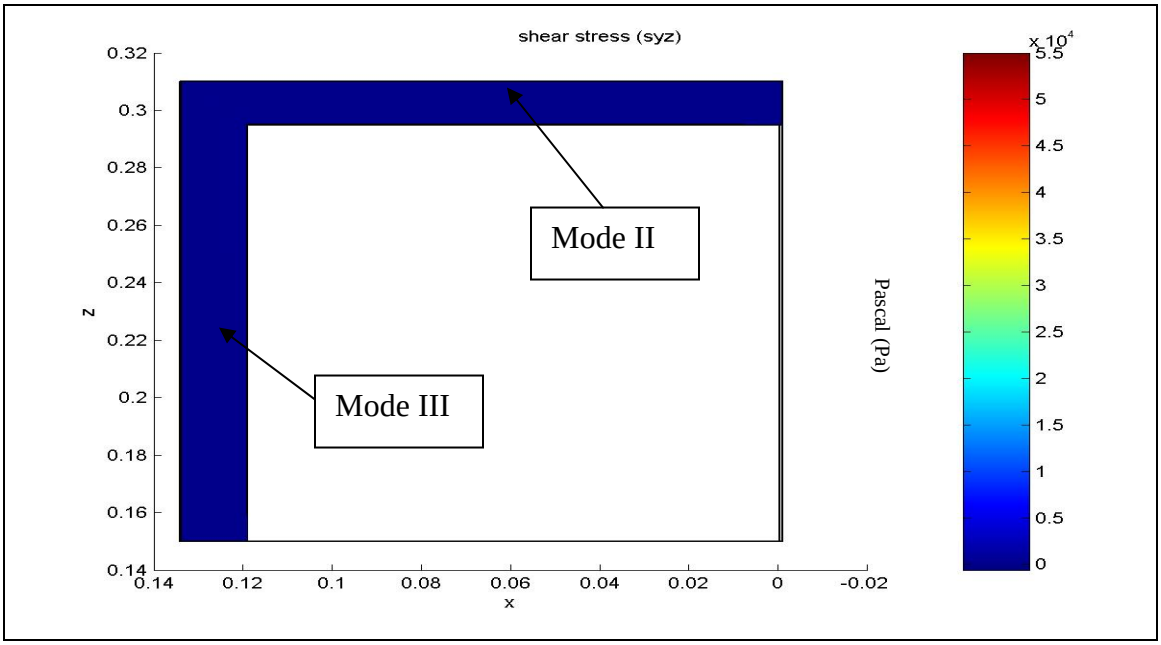

Figure 4.30: Cross-section plot of corner force simulation at 10 N load showing stress, σyz, in xz plane.

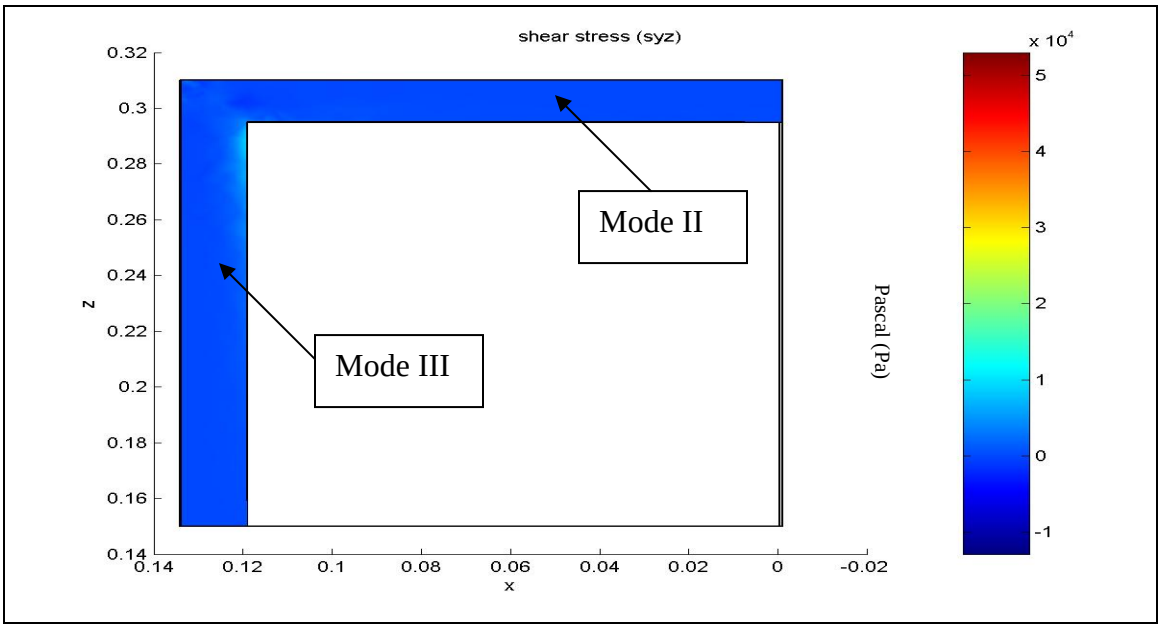

Figure 4.31: Cross-section plot of corner force simulation at 200 N load showing stress, σyz, in xz plane.

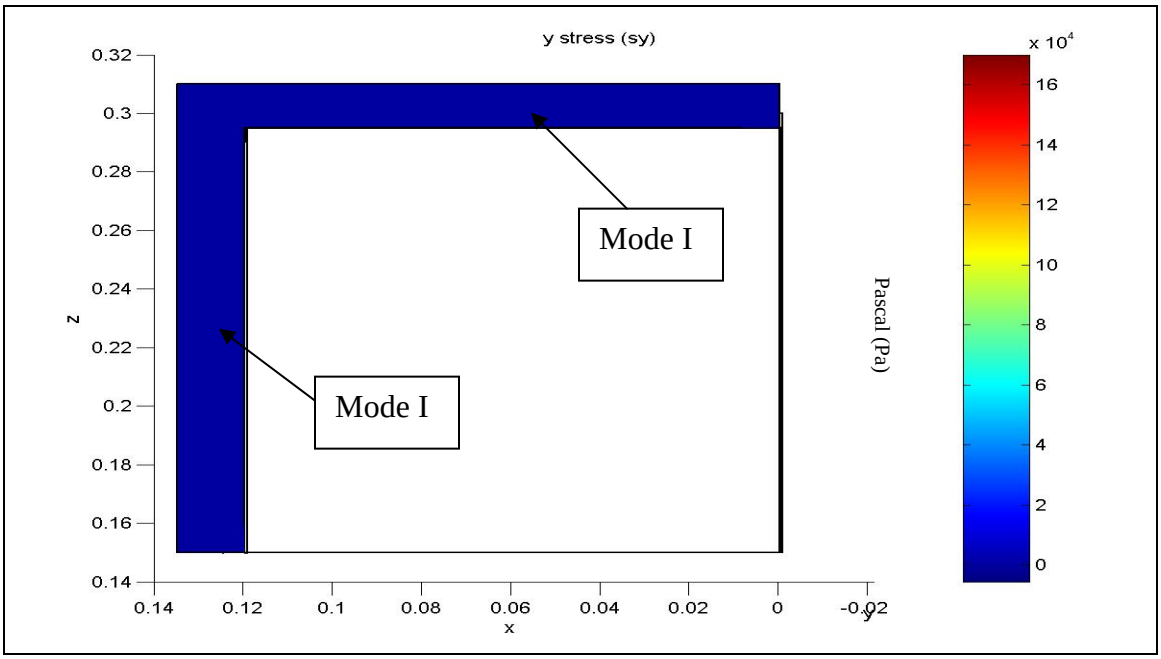

Figure 4.32: Cross-section plot of corner force simulation at 10 N load showing normal stress, σyy, in xz plane.

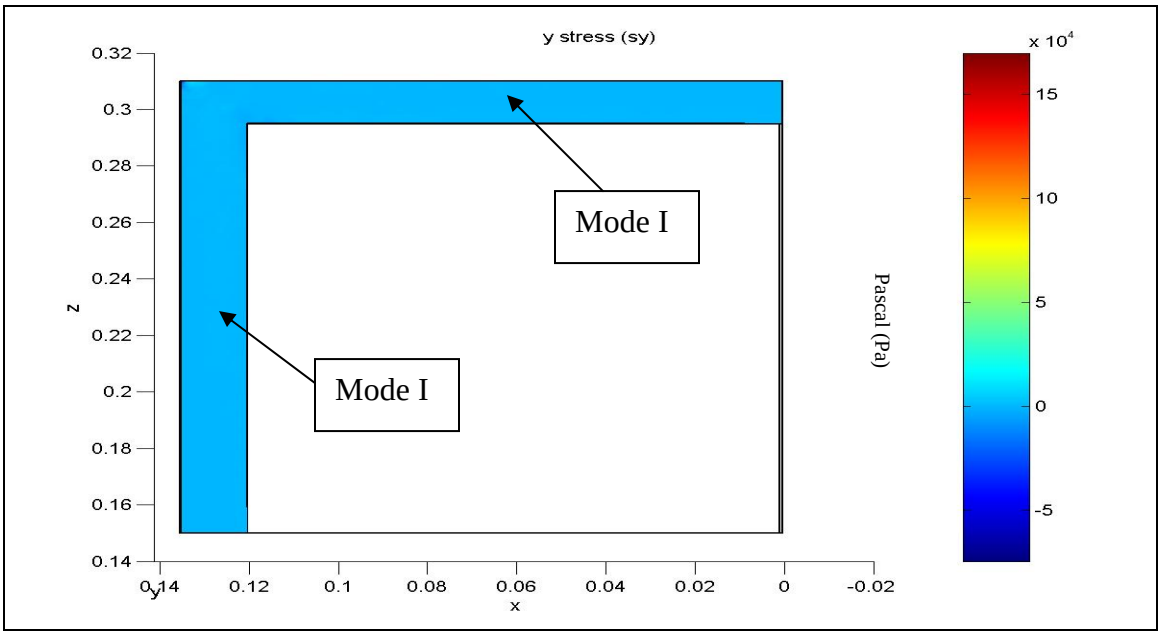

Figure 4.33: Cross-section plot of corner force simulation at 200 N load showing normal stress, σyy, in xz plane.

Table 4.6: Maximum stresses (Mode I, II, and III) produced as a result of pressure and corner load simulations.

Pressure Simulations

Pressure (Pa)	**Pressure (psi)**	Mode I (Pa)	Mode II (Pa)	Mode III (Pa)
2.00E+04	2.9	2.70E+07	1.40E+07	2.0E+06
5.00E+04	7.3	6.70E+07	3.60E+07	5.0E+06
7.50E+04	11.0	1.00E+08	5.50E+07	7.5E+06
1.00E+05	14.5	1.30E+08	7.20E+07	1.0E+07
1.50E+05	21.8	2.00E+08	1.10E+08	1.5E+07
2.00E+05	29.0	2.70E+08	1.40E+08	2.0E+07

Corner Load Simulations

Load (N)	Mode I (Pa)	Mode II (Pa)	Mode III (Pa)
10	3.30E+03	2.0E+02	1.70E+03
50	3.60E+04	7.5E+02	6.70E+03
100	8.00E+04	1.3E+03	1.90E+04
150	1.20E+05	1.8E+05	3.50E+04
200	1.60E+05	2.5E+03	5.30E+04

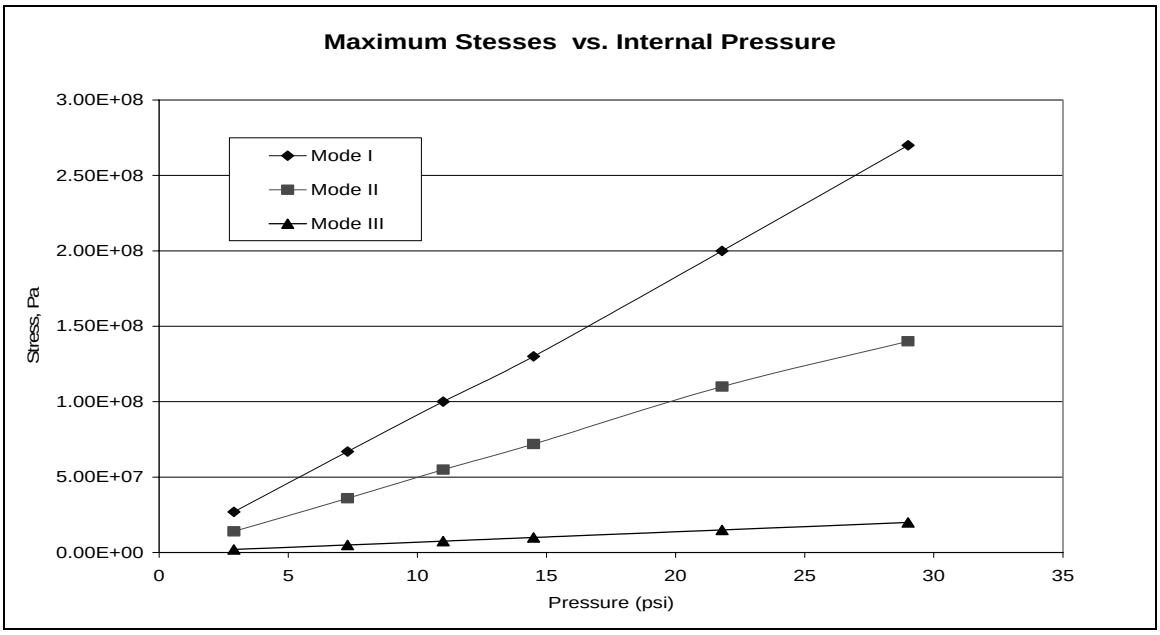

Figure 4.34: Plot of maximum stresses developed in burst simulation with increasing internal pressure.

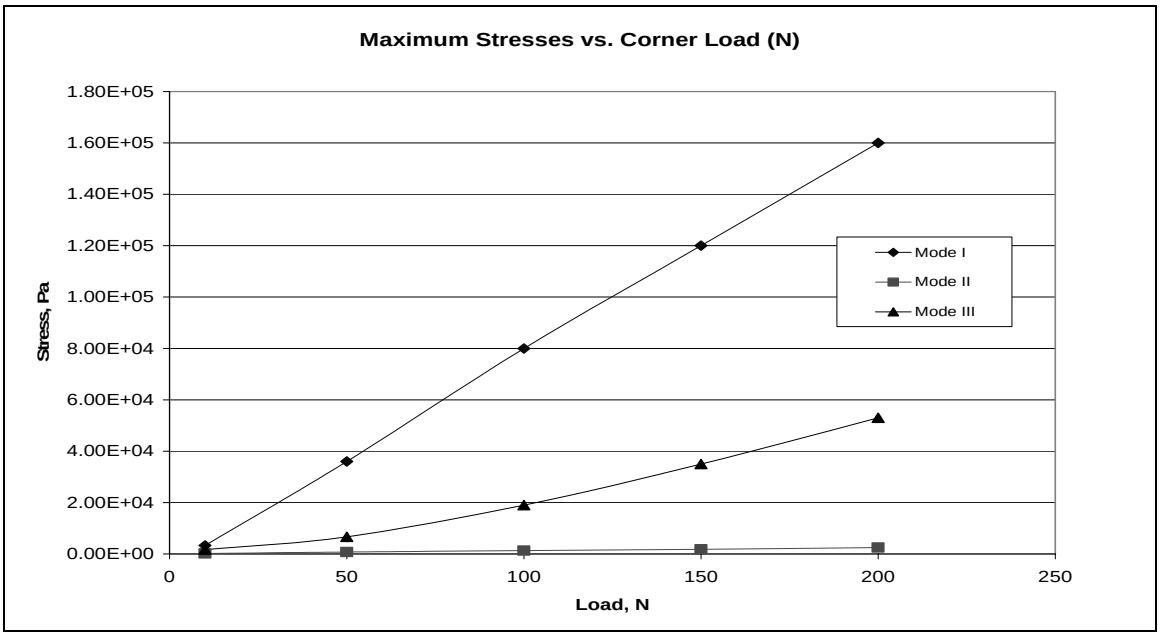

Figure 4.35: Plot of maximum stresses developed in corner force simulation with increasing load.

According to the preceding cross-sections plots, Mode I and Mode II stresses dominate in the pressure simulations; Mode III stresses were negligible. As the polytrays are pressurized, the seal is actually trying to open and shear at the same time; the lid stock is pulling away from the tray, delaminating the PP/PP heat seal. The maximum stress in the y-direction, or Mode I, is actually the largest stress produced in the pressurization simulation which suggests dominate tensile loading in the y-direction.

Mode I and Mode III dominate in the corner load simulations; Mode II stresses are negligible. Side or corner loading produced the largest stresses in Mode I which was seen in Table 4.6. A corner force or loading is more likely to happen while the polytrays are in service or during destination movement. A pressurization of the polytray will not occur in service unless bacteria growth is formed, but in certain loadings in service, these modes of fracture may be present and Mode II and Mode III may dominate.

4.4 Ultrasonic C-scan:

As discussed in Section 3.3.2, ultrasonic techniques can provide an economic means of reducing the incidence of defective packages reaching consumers. With no change in medium under test, there is no waste issue. Two techniques can be utilized, pulse-echo and through-transmission technique. The pulse-echo technique was used for this experiment. The pulse is sent down from the transducer and when it hits an object, the signal is bounced (echoed) back to the transducer in a certain time frame. It is this time that is transformed into a signal that is recorded by the transducer and variations in the intensity of the signal are shown on the screen in waveform. Important parameters in adjusting the C-scan include: gate locations, time of flight, and peak amplitude. Packages with artificial defects made from the Stegner MRE production Trial 1 were used for scanning as well as the Rutgers short seal defective packages described earlier in the peel and burst test sections.

Polytrays were sealed specifically for ultrasonic scanning with all four channel defects on one side of the package. After sealing the wires in place, the four wires were drawn out of seal creating the channel defect. Figure 4.36 is a picture of the C-scan with all four channel defects in place. The wire with the smallest diameter (50.8 micron) is not identifiable, which might require a less sensitive pulse-echo technique. The B scan (surface scan) can be seen in Figure 4.37. Two wires, 254 and 381 micron, can be seen easily within this particular scan. Figure 4.38 is a C-scan of entrapped matter contamination (5% starch solution). The position of the B-scan gate is important because it determines the part of RF waveform to be captured. Although the wires were detected in both the B and C-scans, this Ultrasonic technique is ultimately not useful. The clarity and resolution of the images captured are not of high quality even with the largest of channel defects. Smaller defects, such as the 50.8 micron channel defect, which can be seen with the naked eye, were not present in the images captured. These smaller defects which are more difficult to see are a major concern for the integrity of the seal. If these small defects can not be detected with this technique, it will not be useful on the production line for product inspection.

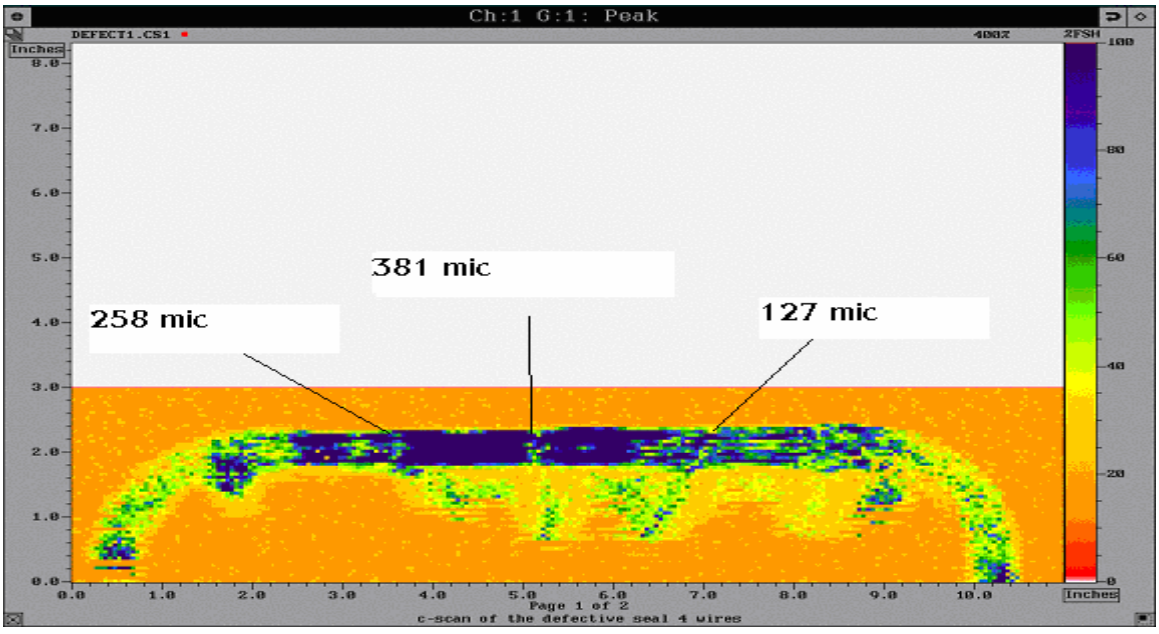

Figure 4.36: Generation of C-scan image with all four channel defects in place.

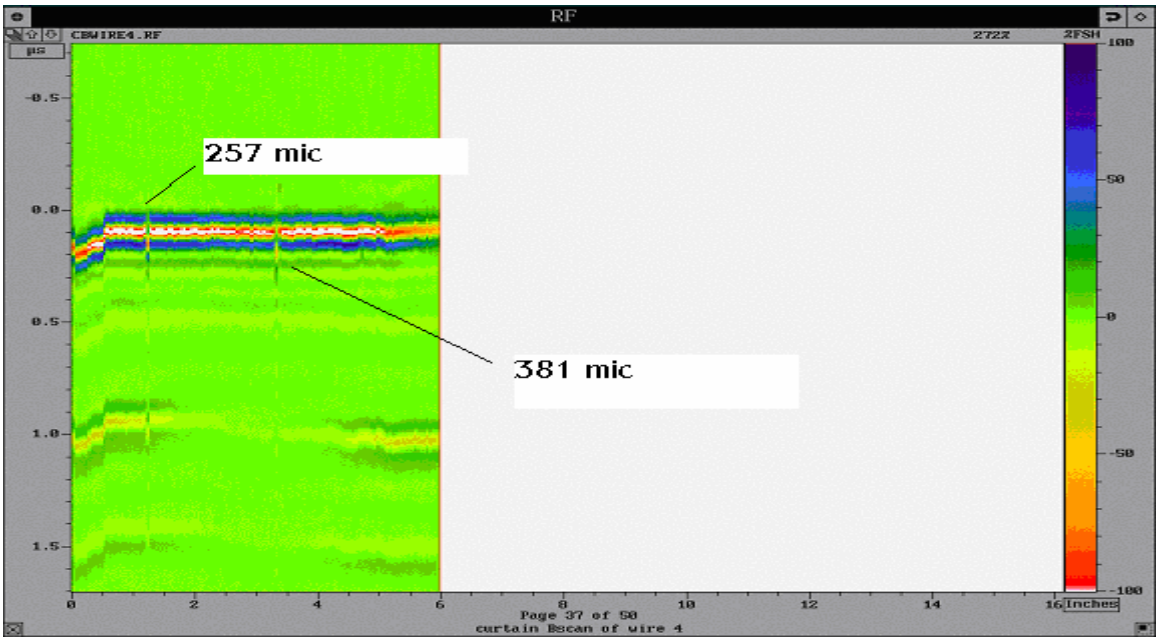

Figure 4.37: B-scan image generated showing the artificial channel defects of 254 and 381 micron.

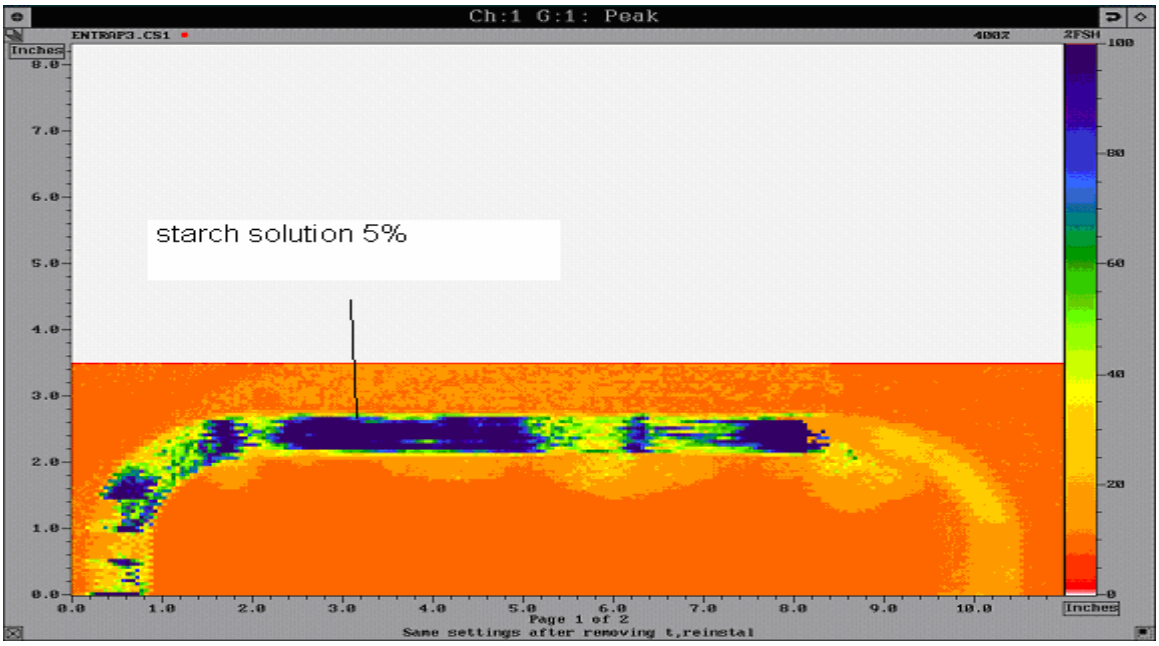

Figure 4.38: C-scan showing entrapped matter contamination (5% starch solution) which appears diffused and spread over a large area.

4.5 Infrared Spectroscopy (FTIR/ATR):

Samples of failed seals (lid-stock side) were examined with FTIR/ATR spectrometry. Through visual inspection, it was concluded that the failed samples delaminated in two places; at the actual seal between the polypropylene of the lid stock and the polypropylene of the tray and between the aluminum and the polypropylene of the lid stock. Through ATR examination of the failed surfaces, the visual inspection was supported. A schematic of the failed specimens of the lid-stock in relation to the ATR crystal can be seen in Figure 4.39.

The Bio-Rad WinIR Pro 3.0 has software which matches spectra to a database of spectra. Figure 4.40 is a spectrum scan of a failed lid-stock surface with an accompanying spectrum from the Bio-Rad WinIR Pro3.0 software [39] database (blue) which matches very closely to the failed surface spectrum; match is ~81% for spectrum compared to database. There was no delamination of the lid stock in these samples; samples failed at the thermally bonded PP/PP seal.

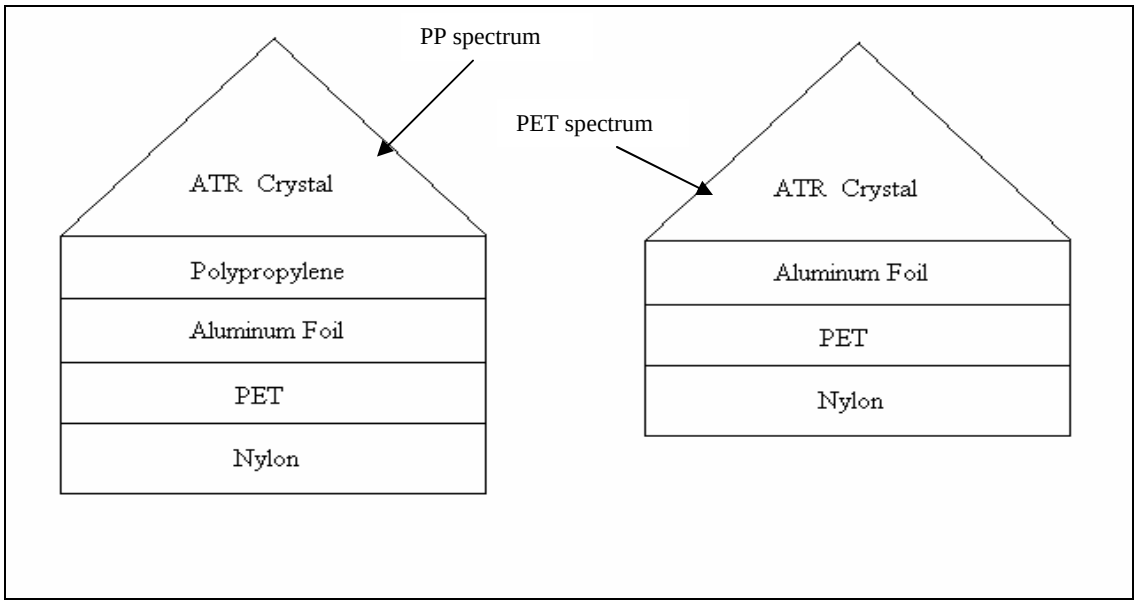

Figure 4.39: Schematic of lid-stock layers in relation to the ATR crystal.

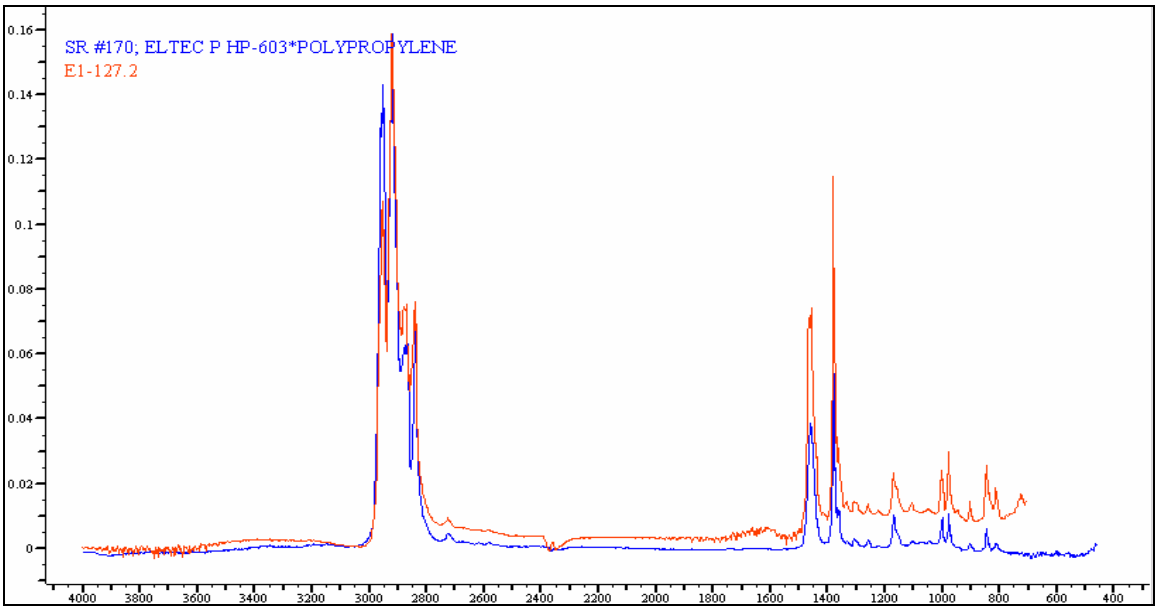

Figure 4.40: Polypropylene spectrum of failed surface (red) with the accompanying database spectrum of polypropylene (blue) from the Bio-Rad WinIR Pro 3.0 software [39].

Figure 4.41 is a spectrum scan of another lid-stock failure surface with an accompanying spectrum from the Bio-Rad WinIR Pro3.0 software (blue) which again matches very closely to the failed surface spectrum; match is ~65% for the spectrum compared to the database. The aluminum foil layer could be seen on the lid-stock after failure, therefore the failure occurred at the PP/Al interface since the PP spectrum was not seen. The depth penetration, dp, orthogonal to that of the incident light through the aluminum was most likely the reason for the revealing of the PET spectrum. Remember that the PET layer is on top of the aluminum layer, but underneath the aluminum in relation to the ATR crystal. In the areas where the lid stock completely delaminated from the tray, a polypropylene spectrum was displayed which supports our visual inspection.

A total of 119 failed samples surrounding various defects were examined with the software. 72 failed samples displayed the polypropylene spectrum which equates to 60.5% of the total samples examined. The remaining samples, 47, displayed a polyester spectrum which is equivalent to 39.5%. A correlation for each particular defect with the

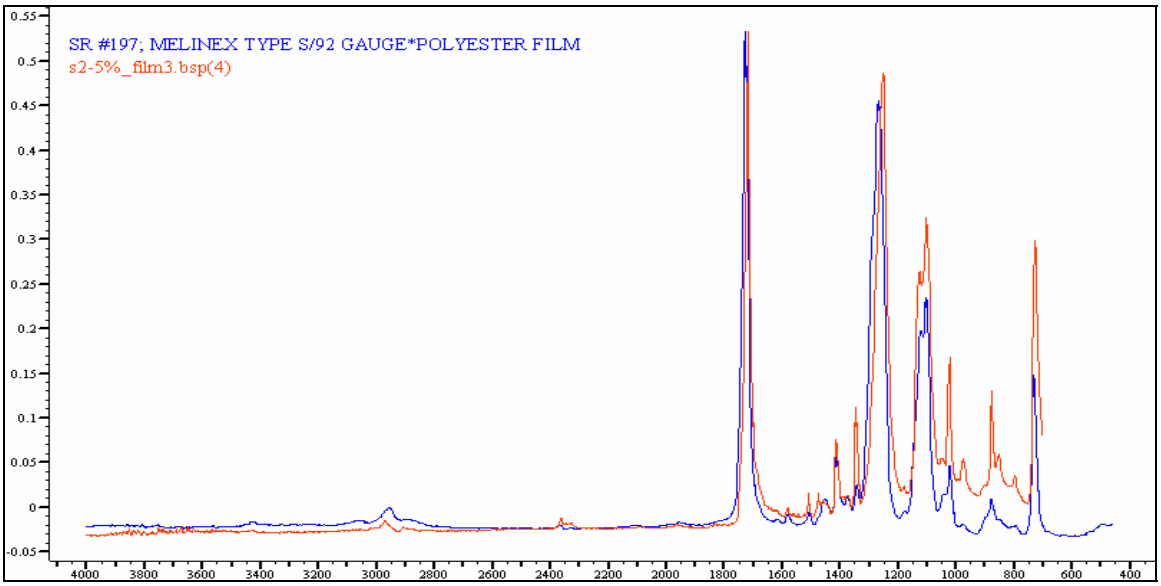

Figure 4.41: PET spectrum of failed surface (red) with the accompanying database spectrum of polyester (blue) from the Bio-Rad WinIR Pro 3.0 software [39].

failed delamination surface could not be generated based on the results. The defects present in the seal had no adverse effect on the particular failure surface of the samples from the burst test experiments.

The ATR/FTIR spectrometry provided insight as to the failed surfaces of the samples from the burst test. 60.5% of the failed samples showed polypropylene as the layer present at the failed surface. If the samples all showed polypropylene, the seal strengths could only be improved by improving the polypropylene/polypropylene fusion seal. On the other hand, 39.5% of the failed samples showed PET as the layer present at the failed surface. The failed surface on these samples was actually between the polypropylene and the aluminum foil in the lid stock. The evanescence of ATR/FTIR incident ray and depth of penetration into the failed surface was most likely the reason for the PET spectra present. The PET layer of the lid-stock is on top of the aluminum layer. If the failed samples all showed the polypropylene/aluminum foil delamination, a better tie layer in the extrusion of the lid-stock would be necessary. Since there were a number of failures in both cases, both the fusion seal of the PP/PP and the tie layer used in the extrusion of the lid-stock should be examined further.

Twenty-three out of the one-hundred nineteen failed surfaces examined were from channel defective polytrays (containing channel diameters of 50.8, 127, 254, and 381 microns) used in the burst test. All of these polytrays leaked during the burst test as seen in Section 4.2.4. Eighteen out of twenty-three failure surfaces from the channel defective polytrays failed at the PP/PP diffusion of the seal. The other 5 failed surfaces were from the PP/Aluminum layer in the lid-stock. The following is a break down of the visual inspection and supported ATR examination: 50.8 μm – 4 samples failed at the PP/Al layer and 2 failed at the PP/PP seal; 127 μm – all 10 samples failed at the PP/PP seal; 254 μm – 3 samples failed at the PP/PP seal and 1 sample failed at the PP/Al layer; 381 μm – all 3 samples failed at the PP/PP seal. From this evaluation no specific channel leak defect could be correlated with a specific failure surface; but the delamination of the PP/PP diffusion seal is more likely to occur with these particular defects. No correlation of burst failure pressure with specific failure samples and their respecting failure surface could be generated.

Chapter 5: Summary and Conclusions

5.1 Summary and Conclusions:

The evaluation of the sealing in military flexible food polytrays was completed by utilizing various destructive and non-destructive techniques. The mechanical properties of the polytrays were found by utilizing the tensile test. The lid-stock and tray samples were taken from the same Sopakco 1 polytrays used for the peel tests. An average elastic modulus value of 1.4 $x10^9$ Pa for the lid-stock was found and was used for the material properties input of finite element analysis. The tray tensile specimens produced an average modulus value of 1.8 x 10^9 Pa and that value was also used in conjunction with the finite element analysis.

Peel testing was performed to gain a perspective on the strength of the seals. Polytrays with no defects from Wornick Food Company were the first samples tested. A wide variation in peak load within the sample set resulted in high standard deviation; 7.67/in lb_f standard deviation, which suggested some uneven thermal sealing of the polytrays. The maximum peak and minimum peak load for the forty sample population was 43.83 lb_f/in and 18.27 lb_f/in respectively. The next set of peel tests were completed on polytrays from Sopakco Food Products. These polytrays also had no visual defects in the sealing area. Although the variation in peak load within these sample sets is smaller than that of the Wornick polytrays, 3.34 lb_f/in standard deviation, the overall maximum peak load is 12 – 15 lb_f/in lower than that of the Wornick polytrays. The maximum peak and minimum peak load for the forty sample population was 30.35 lb_f/in and 17.42 lb_f/in respectively. The variation in peak load, again, suggests some uneven thermal sealing of the polytray.

Polytrays from the Center for Advanced Food Technology at Rutgers that appeared visually intact (100% good seal) were also tested. The maximum and minimum peak loads were plotted for each test and are 31.21 lb_f/in and 20.54 lb_f/in respectively for that population. There is still variation of peak load, but this particular set of polytrays

has one of the lowest standard deviations of all the populations, 3.38 lb_f/in. The first set of defective polytrays used in peel testing was from the Center for Advanced Food Technology at Rutgers University, where a good representation of "short seal" defects on the polytrays was obtained. Samples were tested with areas of the seal within the sample ranging from 0% to ~90% good seal. The maximum and minimum peak loads were 24.01 lb_f/in and 8.42 lb_f/in respectively. The average peak load was obviously lower than that of Wornick and Sopakco polytrays. Again, a large standard deviation of peak loads was obtained, 4.48 lb_f/in, but it can be justified here by the presence of the "short seal" defects.

The last set of peel tests involved polytrays with artificial defects such as entrapped matter made at Stegner Food Company Trial 2. The entrapped oil and starch samples performed just as well or better than the control (defect free) samples produced. The entrapped noodle samples, on the other hand, performed poorly compared to the control samples. The entrapped noodle samples proved to be the worst performing of all peel test sets with an average peak value of 15.31 lb_f/in and the lowest recorded peak force value at 7.17 lb_f/in. Solid entrapped matter, such as the noodle, clearly affects the strength of the seal surrounding the defect.

Two microbial challenge experiments were carried out to see if artificial defects such as channel defects would affect the seal integrity of the polytray when exposed to bacteria. The first challenge produced results as follows: 6 out of 15 polytrays with the 381 micron channel defect were positive (+) for CO_2 gas production, 3 out of 15 polytrays with the 254 micron defect were positive (+) for gas production, and all five inoculated polytrays (positive control) were positive (+) for gas production, where as none of the sound samples failed, and polytrays with channel defect less than or equal to 127 microns did not fail. Fifteen polytrays were also dipped into negative control, chlorinated water (10 ppm FAC), after which none of the polytrays produced gas while in incubation. The most interesting result from this challenge was that none of the trays with the 50.8 and 127 μm channel defects failed, which clearly gives a basis for smallest

channel defect that could be allowed to pass during inspection. The polytrays with channel defect less than or equal to 127 μm were obviously not as serious as the other channel defects.

An experimental mistake made results in microbial challenge #2 difficult to interpret. The polytrays were stacked on their sides in crates rather than on a flat surface. Liquid media leaked out of some of the polytrays and quite possibly contaminated other polytrays. It is for this reason, a negative control is used in the experiment. Failure, or gas production, within the negative control polytrays (chlorinated water), makes these results invalid. Seven polytrays dipped in the 3 log CFU/mL water failed along with six polytrays that were dipped in the 6 log CFU/mL contaminated water. All five positive control samples produced CO_2 gas.

The development of a burst test was necessary to correlate microbial challenge and peel testing results. The initial analog system was constructed to monitor air flow through the polytray versus increasing pressure. Experiments were carried out and a basis for further experiments and development was established. Several control polytrays were used for calibration of the new burst test system. Five polytrays of each artificial channel defect created having diameters of 50.8, 127, 254, and 381 micron were tested. An additional five packages from the Rutgers polytrays, having short seal defects, were also tested.

Air flow was detected exiting on polytrays with channel defects as small as 50.8 μm with as little pressure as 5 psi. All 127 micron diameter channel defect polytrays tested had detectable leaks. A more linear pattern was seen in this experiment as compared to the polytrays with the 50.8 micron diameter channel defects. All five polytrays with 127 μm channel defects burst between 25 and 30 psi. Some 254 μm channel defect polytrays formed severe leaks in the area surrounding the sealing defect. Along with the severe leak, delamination, or peel of the seal, occurred at and around the area surrounding the channel defect. The same results were seen for the polytrays with

381 micron diameter channel defects. The leaks in the 381 μm channel defect polytrays became larger with increasing regulator pressure. The polytrays could not maintain regulator pressure because the air flow exiting the polytray was too great.

Burst tests were also conducted for polytrays made in Trial 2 at Stegner Food Company. Three of each of the following polytrays was pressurized until failure: sound samples, samples with entrapped 6.5% starch solution, samples with entrapped soybean oil and samples with entrapped blanched noodles. All polytrays failed at pressures less than 35 psi. The sound sample, entrapped oil, and entrapped starch (6.5%) all performed similarly. The entrapped noodle polytrays did perform as expected producing leaks and failing at lower pressure values than the other polytrays. The results from these burst tests correlated very nicely with the peel results for the same polytrays seen previously. A PC integrated system was developed as a result of this preliminary testing using the analog system. Based on the results, it was determined that a volumetric flow rate sensitivity of 0.2 mL/min was appropriate to detect leaks in these polytrays. This current burst test system will be used in future experiments. The ultimate goal of designing a test and implementing it was achieved and is extremely useful in the examination of the seal integrity of the polytrays.

Finite element analysis was utilized to study the 3D solid model of the military polytray. FEMLAB® was used for pressurization simulations, which emulates the burst test, and corner force loading, which emulates the polytray landing on its side. Actual stresses and strains produced can be generated and seen at any point within the model. The internal pressure simulations were run at $2.0x10^4$, $5.0x10^4$, $7.5x10^4$, $1.0x10^5$, $1.5x10^5$, and $2.0x10^5$ Pa or 2.9, 7.25, 10.875, 14.5, 21.8, and 29 psi respectively. Corner forces were also simulated on the model polytray at loads of 10, 50, 100, 150 and 200N. Modulus values calculated from the tensile data of the lid stock and tray were used as material property input values.

After finite element simulations were complete, cross-section plots of the seal area were generated. Maximum stresses (σ_{yy}, σ_{xy}, σ_{yz}) present in the seal were obtained. It was found that Mode I and Mode II stresses, or shearing, are at a maximum for the pressurization simulations and Mode I and Mode III stresses, or tearing, are at a maximum for the corner load simulations. There was a definite linear increase in maximum stress as the pressure and load is increased for the burst and corner force simulations respectively. As the polytrays are pressurized, the seal is actually trying to open and shear at the same time; the lid stock is pulling away from the tray, delaminating the PP/PP heat seal. The maximum stress in the y-direction, or Mode I, is actually the largest stress produced in the pressurization simulation which suggests dominate tensile loading in the y-direction. Mode I and Mode III dominate in the corner load simulations. A corner force or loading is more likely to happen while the polytrays are in service or during destination movement and these modes of fracture, Mode II and Mode III, may be present and may dominate.

An ultrasonic C-scan technique could provide an economic means of reducing the incidence of defective packages reaching consumers. With no change in medium under test, there is no waste issue. Packages with artificial defects made from the Stegner MRE production Trial 1 were used for scanning as well as the short seal defective polytrays. Polytrays were sealed specifically for ultrasonic inspection which included all four channel defects on one side of the polytray. Although the wires were detected in both ultrasonic B and C-scans, this technique was ultimately not useful. The clarity and resolution of the images captured were not of high quality even with the largest of channel defects present. Smaller defects, such as the 50.8 micron channel defect, could not be captured in the images. These smaller defects which are more difficult to see are a major concern for the integrity of the seal. These small defects were not detected with this technique, and it would not be useful on the production line for product inspection.

Through visual inspection, it was concluded that the failed burst test samples delaminated in two places; at the actual seal between the polypropylene of the lid stock and the polypropylene of the tray and between the aluminum and the polypropylene of

the lid stock. ATR/FTIR spectrometry was used to examine 119 failed sample surfaces surrounding various defects. 72 of the failed samples displayed the polypropylene spectrum; 60.5% of the total samples examined. The remaining failed samples, 47, displayed a polyester spectrum which is equivalent to 39.5%. A correlation of a particular defect with the failed delamination surface could not be generated based on the results. It was determined that the defects present in the seal, whether artificial or naturally occurring, had no adverse effect on the particular failure surface of the samples from the burst test experiments.

If all failed samples showed polypropylene, the seal strengths could only be improved by improving the polypropylene/polypropylene fusion seal. The failed surface of the samples showing a PET spectrum was actually between the polypropylene and the aluminum foil in the lid stock. The evanescence of ATR/FTIR incident ray and depth of penetration into the failed surface was most likely the reason for the PET spectra present. The PET layer of the lid-stock is on top of the aluminum layer. If the failed samples all showed the polypropylene/aluminum foil delamination, a better tie layer in the extrusion of the lid-stock would be necessary. Because there were a number of failures in both cases, both the fusion seal of the PP/PP and the tie layer used in the extrusion of the lid-stock should be examined in future experiments.

Several types of sealing defects can really affect the seal integrity of the military food polytrays. As seen, naturally occurring short seals can significantly decrease the peel and burst strength of the seal, but might be strong enough to keep the seal intact and free from its surrounding environment. Because of this, it would be safe to say that short seals covering at least 50% of the width of the seal could be passed through visual inspection, as long as no channel defect is present. Channel defects less than or equal to 127 μm may not affect the seal strength surrounding the defect but do need to be taken into consideration because of the possibility of leaks and potential microbial contamination of the contents of the polytray. From the first microbial challenge experiment, channel defects less than or equal to 127 μm did not produce severe gas formation, but air leaks through these defects as small as 50.8 μm were detected in the burst test.

Solid entrapped matter in the seal should not be passed through visual inspection. As seen, entrapped noodles in the seal area significantly reduced the seal strength and the potential for leaks, just as in channel defects, may be present and microbial contamination may take place over time. Fluid entrapped matter defects such as oils and starches did not adversely affect the seal strength of the seal surrounding the defect. These fluid entrapped matter defects produced results equal to or greater than the sound samples in both peel and burst testing. Through this rigorous experimentation, it would be safe to pass defects through visual inspection, as long as no channel defect was present, that had a burst strength of 30 psi or higher and a peel strength of 20 lb_f/in or higher.

5.2 Suggestions for Future Work:

The following suggestions should be considered for the future work with the flexible military polytrays in regards to better understanding the quality of the seals produced.

- Production of polytrays with various solid entrapped matter defects – categorize different solids with seal strength.
- Burst test analysis of more defective polytrays using the current PC integrated system. Monitor air flow and pressure.
- Another microbial challenge to support results found in this project.
- Infrared camera inspection on seals to examine defects present not seen by the naked eye - possible implementation into the production of the polytrays.
- Pressure differential leak detection in place of the current burst test system – polytrays will not be destroyed.
- FEMLAB® simulations of a restrained polytray within the current burst test chamber.
- Bacteria growth detection system implanted into the sidewall or the lid-stock of the polytray – eliminate need for any post production testing.

References:

1. Li, Jun; Shanks, Robert A.; Bray, Tracey; Lau, Andro; and Hubbert, Michael. Control of Adhesion and Removal of Heat Sealable Tops on Polymer Containers. RMIT University, Melbourne, Australia. Jan 1, 2002.
2. Kit, Kevin M. Private communication. Primary advisor and professor of project. Materials Science & Engineering. University of Tennessee, Knoxville, 2002.
3. Kwak, Sang Kyu. *Material Fracture*. Department of Chemical Engineering. State University of New York at Buffalo. Center for Computational Research. Buffalo, New York. October 13, 2004. <http://www.ccr.buffalo.edu/etomica/app/modules/sites/MaterialFracture/Images/SSPicture1.jpg>.
4. SpecialChem. Innovation & Solutions in Adhesives and Sealants. Adhesion Guide. SpecialChem4Adhesives. October14, 2004. <http://www.specialchem4adhesives.com/resources/adhesionguide/index.aspx>
5. Lee, L.H. Adhesive Bonding. Plenum Press, NY, 19, 1991.
6. Kinloch, A.J. Interfacial Fracture Mechanical Aspects of Adhesive Bonded Joints – A Review. *Journal of Adhesion*, 10, 193-219, 1979.
7. Kinloch; Glendhill; and Shaw. A Model for Predicting Joint Durability. *Journal of Adhesion*, 11, 3-15, 1980.
8. Kinloch, A.J. Science of Adhesion. 1. Surface and Interfacial Aspects. *Journal of Materials Science*, 15, 2160-2166, 1980.
9. Clearfield; McNamara; and Davis. Adherend surface preparation fro structural adhesive bonding in: Adhesive Bonding (L.H. Lee, ed.), Plenum Press, NY, 1991.
10. Kinloch, A.J. Adhesion and Adhesives, Science & Technology. Chapman and Hall, London, NY, 1987.
11. Voyutskii, S.S. Autohesion and adhesion of high polymers. Interscience, New York, 1963.
12. Deryagin, B.V. Research, 8, 70, 1913.

13. Goulas, Antonios E; Riganakos, Kyriakos A; and Kontominas, Michael G. Effect of ionizing radiation on physicochemical and mechanical properties of commercial multilayer coextruded flexible plastics packaging materials *Radiation Physics and Chemistry*, Volume 68, Issue 5, December 2003, Pages 865-872.
14. Feliu, Baez R.; Lockhart, H.E.; and Burgess, G. Correlation of peel and burst tests for pouches. School of Packaging Michigan State University, East Lansing, MI. *Packaging-Technology-and-Science*. v 14 n 2 March/April 2001, p 63-69
15. Sanchez, Saul V.; Orona, Filiberto V.; Lopez, M.; Luisa, Q.; Guerrero, Carlos. Multilayer films using modified LLDPE blends. CIQA, Saltillo, Mexico. *Journal-of-Engineering-and-Applied-Science*. v 2 1996, p 2642-2644.
16. Wilson, P. D. G.; Brocklehurst, T. F.; Arino, S.; Thuault, D.; Jakobsen, M.; Lange, M.; Farkas, J.; Wimpenny, J. W. T.; and Van Impe, J. F. Modeling microbial growth in structured foods: towards a unified approach. Institute of Food Research, Norwich Research Park, Norwich, NR4 7UA, UK.
17. Uyttendaele M.; Rajkovic A.; Benos G.; Francois K.; Devlieghere F.; and Debevere, J. Evaluation of a challenge testing protocol to assess the stability of ready-to-eat cooked meat products against growth of Listeria monocytogenes. *INTERNATIONAL JOURNAL OF FOOD MICROBIOLOGY* .90 (2): 219-236 January, 15 2004.
18. MicroMemAnalytical. “Fourier Transform Infrared Spectrometry”. A Division of the Orange County Water District. Fountain Valley, CA. October 22, 2004. <http://www. micromemanalytical.com/ATR_Ken/ATR.htm>
19. Ridgway, H.; Ishida, K; Rodriguez, G.; Safarik, J.; Knoell, T.; and Bold, R.. 1999. Biofouling of membranes: Membrane preparation, characterization and analysis of bacterial adhesion, p. 463-494. In R. J. Doyle (ed.), *Methods in Enzymology*, Vol. 310. Academic Press, New York.

20. Campbell, P.; Srinivasan, R.; Knoell, T.; Phipps, D.; Ishida, K.; Safarik, J.; Cormack, T.; and Ridgway, H. Quantitative structure-activity relationship (QSAR) analysis of surfactants influencing attachment of a *Mycobacterium sp.* to cellulose acetate and aromatic polyamide reverse osmosis membranes. *Biotechnol*. Bioeng, 64, 527-544. 1999.
21. Bold, R. M.; K. P. Ishida; and Ridgway, H. R. 1999. Effect of adsorbed surfactant on bacterial attachment at an aqueous-polymer membrane interface as determined by attenuated total reflection Fourier transform spectrometry and differential interference contrast microscopy. Poster presentation. AWWA Membrane Technology Conference Proceedings. Feb. 28-Mar. 3, Long Beach, CA.
22. Ishida, K. P. and Ridgway, H. R. Influence of dodecylbenzenesulfonic acid treatment on model organic molecular conditioning films formed on cellulose acetate as determined by attenuated total reflection Fourier transform infrared spectrometry. AWWA Membrane and Technology Conference Proceedings. Feb. 28-Mar. 3, Long Beach, CA. 1999.
23. Chittur, Krishnan K. "FTIR and Protein Structure at Interfaces". December 9, 1997 Chemical and Materials Engineering Department. University of Alabama, Huntsville. October 25, 2004. <http://www.eng.uah.edu/~kchittur/bmreview/node2.html>.
24. Pike Technologies. Spectroscopic Creativity: ATR Theory and Applications. <http://www.piketech.com/technical/application-pdfs/ATR-theory-apps.pdf> Application Note – 0402. October 25, 2004. <http://www.piketech.com>.
25. Pascall, M.A.; Richtsmeier, J.; Riemer, J.; and Farahbaksh, B. Non-destructive packaging seal strength analysis and leak detection using ultrasonic imaging Dept. of Food Science and Technology, Ohio State University, Columbus, OH.
26. Kaliakin, V.N. *Introduction to Approximation and to the Finite Element Method.* Department of Civil Engineering. University of Delaware, pp. 81-83, 1992.

27. Margaritas, G.; Sikorski, S.A.; and McGarry, F.J. Elastic-plastic finite element analysis and application of the island blister test. Materials Science & Engineering, MIT, Cambridge, MA.
28. ASTM Standard D1876 – 01. Standard Test Method for Peel Resistance of Adhesives (T-Peel Test). 2001.
29. ASTM Standard F88 – 00. Standard Test Method for Seal Strength of Flexible Barrier Materials. 2000
30. ASTM Standard D882 – 02. Standard Test Method for Tensile Properties of Thin Plastic Sheeting. 2002.
31. ASTM Standard F 2054 – 00. Standard Test Method for Burst Testing of Flexible Package Seals Using Internal Air Pressurization within Restraining Plates. 2000.
32. Dyer, John R. Applications of Absorption Spectroscopy of Organic Compounds. Georgia Inst. Of Tech. Prentice-Hall, Inc., NJ, 1965.
33. "Singular Stress and Displacement Fields." Engineers Toolbox. Rapid Solutions for Engineers. <http://www.engineerstoolbox.com/doc/etb/mod/fm1/crack stress/ crackstress_help.html> October 25, 2004. <http://www.engineerstoolbox.com>.
34. Anderson, T. L. *Fracture Mechanics Fundamentals and Applications - 2nd Edition*, CRC Press Florida, 1995.
35. Westergaard, H.M. "Bearing Pressures and Cracks," *Journal of Applied Mechanics*, Vol. 6, pp. 49-53, 1939.
36. Irwin, G.R. "Analysis of Stresses and Strains near the End of a Crack Traversing a Plate," *Journal of Applied Mechanics*, Vol. 24, pp. 361-364, 1957.
37. Sneddon, I.N. "The Distribution of Stress in the Neighborhood of a Crack in an Elastic Solid," Proceedings, *Royal Society of London*, Vol. A-187, pp. 229-260, 1946.
38. Williams, M.L. "On the Stress Distribution at the base of a Stationary Crack," *Journal of Applied Mechanics*, Vol. 24, pp. 109-114, 1957.
39. Bio-Rad WinIR Pro 3.0 software spectra search database.

Appendix A: Tray Production and Retort Conditions

Table A.1: Empty polytray production with varying channel defects: Trial 1 Stegner Food Products 6/5/2003.

Empty MRE Packages (E): 50 total						
Destructive/Mechanical Testing						
Sample	**Wire (μm)**	**Time (put in production)**		**Sample**	**Wire (μm)**	**Time (put in production)**
E1-0	0.0	4:55		E6-50.8	50.8	6:00
E2-0	0.0	4:55		E7-50.8	50.8	6:00
E3-0	0.0	4:55		E8-50.8	50.8	6:00
E4-0	0.0	4:55		E9-50.8	50.8	6:00
E5-0	0.0	4:55		E10-50.8	50.8	6:00
E6-0	0.0	4:55		E1-127	127.0	6:00
E7-0	0.0	4:55		E2-127	127.0	6:00
E8-0	0.0	4:55		E3-127	127.0	6:00
E9-0	0.0	4:55		E4-127	127.0	6:00
E10-0	0.0	4:55		E5-127	127.0	6:00
E1-254	254.0	5:15		E6-127	127.0	6:00
E2-254	254.0	5:15		E7-127	127.0	6:00
E3-254	254.0	5:15		E8-127	127.0	6:00
E4-254	254.0	5:15		E9-127	127.0	6:00
E5-254	254.0	5:15		E10-127	127.0	6:00
E6-254	254.0	5:15		E1-381	381.0	5:15
E7-254	254.0	5:15		E2-381	381.0	5:15
E8-254	254.0	5:15		E3-381	381.0	5:15
E9-254	254.0	5:15		E4-381	381.0	5:15
E10-254	254.0	5:15		E5-381	381.0	5:15
E1-50.8	50.8	6:00		E6-381	381.0	5:15
E2-50.8	50.8	6:00		E7-381	381.0	5:15
E3-50.8	50.8	6:00		E8-381	381.0	5:15
E4-50.8	50.8	6:00		E9-381	381.0	5:15
E5-50.8	50.8	6:00		E10-381	381.0	5:15

Table A2: Empty polytray production with all channel defects on one polytray: Trial 1 Stegner Food Products 6/5/2003.

Empty MRE Packages (E): 10 total						
Destructive/Mechanical Testing: All wire sizes on one package						
Sample	**Wire (μm)**	**Time (put in production)**		**Sample**	**Wire (μm)**	**Time (put in production)**
E1-all	all sizes	6:20		E6-all	all sizes	6:20
E2-all	all sizes	6:20		E7-all	all sizes	6:20
E3-all	all sizes	6:20		E8-all	all sizes	6:20
E4-all	all sizes	6:20		E9-all	all sizes	6:20
E5-all	all sizes	6:20		E10-all	all sizes	6:20

Table A3: Media filled polytray production with various channel defects: Trial 1 Stegner Food Products 6/5/2003.

Media Filled Packages (MF): 80 total						
Microbial Challenge						
Chlorinated Water (10 ppm FAC)				**Contaminated Water (3 log CFU/ml)**		
Sample	**Wire (μm)**	**Time (put in production)**		**Sample**	**Wire (μm)**	**Time (put in production)**
MF1-0-Cl	0	11:05		MF1-0-3 log	0	11:40
MF2-0-Cl	0	11:05		MF2-0-3 log	0	11:40
MF3-0-Cl	0	11:05		MF3-0-3 log	0	11:40
MF4-0-Cl	0	11:05		MF4-0-3 log	0	11:40
MF5-0-Cl	0	11:05		MF5-0-3 log	0	11:40
MF1-254-Cl	254	12:40		MF1-254-3 log	254	1:05
MF2-254-Cl	254	12:40		MF2-254-3 log	254	1:05
MF3-254-Cl	254	12:40		MF3-254-3 log	254	1:05
MF4-254-Cl	254	12:40		MF4-254-3 log	254	1:05
MF5-254-Cl	254	12:40		MF5-254-3 log	254	1:05
MF1-50.8-Cl	50.8	2:30		MF1-50.8-3 log	50.8	2:55
MF2-50.8-Cl	50.8	2:30		MF2-50.8-3 log	50.8	2:55
MF3-50.8-Cl	50.8	2:30		MF3-50.8-3 log	50.8	2:55
MF4-50.8-Cl	50.8	2:30		MF4-50.8-3 log	50.8	2:55
MF5-50.8-Cl	50.8	2:30		MF5-50.8-3 log	50.8	2:55
MF1-127-Cl	127	2:00		MF1-127-3 log	127	2:00
MF2-127-Cl	127	2:00		MF2-127-3 log	127	2:00
MF3-127-Cl	127	2:00		MF3-127-3 log	127	2:00
MF4-127-Cl	127	2:00		MF4-127-3 log	127	2:00
MF5-127-Cl	127	2:00		MF5-127-3 log	127	2:00
MF1-381-Cl	381	11:05		MF1-381-3 log	381	11:40
MF2-381-Cl	381	11:05		MF2-381-3 log	381	11:40
MF3-381-Cl	381	11:05		MF3-381-3 log	381	11:40
MF4-381-Cl	381	11:05		MF4-381-3 log	381	11:40
MF5-381-Cl	381	11:05		MF5-381-3 log	381	11:40

Table A3: Continued.

Contaminated Water (6 log CFU/ml)		
Sample	**Wire (μm)**	**Time (put in production)**
MF1-0-6 log	0	12:30
MF2-0-6 log	0	12:30
MF3-0-6 log	0	12:30
MF4-0-6 log	0	12:30
MF5-0-6 log	0	12:30
MF1-254-6 log	254	1:05
MF2-254-6 log	254	1:05
MF3-254-6 log	254	1:05
MF4-254-6 log	254	1:05
MF5-254-6 log	254	1:05
MF1-50.8-6 log	50.8	2:55
MF2-50.8-6 log	50.8	2:55
MF3-50.8-6 log	50.8	2:55
MF4-50.8-6 log	50.8	2:55
MF5-50.8-6 log	50.8	2:55
MF1-127-6 log	127	2:00
MF2-127-6 log	127	2:00
MF3-127-6 log	127	2:00
MF4-127-6 log	127	2:00
MF5-127-6 log	127	2:00
MF1-381-6 log	381	12:30
MF2-381-6 log	381	12:30
MF3-381-6 log	381	12:30
MF4-381-6 log	381	12:30
MF5-381-6 log	381	12:30

Positive Control (post cool inoculated)		
Sample	**Wire (μm)**	**Time (put in production)**
MF1-0-PCI	0	11:55
MF2-0-PCI	0	11:55
MF3-0-PCI	0	11:55
MF4-0-PCI	0	11:55
MF5-0-PCI	0	11:55

Table A.4: Retort process conditions for Stegner Trial 1.

ICON 2000 Sterilization Report

Preheat					
	Time	Process Vessel Temp (F)	System Pressure (psi)	Water Level (%)	Flow (gal/min)
Step Begin	3:04:44	98.3	0.4	23	0
Step End	3:11:23	110	4.9	27	0
Total Time in Step	0:06:39				
Come Up					
	Time	Process Vessel Temp (F)	System Pressure (psi)	Water Level (%)	Flow (gal/min)
Step Begin	3:11:23	110	4.9	27	0
Step End	3:18:35	201.2	15.1	19	1100
Total Time in Step	0:07:12				
Come Up					
	Time	Process Vessel Temp (F)	System Pressure (psi)	Water Level (%)	Flow (gal/min)
Step Begin	3:18:35	201.2	15.1	19	1100
Step End	3:24:35	256	34.2	21	1357
Total Time in Step	0:06:00				
Come Up					
	Time	Process Vessel Temp (F)	System Pressure (psi)	Water Level (%)	Flow (gal/min)
Step Begin	3:24:35	256	34.2	21	1357
Step End	3:28:05	255.6	34.2	20	1354
Total Time in Step	0:03:30				
Cook					
	Time	Process Vessel Temp (F)	System Pressure (psi)	Water Level (%)	Flow (gal/min)
Step Begin	3:28:05	255.6	34.2	20	1354
Step End	4:55:10	252.9	34.1	20	1371
Total Time in Step	1:27:05				

Table A4: Continued

Micro Cool					
	Time	Process Vessel Temp (F)	System Pressure (psi)	Water Level (%)	Flow (gal/min)
Step Begin	4:55:10	252.9	34.1	20	1371
Step End	4:57:26	237	33.9	20	1355
Total Time in Step	0:02:16				
Cool					
	Time	Process Vessel Temp (F)	System Pressure (psi)	Water Level (%)	Flow (gal/min)
Step Begin	4:57:26	237	33.9	20	1355
Step End	5:02:26	193.8	34.9	21	1236
Total Time in Step	0:05:00				
Cool					
	Time	Process Vessel Temp (F)	System Pressure (psi)	Water Level (%)	Flow (gal/min)
Step Begin	5:02:26	193.8	34.9	21	1236
Step End	5:08:26	125.4	30	20	1338
Total Time in Step	0:06:00				
Cool					
	Time	Process Vessel Temp (F)	System Pressure (psi)	Water Level (%)	Flow (gal/min)
Step Begin	5:08:26	125.4	30	20	1338
Step End	2:28:26	79.4	15.1	21	1353
Total Time in Step	1:20:00				

Polytrays were again manufactured at Stegner Food Company in February 2004. The same process was used here for Trial 2 to fill and seal the packages. The 254 and 381 micron wires were not used in this trial because prior testing, which can be seen in the Results and Discussion section, proved the channel defects to be too severe. The 50.8 micron wire and ~12 micron carbon fibers were used in this trial to create channel defects. The carbon fibers proved to be entirely too small to create a channel defect. The fibers would break very similarly to the 12.7 micron wire in production. As the lid stock was sealed to the tray, the fibers would break and could not be pulled from the seal to create a channel defect. Sound samples were made along with samples with entrapped matter. To understand some of the problems occurring in process, soy bean oil, starch solution (6.5%) and blanched noodles were placed across the tray before sealing. This in turn creates an artificial defect in the sealing area. The defects were clearly visible and samples could then be cut from the area surrounding the defect for mechanical testing. The polytrays were not placed in retort at the Stegner plant for Trial 2; instead the media filled polytrays were placed in retort at the University of Tennessee, Knoxville in the Food Science and Technology Building. The retort conditions can be found in below in Table A.5.

Table A.5: Retort process conditions for Stegner Trial 2: University of Tennessee, Knoxville, Food Science and Technology Department.

Temperature (F)	Time (min)	Pressure (psi)
100	5	5
150	6	5
200	6	15
256	6	34
255.6	3	34.2
252	30	34.1
237	2	33
150	5	33
125	5	20
105	10	10
100	1	1

Appendix B: Microbial Challenge Results and Microorganism Preparation

Sample (polytrays and microorganism) preparations for microbial challenge 1:

Polytray Preparation

Chlorinated Water (10 ppm FAC)	
Test Samples – 4 wire sizes X 5 polytrays	20 samples
Sound Samples	5 samples
Contaminated Water (3 log CFU/mL)	
Test Samples – 4 wire sizes X 5 polytrays	20 samples
Sound Samples	5 samples
Contaminated Water (6 log CFU/mL)	
Test Samples – 4 wire sizes X 5 polytrays	20 samples
Sound Samples	5 samples
Positive Control (post cool inoculated)	5 samples
Total Polytrays	80

Microorganism Washes

1. Prepare Cultures of *Enterobacter aerogenes*
    a. 5 tubes (10 mL each) in trypticase soy broth + starch
    b. Incubate 24 hr. at 37C
    c. Check for Gas formation (CO2)
2. Wash and rinse 3-5 gallon buckets with chlorinated water
3. Fill and add sodium thiosulfate to 2 of the buckets
4. Add 10 ppm (mg/L) sodium hypochlorite to the third bucket:
    a. Chlorox or Purex (5,25% sodium hypochlorite)
    b. Needed 10 mg/L for 18.9 L = 0.189 mg
    c. Add 3.6 mL (0.0525 mg) of 5.25% Chlorox or Purex in 5 gallons of water
5. High initial number – 6 log CFU/mL
    a. Add two tubes (20 mL) of *Enterobacter aerogenes* culture to 5 gallons of water with sodium thiosulfate
    b. Ca. 9 log CFU/Ml X 20 mL = $2x10^{10}$ CFU
    c. $2x10^{10}$ CFU/18,925 ml = 1.06×10^{6} CFU/mL
6. Low initial number – 3 log CFU/mL
    a. Add 100 mL from high initial number *Enterobacter aerogenes* bucket to 5 gallon water with thiosulfate
    b. 1.06×10^{8} CFU/18,925 mL – 5.6×10^{3} CFU/mL
7. Dip all retorted polytrays for 2 minutes and agitate manually
8. For positive controls, add 1.0 mL of culture into a sound polytray

Sample (polytrays) preparations for microbial challenge 2.

Sample Preparation

Chlorinated Water (10 ppm FAC)	
Test Samples – 2 wire sizes (50.8, C Fiber) X 5 polytrays	10 samples
Control Samples	5 samples
Contaminated Water (3 log CFU/mL)	
Test Samples – 2 wire sizes (50.8, C Fiber) X 5 polytrays	10 samples
Control Samples	5 samples
Contaminated Water (6 log CFU/mL)	
Test Samples – 2 wire sizes (50.8, C Fiber) X 5 polytrays	10 samples
Control Samples	5 samples
Positive Control (post cool inoculated)	5 samples
Total Polytrays for Microbial Challenge 2	50

Table B.1: Results of Microbial Challenge 1 of Stegner Trial 1 Polytrays.

SAMPLE NO.	WIRE	DAY										
		1	2	3	4	5	6	7	8	9	10	11
Chlorinated Water (7-9 ppm FAC)												
MF1-0-CI	0	-	-	-	-	-	-	-	-	-	-	-
MF2-0-CI	0	-	-	-	-	-	-	-	-	-	-	-
MF3-0-CI	0	-	-	-	-	-	-	-	-	-	-	-
MF4-0-CI	0	-	-	-	-	-	-	-	-	-	-	-
MF5-0-CI	0	-	-	-	-	-	-	-	-	-	-	-
MF1-254-CI	254	-	-	-	-	-	-	-	-	-	-	-
MF2-254-CI	254	-	-	-	-	-	-	-	-	-	-	-
MF3-254-CI	254	-	-	-	-	-	-	-	-	-	-	-
MF4-254-Cl	254	-	-	-	-	-	-	-	-	-	-	-
MF5-254-CI	254	-	-	-	-	-	-	-	-	-	-	-
MF1-50.8-CI	50.8	-	-	-	-	-	-	-	-	-	-	-
MF2-50.8-CI	50.8	-	-	-	-	-	-	-	-	-	-	-
MF3-50.8-CI	50.8	-	-	-	-	-	-	-	-	-	-	-
MF4-50.8-CI	50.8	-	-	-	-	-	-	-	-	-	-	-
MF5-50.8-CI	50.8	-	-	-	-	-	-	-	-	-	-	-
MF1-127-CI	127	-	-	-	-	-	-	-	-	-	-	-
MF2-127-CI	127	-	-	-	-	-	-	-	-	-	-	-
MF3-127-CI	127	-	-	-	-	-	-	-	-	-	-	-
MF4-127-CI	127	-	-	-	-	-	-	-	-	-	-	-
MF5-127-CI	127	-	-	-	-	-	-	-	-	-	-	-
MF1-381-CI	381	-	-	-	-	-	-	-	-	-	-	-
MF2-381-CI	381	-	-	-	-	-	-	-	-	-	-	-
MF3-381-CI	381	-	-	-	-	-	-	-	-	-	-	-
MF4-381-CI	381	-	-	-	-	-	-	-	-	-	-	-
MF5-381-CI	381	-	-	-	-	-	-	-	-	-	-	-
3 log CFU/ml												
MF1-0-3 log	0	-	-	-	-	-	-	-	-	-	-	-
MF2-0-3 log	0	-	-	-	-	-	-	-	-	-	-	-
MF3-0-3 log	0	-	-	-	-	-	-	-	-	-	-	-
MF4-0-3 log	0	-	-	-	-	-	-	-	-	-	-	-
MF5-0-3 log	0	Lost										
MF1-254-3 log	254	-	+									
MF2-254-3 log	254	-	-	-	-	-	-	-	-	-	-	-
MF3-254-3 log	254	-	-	-	-	-	-	-	-	-	-	-
MF4-254-3 log	254	-	-	-	-	-	-	-	-	-	-	-
MF5-254-3 log	254	-	-	-	-	-	-	-	-	-	-	-
MF1-50.8-3 log	50.8	-	-	-	-	-	-	-	-	-	-	-
MF2-50.8-3 log	50.8	-	-	-	-	-	-	-	-	-	-	-

Table B.1: Continued

SAMPLE NO.	WIRE	DAY										
		1	2	3	4	5	6	7	8	9	10	11
MF3-50.8-3 log	50.8	-	-	-	-	-	-	-	-	-	-	-
MF4-50.8-3 log	50.8	-	-	-	-	-	-	-	-	-	-	-
MF5-50.8-3 log	50.8	-	-	-	-	-	-	-	-	-	-	-
MF1-127-3 log	127	-	-	-	-	-	-	-	-	-	-	-
MF2-127-3 log	127	-	-	-	-	-	-	-	-	-	-	-
MF3-127-3 log	127	-	-	-	-	-	-	-	-	-	-	-
MF4-127-3 log	127	-	-	-	-	-	-	-	-	-	-	-
MF5-127-3 log	127	-	-	-	-	-	-	-	-	-	-	-
MF1-381-3 log	381	-	-	-	-	-	-	-	-	-	-	-
MF2-381-3 log	381	-	+									
MF3-381-3 log	381	-	+									
MF4-381-3 log	381	-	-	-	-	-	-	-	-	-	-	-
MF5-381-3 log	381	-	-	-	-	-	-	-	-	-	-	-
6 log CFU/ml												
MF1-0-6 log	0	-	-	-	-	-	-	-	-	-	-	-
MF2-0-6 log	0	-	-	-	-	-	-	-	-	-	-	-
MF3-0-6 log	0	-	-	-	-	-	-	-	-	-	-	-
MF4-0-6 log	0	-	-	-	-	-	-	-	-	-	-	-
MF5-0-6 log	0	-	-	-	-	-	-	-	-	-	-	-
MF1-254-6 log	254	-	-	-	-	-	-	-	-	-	-	-
MF2-254-6 log	254	-	-	-	-	-	-	-	-	-	-	-
MF3-254-6 log	254	-	-	+								
MF4-254-6 log	254	-	-	+								
MF5-254-6 log	254	-	-	-	-	-	-	-	-	-	-	-
MF1-50.8-6 log	50.8	-	-	-	-	-	-	-	-	-	-	-
MF2-50.8-6 log	50.8	-	-	-	-	-	-	-	-	-	-	-
MF3-50.8-6 log	50.8	-	-	-	-	-	-	-	-	-	-	-
MF4-50.8-6 log	50.8	-	-	-	-	-	-	-	-	-	-	-
MF5-50.8-6 log	50.8	-	-	-	-	-	-	-	-	-	-	-
MF1-127-6 log	127	-	-	-	-	-	-	-	-	-	-	-
MF2-127-6 log	127	-	-	-	-	-	-	-	-	-	-	-
MF3-127-6 log	127	-	-	-	-	-	-	-	-	-	-	-
MF4-127-6 log	127	-	-	-	-	-	-	-	-	-	-	-
MF5-127-6 log	127	-	-	-	-	-	-	-	-	-	-	-
MF1-381-6 log	381	-	+									
MF2-381-6 log	381	-	-	-	-	-	-	-	-	-	-	-
MF3-381-6 log	381	-	+									
MF4-381-6 log	381	-	+									
MF5-381-6 log	381	-	+									

Table B.1: Continued

SAMPLE NO.	WIRE	DAY										
		1	2	3	4	5	6	7	8	9	10	11
Positive Control (Inoculated)												
MF1-0-PCI	0	+										
MF2-0-PCI	0	+										
MF3-0-PCI	0	+										
MF4-0-PCI	0	+										
MF5-0-PCI	0	+										

Table B.2: Raw results of microbial challenge 2 of Stegner Trial 2 polytrays.

Stegner Project--Began incubation 2/13/2004		
Tray	**Date observed**	**Observation**
MF1-0-PCL	2/16/2004	gas production (++++++), odor associated with organism, cloudy
MF2-0-PCL	2/16/2004	gas production (++++++), odor associated with organism, cloudy
MF3-0-PCL	2/16/2004	gas production (++++++) indicating major growth, odor associated with organism, cloudy
MF4-0-PCL (lost caulk)	2/16/2004	gas production (++++++), odor associated with organism
MF5-0-PCL	2/16/2004	gas production (++++++), odor associated with organism, cloudy
MF1-0-CL	2/20/2004	negative
MF2-0-CL	2/20/2004	negative
MF3-0-CL	2/20/2004	gas production (+) throughout
MF4-0-CL	2/20/2004	negative
MF5-0-CL	2/20/2004	negative
MF1-0-3 log	2/20/2004	negative
MF2-0-3 log	2/20/2004	negative
MF3-0-3 log	2/20/2004	negative
MF4-0-3 log	2/20/2004	negative--slight bubbling around one corner
MF5-0-3 log	2/20/2004	negative
MF1-0-6 log	2/20/2004	negative, tight swelling of cover
MF2-0-6 log	2/20/2004	gas production (++), cloudy
MF3-0-6 log	2/20/2004	gas production (+++), cloudy
MF4-0-6 log	2/20/2004	only slight bubbles, cloudy
MF5-0-6 log	2/20/2004	negative

Table B.2: Continued

Tray	Date observed	Observation
MF1-50.8-CL	2/20/2004	negative
MF2-50.8-CL	2/20/2004	gas production (+) around corners not near tape
MF3-50.8-CL	2/20/2004	gas production (++), cloudy
MF4-50.8-CL	2/20/2004	gas production (++), cloudy
MF5-50.8-CL	2/20/2004	negative
MF1-50.8-3log	2/16/2004	possibly?? (-), maybe a couple of bubbles (+), different odor (bad)
MF2-50.8-3 log	2/20/2004	gas production (+) around 3 edges
MF3-50.8-3 log	2/20/2004	negative
MF4-50.8-3 log	2/20/2004	tight swelling of cover, gas production (+++) cloudy, odor
MF5-50.8-3 log	2/20/2004	tight swelling of cover, gas production (+) around tape
MF1-50.8-6 log	2/20/2004	gas production (+) confined to around sides
MF2-50.8- 6 log	2/20/2004	negative
MF3-50.8-6 log	2/20/2004	negative
MF4-50.8-6 log	2/20/2004	negative
MF5-50.8-6log	2/16/2004	gas production (++)
MF1-CF-CL	2/16/2004	few bubbles indicating slight gas production (++), slightly bad odor
MF2-CF-CL	2/20/2004	negative
MF3-CF-CL	2/20/2004	negative, slightly cloudy but no bubbles
MF4-CF-CL	2/20/2004	negative
MF5-CF-CL	2/20/2004	gas production (+++), cloudy, odor
MF1-CF-3 log	2/20/2004	negative
MF2-CF-3 log	2/20/2004	negative

Table B.2: Continued

Tray	Date observed	Observation
MF3-CF-3 log	2/20/2004	tight swelling of cover, gas production (+) confined to one side not around tape
MF4-CF-3 log	2/20/2004	gas production (+) around sides
MF5-CF-3 Log	2/20/2004	negative
MF1-CF-6 log	2/20/2004	negative
MF2-CF-6 log	2/20/2004	negative
MF3-CF-6 log	2/20/2004	gas production (+)
MF4-CF-6 log	2/20/2004	negative
MF5-CF-6 log	2/20/2004	negative
		+ indicates slight gas production (only a few bubbles)
		++++++ indicates major gas production
		- indicates negative gas production

Table B.3: Compiled results for microbial challenge 2 of Stegner trial 2.

Stegner Project Results				
Tray	**Observation**	**Date observed**		
MF1-0-PCL	+	2/16/2004		
MF2-0-PCL	+	2/16/2004		+
MF3-0-PCL	+	2/16/2004		
MF4-0-PCL	+	2/16/2004		-
MF5-0-PCL	+	2/16/2004		
MF1-0-CL	-	2/20/2004		+/-
MF2-0-CL	-	2/20/2004		
MF3-0-CL	-/+	2/20/2004		-/+
MF4-0-CL	-	2/20/2004		
MF5-0-CL	-	2/20/2004		
MF1-0-3 log	-	2/20/2004		
MF2-0-3 log	-	2/20/2004		
MF3-0-3 log	-	2/20/2004		
MF4-0-3 log	-	2/20/2004		
MF5-0-3 log	-	2/20/2004		
MF1-0-6 log	-	2/20/2004		
MF2-0-6 log	+/-	2/20/2004		
MF3-0-6 log	+/-	2/20/2004		
MF4-0-6 log	-/+	2/20/2004		
MF5-0-6 log	-	2/20/2004		
MF1-50.8-CL	-	2/20/2004		
MF2-50.8-CL	-/+	2/20/2004		
MF3-50.8-CL	-/+	2/20/2004		
MF4-50.8-CL	-/+	2/20/2004		
MF5-50.8-CL	-	2/20/2004		
MF1-50.8-3log	-/+	2/16/2004		
MF2-50.8-3 log	-/+	2/20/2004		
MF3-50.8-3 log	-	2/20/2004		
MF4-50.8-3 log	+/-	2/20/2004		

Table B.3: Continued

Tray	Observation	Date observed		
MF5-50.8-3 log	-/+	2/20/2004		
MF1-50.8-6 log	-/+	2/20/2004		
MF2-50.8- 6 log	-	2/20/2004		
MF3-50.8-6 log	-	2/20/2004		
MF4-50.8-6 log	-	2/20/2004		
MF5-50.8-6log	+/-	2/16/2004		
MF1-CF-CL	+/-	2/16/2004		
MF2-CF-CL	-	2/20/2004		
MF3-CF-CL	-	2/20/2004		
MF4-CF-CL	-	2/20/2004		
MF5-CF-CL	+/-	2/20/2004		
MF1-CF-3 log	-	2/20/2004		
MF2-CF-3 log	-	2/20/2004		
MF3-CF-3 log	-/+	2/20/2004		
MF4-CF-3 log	-/+	2/20/2004		
MF5-CF-3 Log	-	2/20/2004		
MF1-CF-6 log	-	2/20/2004		
MF2-CF-6 log	-	2/20/2004		
MF3-CF-6 log	-/+	2/20/2004		
MF4-CF-6 log	-	2/20/2004		
MF5-CF-6 log	-	2/20/2004		

Appendix C: Designs of Burst Chamber and FEMLAB 3D Modeling

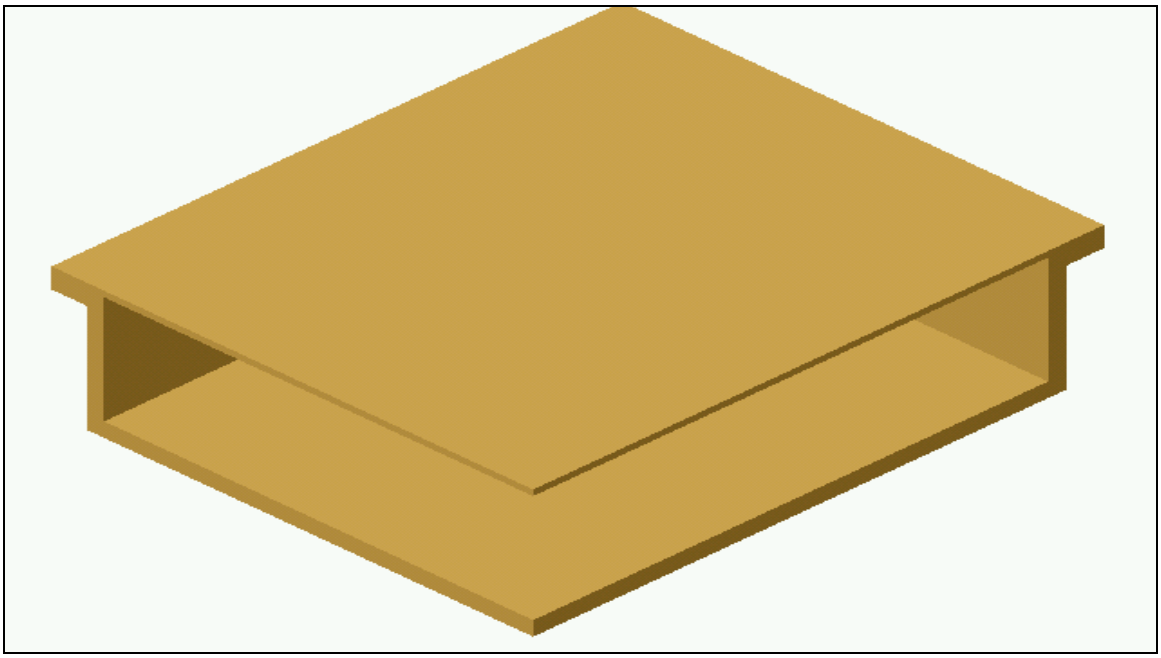

Figure C.1: SolidWorks® drawing of a quartered polytray: isometric view.

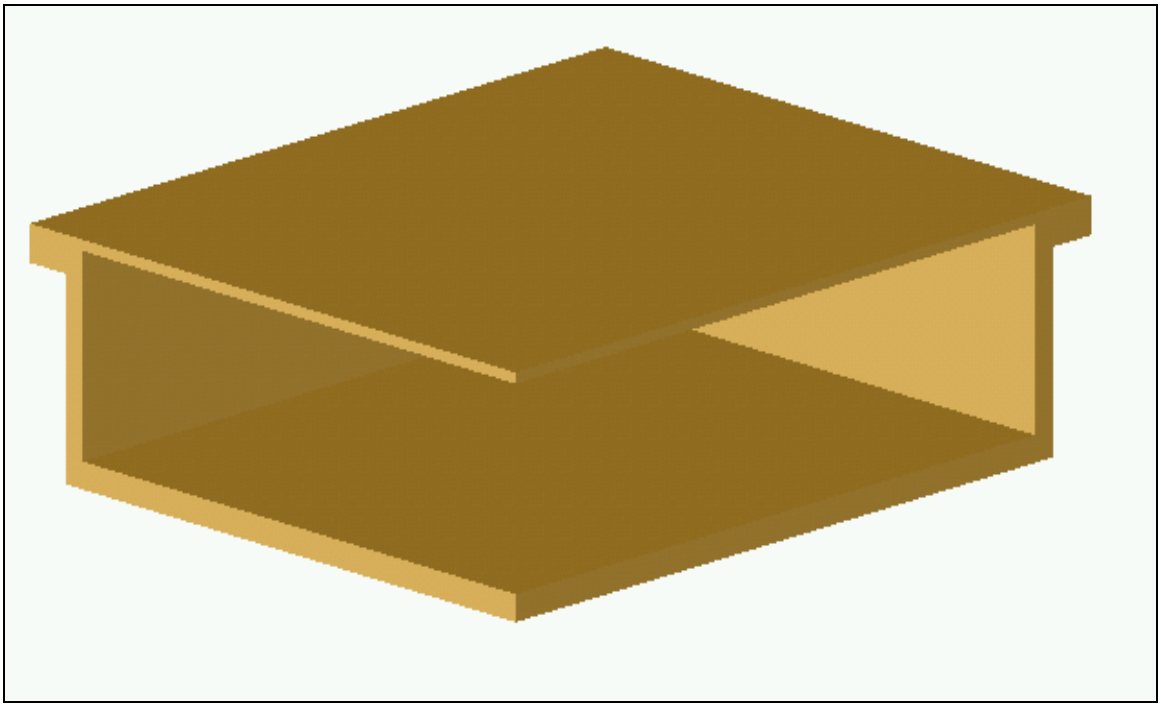

Figure C.2: SolidWorks® drawing of a quartered polytray: diametric view.

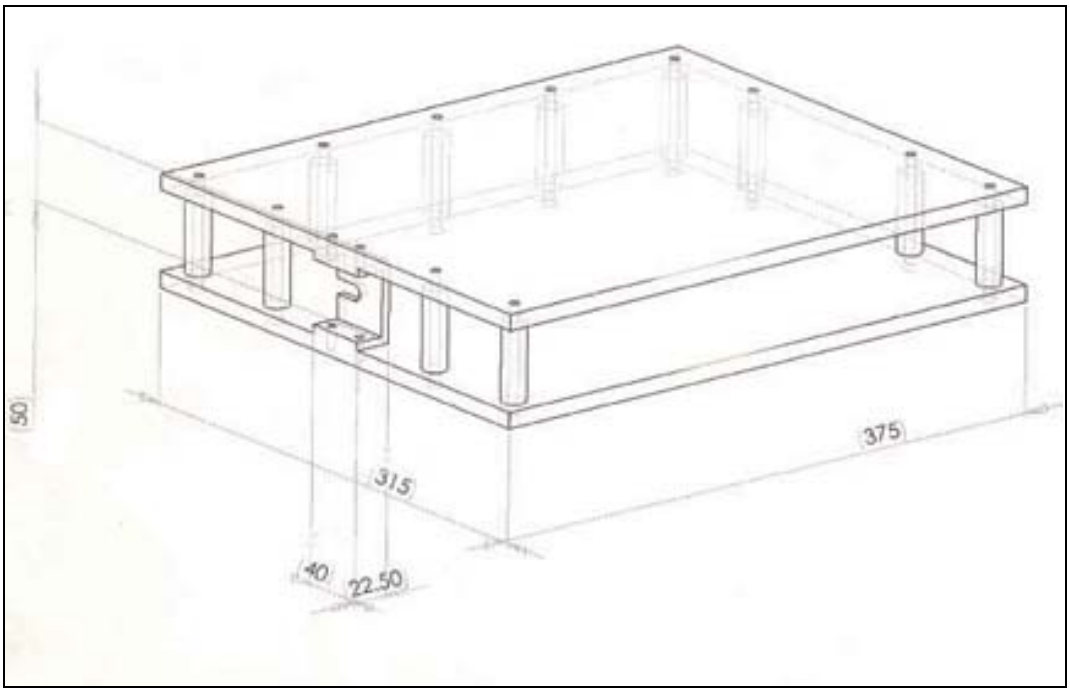

Figure C.3: SolidWorks® drawing of a burst chamber: isometric view.

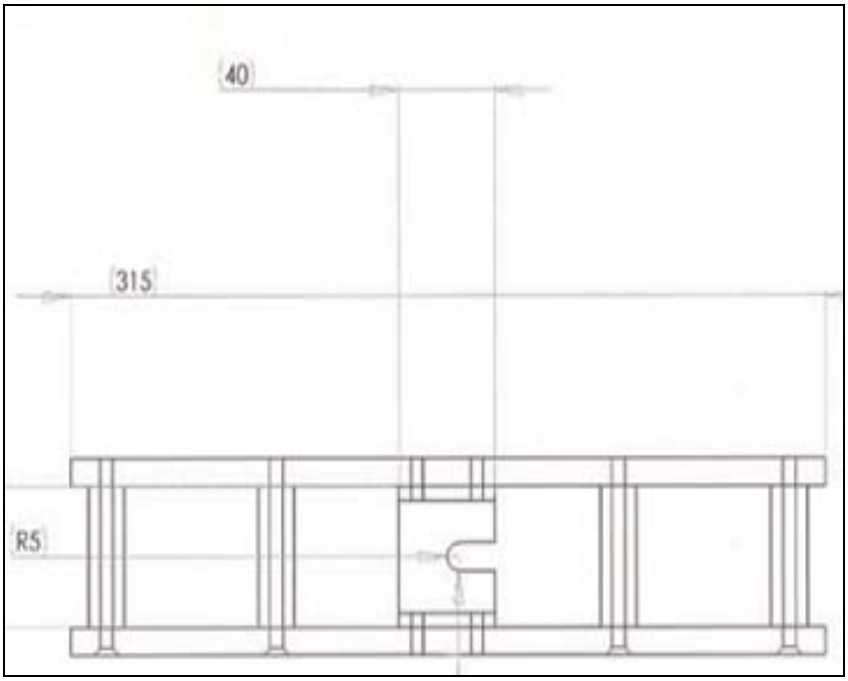

Figure C.4: SolidWorks® drawing of a burst chamber: side view.

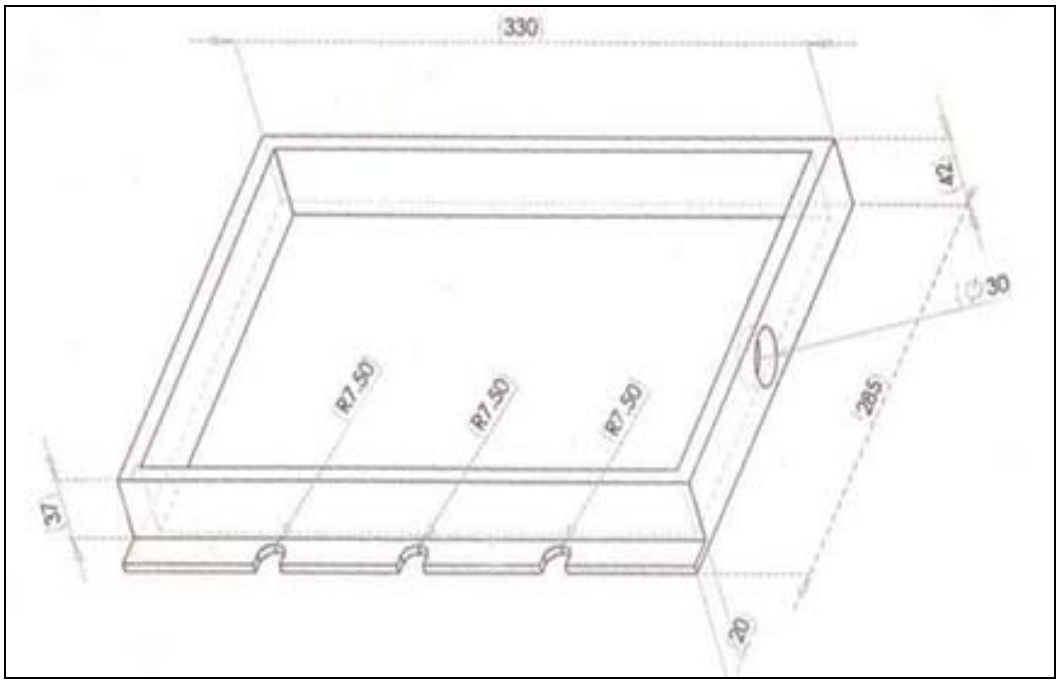

Figure C.5: SolidWorks® drawing of a burst tray insert: isometric view.

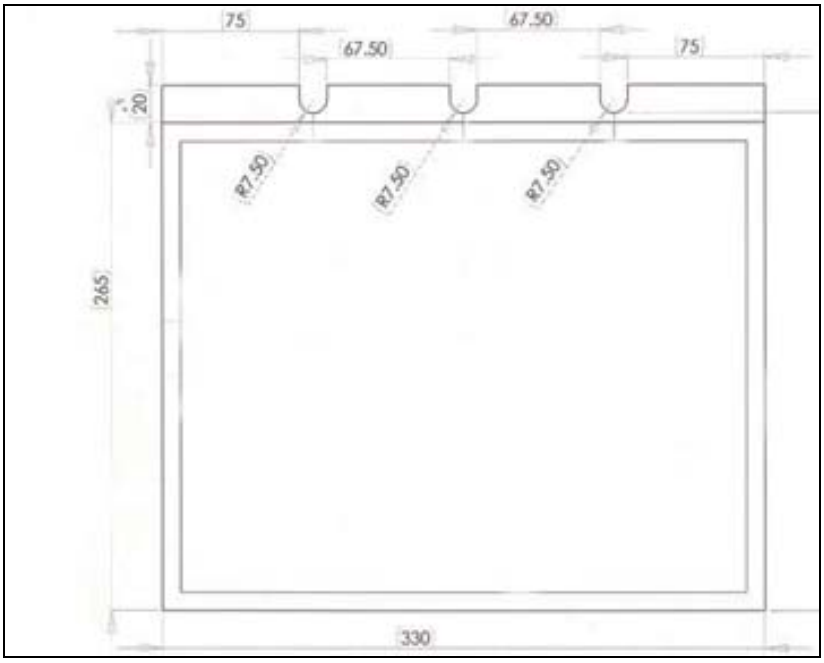

Figure C.6: SolidWorks® drawing of a burst tray insert: top view.

Vita:

William James Barlow, Jr. was born in Dearborn Heights, Michigan on August 19, 1979 to William James Barlow, Sr. and Mariella D. Barlow. He moved to Tennessee in 1991 and has lived there since. He attended high school at Battle Ground Academy in Franklin, Tennessee and graduated in 1997. He attended the University of Tennessee, Knoxville in 1997 and received his Bachelor of Science degree in Materials Science & Engineering in May of 2002. He continued his stay at the University of Tennessee, Knoxville for his Master of Science degree in Polymer Engineering and graduated in December of 2004.